Chapter 1

VOLCANIC-GAS STUDIES: METHODS, RESULTS, AND APPLICATIONS

Robert B. Symonds[1], William I. Rose[2], Gregg J. S. Bluth[2] and Terrrence M. Gerlach[1]

[1]*United States Geological Survey, Cascades Volcano Observatory*
5400 MacArthur Blvd.
Vancouver, Washington 98661 USA

[2]*Department of Geological Engineering, Geology, and Geophysics*
Michigan Technological University
Houghton, Michigan 49931 USA

INTRODUCTION

This chapter reviews several facets of the study of volcanic gases. The focus of the review is generally, but not exclusively on "high-temperature volcanic gases"—i.e., gases emitted at temperatures over 500°C from various sources at active volcanoes (erupting magma, lava flows, lava lakes, lava domes, eruption vents, fumaroles, fractures, etc.)—since these gases contain a substantial proportion of volatiles released directly from shallow magmas. Shallow magmas beneath active volcanoes release volatiles during both passive degassing and volcanic eruption. Passively degassing volcanoes often permit direct sampling of volcanic gases from ground-level sources and from volcanic plumes. Investigations of volcanic gases during eruptive degassing generally require remote sensing methods, including satellite-based methods. Because of the close tie to magma degassing, investigations of high-temperature volcanic gases provide important data for constraining the compositions, amounts, and origins of volatiles in magma. Volcanic gas data provide insights into magma degassing processes and critical information for evaluating volcanic hazards. In recent years, volcanic gas emissions have also received attention because of their effects on the atmosphere and climate, and as benchmarks for comparison with anthropogenic gas emissions.

SAMPLING AND IN-SITU MEASUREMENTS AT HIGH-TEMPERATURE SITES

Inherent risks and limitations

Health and safety hazards. Getting to high-temperature sites on volcanoes inevitably involves higher than normal risks regardless of the mode of transport (hiking, climbing, helicopter flight). At the site, there are serious risks from direct exposure to eruptions, explosions, lava spraying, and hot gases (Williams, 1993). Furthermore, it is virtually impossible to work at these sites without some exposure to corrosive and toxic gases, aerosols, and toxic trace metals.

Sampling bias. Unfortunately, sampling is only feasible at the Earth's surface, so all volcanic-gas samples represent low-pressure (~1 bar) discharges. A potentially more significant problem is that the samples may represent fractionated gases from very degassed magma.

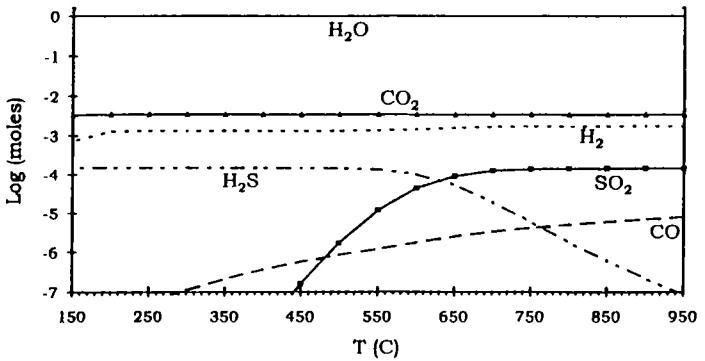

Figure 1. Calculated distribution of species for closed-system cooling of the August 11, 1960 gas sample from Showa-Shinzan's A-1 fumarole at 1 atm pressure. Gas analysis is from Mizutani and Sugiura (1982). For clarity, we exclude HCl (-3.4 log moles) and HF (-3.7 log moles) from the plot; all other species included in the calculations are shown.

Contamination. The ideal volcanic-gas sample would contain only magmatic volatiles. However, high-temperature volcanic gases are commonly mixtures of magmatic volatiles, air, meteoric steam, and gases from hydrothermal systems. It is often difficult to avoid some air contamination, because air can mix with magmatic gases at depth, in the vent, or during sampling. The common presence of meteoric water and hydrothermal fluids in volcanoes often leads to contamination of gas samples by meteoric steam and hydrothermal gases.

Reactions during cooling. For purposes of constraining magmatic-volatile compositions, volcanic-gas samples should be collected at magmatic temperatures. Unfortunately, most samples come from vents that are tens to hundreds of degrees Celsius cooler than the parental magma. During cooling, the concentrations of gas species can change (Fig. 1), although the changes are usually arrested by quenching of gas reactions at temperatures hotter than the vent temperature (Le Guern et al., 1982; Gerlach and Casadevall, 1986a).

Methods

Solution-filled collection bottles. The most common present-day method for sampling volcanic gases is to collect them in solution-filled bottles and analyze the mixtures in the laboratory (Giggenbach and Matsuo, 1991). This method was developed by Giggenbach (1975) and Giggenbach and Goguel (1989). A typical sampling setup is shown in Figure 2. A titanium or silica tube is inserted into the vent and attached to a dewared tube that minimizes condensation. The sampling train connects to an evacuated, pre-weighed sampling bottle partly filled with 4N NaOH solution. During sampling, the gas bubbles through the NaOH solution. H_2O condenses and the acid gases (CO_2, SO_2, H_2S, HCl, HF) are absorbed by the NaOH solution by the following reactions:

$$CO_2 + 2\ OH^-(aq) = CO_3^{2-}(aq) + H_2O \quad (1)$$

$$4\ SO_2 + 7\ OH^-(aq) = 3\ SO_4^{2-}(aq) + HS^-(aq) + 3\ H_2O \quad (2)$$

$$H_2S + OH^-(aq) = HS^-(aq) + H_2O \quad (3)$$

$$HCl + 2\ OH^-(aq) = 2Cl^-(aq) + H_2O \quad (4)$$

$$HF + 2\ OH^-(aq) = 2F^-(aq) + H_2O \quad (5)$$

The noncondensable gases (H_2, CO, CH_4, COS, N_2, Ar, O_2) collect in the headspace. In the laboratory, the bottles are reweighed to determine the weight gain during collection.

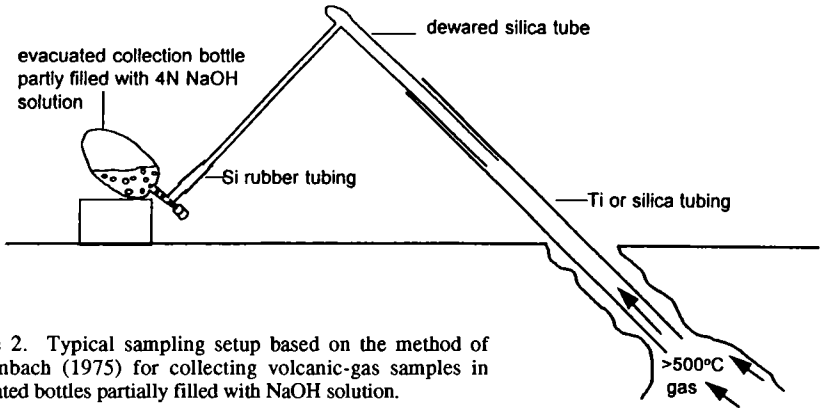

Figure 2. Typical sampling setup based on the method of Giggenbach (1975) for collecting volcanic-gas samples in evacuated bottles partially filled with NaOH solution.

The headspace gases are analyzed (normally by gas chromatography) to determine the molar amounts of each gaseous species collected. The solutions are analyzed by various techniques (e.g., wet-chemical methods, ion chromatography, selective ion electrode) for CO_3^{2-}, SO_4^{2-}, HS^-, total sulfur, Cl^-, and F^- to reconstruct the molar amounts of absorbed acid gases. H_2O is determined by difference (weight gain minus weight determined for non-H_2O gas species).

HS^- may oxidize to SO_4^{2-} after collection if the sample is contaminated with air. To preserve the original quantity of HS^-, some gas geochemists spike their NaOH solutions with Cd^{2+} or collect a second bottle filled with NH_4OH-$AgNO_3$ solution (Greenland, 1987b; Giggenbach and Matsuo, 1991). During collection, the HS^- reacts with the Cd^{2+} or Ag^+ to form CdS or AgS precipitate, which enables determination of the amount of H_2S by weighing the amount of sulfide precipitate or by determining the amount of Cd^{2+} or Ag^+ consumed by the precipitation reaction.

Another significant post-collection reaction is conversion of CO to formate (HCO_2^-):

$$CO + OH^-(aq) = HCO_2^-(aq) \quad (6)$$

(Giggenbach and Matsuo, 1991). This reaction is controlled kinetically; CO loss depends on time and the normality of the NaOH solution, and is less of a problem when using higher normality (~4N) NaOH solutions and when collecting gases rich in acidic species (Giggenbach and Matsuo, 1991). Preliminary results suggest that CO loss follows the radioactive isotope decay equation; hence, the initial CO concentration in the gas may be determined by obtaining several CO analyses over time and extrapolating back to the time of collection (Giggenbach and Matsuo, 1991).

Samples obtained in solution-filled bottles can be affected by several alterations during collection. Condensation or re-evaporation of liquid in the sampling train due to temperature fluctuations below and above the H_2O boiling point may severely disturb H_2O, HCl, and SO_2 concentrations (Gerlach, 1980b; Giggenbach and Matsuo, 1991). Condensation can be minimized by using a dewared sampling train as shown in Figure 2. Spilling of solution from the sampling bottle during collection decreases the determined amount of H_2O but has little effect on the determined quantities of other gas species (Gerlach, 1993b). Chemical reactions between the volcanic gases and titanium sampling tubes produce excess H_2. Silica and mullite tubes do not react with high-temperature volcanic gases, but may be too fragile to use in vigorous vents (Greenland, 1987b; Giggenbach and Matsuo, 1991). Titanium tubing withstands rough field use and is

probably unreactive in ≤400°C vents (Giggenbach and Matsuo, 1991). However, when used in >400°C vents, titanium may react with the gases to produce H_2, especially if the gases contain >0.1% HCl (Greenland, 1987b; Giggenbach and Matsuo, 1991). The predicted reaction[1] between the titanium tube and the gas is as follows:

$$Ti(s) + 2\ H_2O \Rightarrow TiO_2(s) + 2\ H_2 \quad (7)$$

Finally, minor amounts of sulfur may be lost by deposition of native sulfur prior to gas entry into the collection bottle (Matsuo, 1961; Gerlach, 1993b) by the reactions:

$$2\ H_2S + SO_2 \Rightarrow 3\ S(s) + 2\ H_2O \quad (8)$$

$$S_2 \Rightarrow 2\ S(s) \quad (9)$$

Native sulfur typically saturates at temperatures between 100° and 200°C (Bernard, 1985; Quisefit et al., 1989). Because temperatures of the gases often drop to ~100°C prior to entry into the collection bottle, loss of native sulfur is potentially a problem.

Pre-1975 collection techniques. Prior to 1975, most volcanic-gas samples were collected in flow-through or evacuated bottles without a solution to absorb the condensable gases, although notable exceptions are the 1954-1985 Showa-Shinzan samples (Nemoto et al., 1957; Mizutani 1962a,b; Mizutani and Sugiura, 1982). H_2O was not determined in many of the pre-1975 dry-bottle samples, although some analysts obtained estimates of the H_2O contents by determining the amount of condensate in the bottle (Giggenbach and Le Guern, 1976), by adding $CaC_2(s)$ and determining H_2O from the acetylene (C_2H_2) generated (Tazieff et al., 1972), by adding silica gel to the bottles to absorb H_2O (Huntingdon, 1973), or by condensing the H_2O prior to entry of gas into the bottle (Sigvaldason and Elisson, 1968). Dry-bottle samples are also affected by loss of sulfur from Reactions (8) and (9) and by the disproportionation of SO_2 in condensed H_2O:

$$4\ SO_2 + 4\ H_2O \Rightarrow H_2S + 6\ H^+(aq) + 3\ SO_4^{2-}(aq) \quad (10)$$

Some pre-1975 collection techniques exposed the sampled gases to reactive metals (steel, Cu, Al) that caused copious H_2 generation from reaction with H_2O and HCl (Gerlach, 1979; Gerlach, 1980c; Giggenbach and Matsuo, 1991).

In-situ gas chromatography. Some investigators have obtained analyses of volcanic gases by injecting them directly into a field gas chromatograph (hereafter, FGC; Le Guern et al., 1982). This method can determine H_2O, H_2, CO_2, CO, SO_2, H_2S, and atmospheric gases, but HCl and HF must be determined by the bottle-sampling approach (Le Guern et al., 1982). This method potentially yields real-time data on gas composition before leaving the field. Successful application of FGC is limited to sites where it is possible to work for an extended period of time (hours to days). The bottle-sampling approach is more desirable than FGC for hazardous sites where an extended stay is impractical or unsafe and where the results are not needed immediately. Other disadvantages of FGC are relatively large errors in H_2O and the inability to measure HCl and HF.

Oxygen fugacity probes. Some workers have used solid electrolyte probes to measure the oxygen fugacity (fO_2) of the gas in the field (Gantes et al., 1983). The most common probe consists of an electrolyte core, generally made of Zr and Y oxides, coated by a porous noble metal such as Pt (Gantes et al., 1983). The exchange of oxygen ions between the electrolyte core and the noble metal coating fuels the oxidation process of reduced volcanic-gas species and produces a current that is a function of fO_2.

[1]Reaction predicted by reacting a small amount of Ti(s) with a range of volcanic-gas compositions at 400° to 1200°C using thermochemical equilibrium program, GASWORKS (Symonds and Reed, 1993). The results show that Ti(s) reacts to form rutile (TiO_2) in preference to 28 other Ti-bearing gases and solids.

EVALUATION OF VOLCANIC-GAS ANALYSES

General guidelines

We suggest several guidelines to aid in selecting and evaluating gas samples that are likely to contain a high proportion of magmatic volatiles. A high collection temperature (>500°C) is one of the best indicators that a volcanic-gas sample is mainly from a magmatic source. Samples obtained in solution-filled bottles or from in-situ FGC are in general preferable to samples collected in flow-though or evacuated bottles without caustic solution. After collection, gas samples can be evaluated in several ways. When available, stable isotope data ($\delta^{18}O$ and δD data on H_2O, $\delta^{13}C$ data on CO_2 and CH_4, and $\delta^{34}S$ data on total sulfur) are extremely valuable to help determine whether these constituents come from magma, meteoric fluids, sedimentary rocks or fluids within them, seawater, or from some other source (Allard, 1983; Taylor, 1986).For thermochemical evaluation of a gas sample, it is desirable to have analytical data for as many species as possible, although it is common for analyses to lack data for critical species (e.g., SO_2, H_2, H_2S, CO) either because no determinations were made or because of detection limitations. Finally, gas samples are preferred that contain <1% air contamination or that permit reliable removal of air-contamination effects.

The above guidelines should only be viewed as aids in selecting gas samples likely to be enriched in magmatic volatiles. Judgment is required, however, because the guidelines may exclude "good" samples. For instance, the 1918-19 J-series Kilauea samples display only minor modifications from their exhaled equilibrium state even though the samples contain up to 90% air and were collected in evacuated bottles without caustic solution (Gerlach, 1980a). Finally, some samples satisfy the above guidelines, but are nonetheless "bad" for other reasons. We now consider more systematic evaluation procedures.

Evaluation procedures

Air contamination. Air contamination is a common and sometimes serious problem with volcanic-gas samples. Of the three most abundant gases in air, Ar is unreactive and N_2 reacts very little with high-temperature volcanic gases (Giggenbach, 1980, 1987), but O_2 may react significantly with reduced-gas species. Air contamination commonly causes the N_2/Ar ratio of the sample to match approximately the value for air (83.6). N_2/Ar ratios that are much higher than 83.6 or that are about equal to 38.5 (air-saturated groundwater) suggest that N_2 and Ar may come from a deeper magmatic or sedimentary source, or from air-saturated-groundwater, respectively (Magro and Pennisi, 1991). Most gas analyses that contain more than 1% N_2 have N_2/Ar ratios close to air (Fig. 3). The amount of air in such samples can be determined with the equation:

$$\text{air} = N_2 + Ar + 0.268\ N_2 \qquad (11)$$

where all terms are in moles and the term, 0.268 N_2, estimates the original amount of oxygen before any reaction with the sample. Sometimes Ar is not determined separately, but is analyzed as O_2 + Ar. In this case, air contamination gives $N_2/(O_2 + Ar)$ about equal to the value for air (3.6), although the ratio will be greater if some O_2 reacted with the sample. The isotopes, ^{20}Ne, ^{22}Ne, ^{36}Ar, and ^{38}Ar, are atmospheric tracers that may also help discern air contamination in volcanic gases (Magro and Pennisi, 1991).

The severity of air contamination depends on how much atmospheric O_2 reacts with the sample. If all the N_2 in a sample comes from air, then the amount of reacted O_2, $(O_2)_r$, can be estimated with the equation:

$$(O_2)_r = 0.268\ N_2 - (O_2)_m \qquad (12)$$

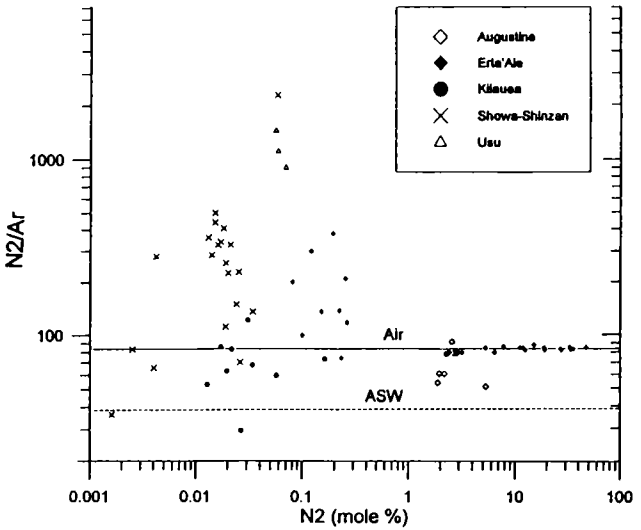

Figure 3. Plot showing N_2/Ar ratios versus total N_2 for selected analyses of high-temperature vol-canic gases. The solid and dashed lines show the N_2/Ar ratios of air and air saturated water (ASW), respectively. Sources of data are in Tables 3-5 (below).

where all terms are in moles and $(O_2)_m$ is the analyzed amount of O_2. Ideally, $(O_2)_r$ should account for all oxidation of reduced-gas species (Gerlach and Casadevall, 1986a). If they are determined to come from the atmosphere, N_2 and Ar are removed from gas analyses. O_2 is also removed from gas analyses, although if it has reacted with the reduced-gas species, the procedure is somewhat more complex (see below).

Equilibrium-disequilibrium analysis. Past investigations indicate that high-temperature volcanic gases initially approach a state of thermodynamic equilibrium (Ellis, 1957; Heald et al., 1963; Nordlie, 1971; Giggenbach and Le Guern, 1976; Gerlach, 1980a-d, 1993a,b; Le Guern et al., 1982; Gerlach and Casadevall, 1986a; Giggenbach, 1987). The strongest support for the equilibrium model of high-temperature volcanic gases is that some samples have equilibrium compositions (e.g., Le Guern et al., 1982; Gerlach and Casadevall, 1986a; Gerlach, 1993a,b) and the equilibrium compositions invariably imply equilibrium temperatures that are greater that the corresponding collection temperatures. These observations suggest that the equilibrium compositions represent the last equilibrium of the high-temperature volcanic gases before the gases stopped reacting (quenched) during cooling. Samples with "quenched equilibrium compositions", however, are relatively uncommon. Most analyses of samples collected before 1975 show evidence of severe disequilibrium (Gerlach, 1980a-d), and modern collection and analytical methods often give samples with mild to moderate disequilibrium (Gerlach, 1993b). To distinguish equilibrium and disequilibrium samples, we turn to thermodynamic modeling.

A flow chart for the equilibrium-disequilibrium determination is shown in Figure 4. We illustrate the procedure for SOLVGAS[2], an equilibrium computer program for gases (Symonds and Reed, 1993), although the same results can be achieved with other computer programs (e.g., Heald et al., 1963; Gerlach, 1980a, 1993b) or graphical methods (Greenland, 1987b). The procedure involves calculating correspondence temperatures (CTs) for the analyzed species to evaluate whether or not a sample is an equilibrium mixture. A CT is the temperature at which the calculated equilibrium molar abundance of

[2]The latest versions of programs SOLVGAS and GASWORKS, the GASTHERM thermochemical data base, and the accompanying manuals are now available for distribution. These are FORTRAN 77 programs and run on 80386- and 80486-level IBM-compatible personal computers, and also on IBM and VAX mainframe computers. They can be obtained for a small distribution cost from the senior author.

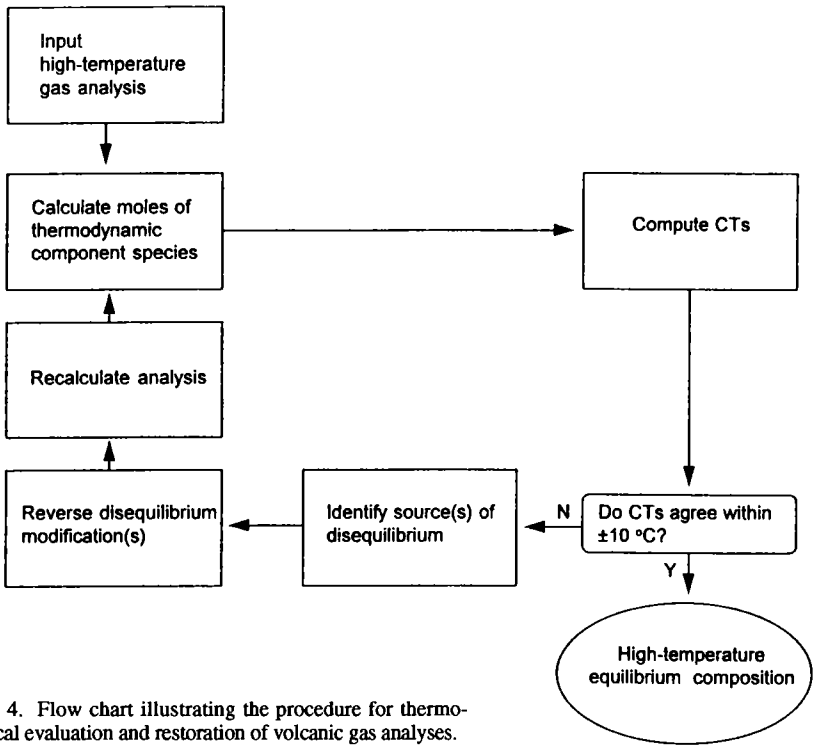

Figure 4. Flow chart illustrating the procedure for thermochemical evaluation and restoration of volcanic gas analyses.

species equals its measured molar abundance (Nordlie, 1971). If the CTs for all species agree within ±10°C, an acceptable limit for typical analytical error, the analysis is interpreted to be a quenched equilibrium composition (Gerlach, 1993b). If the CTs do not agree within ±10°C, the analysis is a disequilibrium composition.

Equilibrium-disequilibrium determinations normally include H_2O, CO_2, SO_2, H_2, H_2S, HCl, HF, and CO but exclude free O_2 and the amounts of N_2 and Ar indicated to be from air contamination. CH_4 and NH_3 are often excluded because they are almost always extraneous (see below). The analysis is recast in terms of thermodynamic component species, as shown in Table 1 for the August 11, 1960 sample from the A-1 vent at Showa-Shinzan (case without N_2, CH_4, and NH_3). SOLVGAS computes the distribution of gas species as a function of temperature using the mass balances of component species. In these calculations, only reactions between the selected analyzed species, H_2O, CO_2, H_2, HCl, HF, SO_2, CO, and H_2S in this case, are considered. Comparisons of the calculated moles of each species with the observed moles determine the CTs. We illustrate this graphically by plotting the logarithms of the calculated/observed moles versus temperature for each species, since this quantity equals zero at the CT but nonzero above and below the CT. The graphical (Fig. 5) and tabular (Table 1) results for the 1960 Showa-Shinzan sample show that the CTs for H_2O, H_2, SO_2, H_2S, CO_2, and CO converge at 735 ± 4°C. We do not report CTs for HCl and HF; their calculated and measured amounts are equal at all temperatures, since volcanic gases lack measurable amounts of other Cl- and F-bearing species that react with HCl and HF. The analysis is interpreted to be a quenched equilibrium composition because the divergence of CTs is less than ±10°C. If CTs diverge by more than ±10°C, the analysis is a disequilibrium composition, and the potential causes of disequilibrium are evaluated.

Table 1. Gas analysis, moles of component species, correspondence temperatures (CTs), and restored composition for the August 11, 1960 gas sample collected from the A-1 vent at Showa-Shinzan. The moles of component species are shown along with CTs are shown for cases with and without CH_4, NH_3, and N_2.

		With CH_4, NH_3, and N_2		Without CH_4, NH_3, and N_2		
Species	*Gas analysis† (moles)*	*Recast to component cpecies‡ (moles)*	*CTs (°C)*	*Recast to component cpecies‡ (moles)*	*CTs (°C)*	*Restored composition (moles)*
H_2O	99.39	99.41692	726	99.4176	739	99.39
CO_2	0.34	0.34074	903	0.34040	731	0.34
H_2	0.17	0.129835	720	0.12840	739	0.17
HCl	0.042	0.042	---	0.042	---	0.042
N_2	0.024	0.024025	194	---	---	---
HF	0.019	0.019	---	0.019	---	0.019
SO_2	0.014	---	740	---	739	0.014
H_2S	0.0008	0.0148	740	0.0148	739	0.0008
CO	0.00040	---	729	---	731	0.00040
CH_4	0.00034	---	210	---	---	6.4×10^{-12}
Ar	0.00016	---	---	---	---	---
O_2	0.0000	---	---	---	---	---
NH_3	0.00005	---	194	---	---	---
S_2	---	---	---	---	---	1.5×10^{-5}
log fO_2						-14.38
T(°C)	722 (obs)					735 (calc)

† Mizutani and Sugiura (1962)

‡ SO_2, CO, CH_4, and NH_3 are not component species, so they are re-expressed interms of the other species (see Symonds and Reed, 1993); Ar and O_2 are excluded.

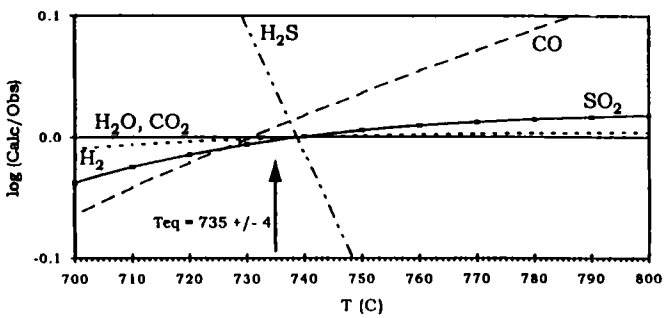

Figure 5. Log (calculated/observed) moles vs. temperature plot for a Showa-Shinzan gas sample collected by Mizutani and Sugiura (1982) from the A-1 vent, August 11, 1960. The CT for a species is the temperature at which the log (calculated/observed) moles equals zero. The plotted species are the only ones included in the calculations; we removed CH_4, NH_3,N_2, and O_2 from the original analysis before calculating the CTs. Note that the scales on the vertical axes conceal the tiny variations in the H_2O, CO_2, and N_2 lines.

Common causes of disequilibrium

There are many causes of disequilibrium in high-temperature volcanic-gas samples. Naturally occurring volatile compounds from non-magmatic sources (heated rock, hydrothermal systems, meteoric water, air, etc.) may contaminate a high-temperature gas initially at equilibrium and produce a disequilibrium mixture that never equilibrates fully

before collection. A variety of collection-related factors (poor sampling design, equipment failures, operator errors, etc.) may cause modifications of high-temperature equilibrium gas compositions and result in an analysis with a disequilibrium composition. Inadequate stabilization of a sample after collection (leakage, post-collection reactions, etc.) may give a similar result. Finally, analytical errors may result in a disequilibrium analytical composition.

Oxidation of H_2, H_2S, or CO. The main cause of disequilibrium is oxidation of H_2, H_2S, or CO by the reactions:

$$H_2 + 1/2\ O_2 = H_2O \quad (13)$$

$$H_2S + 3/2\ O_2 = SO_2 + H_2O \quad (14)$$

$$CO + 1/2\ O_2 = CO_2 \quad (15)$$

Atmospheric oxidation of one of these species is potentially significant if $(O_2)_r$ (Eqn. 12) is greater than the concentration of that species. Nonequilibrium oxidation of H_2 to H_2O produces low CTs for H_2O, H_2, SO_2, and H_2S but high CTs for CO_2 and CO, whereas disequilibrium oxidation of H_2S to SO_2 or CO to CO_2 produce high CTs for H_2O, H_2, SO_2, and H_2S but low CTs for CO_2 and CO (Table 2).

Gains or losses of H_2O. Common sources of disequilibrium related to gains/losses of H_2O include condensation of H_2O in the intake line (Gerlach, 1980b), spilling of solution from the sampling bottle (Gerlach, 1993b), analytical errors (Gerlach, 1980b), and contamination of magmatic gases with unequilibrated meteoric steam (Symonds and Mizutani, in prep.). Condensate will form in the intake line if the gas drops below the boiling point of H_2O. Formation of condensate during collection can give samples with disequilibrium compositions from H_2O loss. However, sometimes increased gas flow during collection will cause condensate to re-evaporate and the sample may show disequilibrium from gains in H_2O. Spilling of solution from sampling bottles is a common problem. The main effect of spilling is disequilibrium related to H_2O loss, since water is determined by difference (Gerlach, 1993b). Disequilibrium can also result from analytical errors in determinations of H_2O concentrations. For instance, the 1971 Erta'Ale gas analyses display disequilibrium and contain highly variable amounts of H_2O because water was determined by an inefficient analytical method (conversion of H_2O to acetylene by CaC_2; Giggenbach and Le Guern, 1976). The H_2O analytical errors in consecutive samples from the same vent over a short period of time produce large variations in H/C while C/S ratios are relatively constant (Fig. 6). When H_2O concentrations are determined by difference, they may contain significant error if the mass of sample collected is close to the analytical error of the balance. Contamination of volcanic gases with unequilibrated meteoric steam prior to collection is yet another potential source of disequilibrium from H_2O gains. In these cases, δD and $\delta^{18}O$ data for H_2O may be a great help diagnosing mixing of meteoric and magmatic gases (Mizutani and Sugiura, 1982; Taylor, 1986). Gain of unequilibrated H_2O will produce low CTs for H_2O, H_2, SO_2, and H_2S but high CTs for CO_2 and CO (Table 2). In contrast, loss of H_2O without re-equilibration will produce high CTs for H_2O, H_2, SO_2, and H_2S but low CTs for CO_2 and CO (Table 2).

Extraneous CH_4 and NH_3. In high-temperature volcanic gases, the CTs for CH_4 and NH_3 are typically much lower than the CTs for other significant species. Samples with NH_3 may also have low CTs for N_2 because it is the only significant nitrogen species that reacts with NH_3. The Showa-Shinzan sample reported in Table 1 is an example of a gas analysis that has much lower CTs for N_2, CH_4, and NH_3 than for H_2O, CO_2, H_2, H_2S, SO_2, and CO. Low CTs for N_2, CH_4, and NH_3 arise from the relatively high concentrations of CH_4 and NH_3 in these samples, since their predicted equilibrium concentrations increase with decreasing temperature. This extraneous CH_4 and NH_3

probably comes from deep hydrothermal (Giggenbach, 1987) or sedimentary (Kodosky et al., 1991; Symonds and Mizutani, in prep.) gases that mix with the high-temperature magmatic gases without equilibrating with them. Sometimes, $\delta^{13}C$ data may support a sedimentary origin for CH_4 (Kodosky et al., 1991). Unequilibrated CH_4, NH_3, and N_2 are generally removed from the analysis, and the CTs are recalculated (Table 2).

Table 2. Summary of common disequilibrium modifications of volcanic-gas samples and restoration procedures to correct them.

Modification	*Evidence*	*Restoration procedure*
Extraneous CH_4 in sample	1-2	Remove CH_4 from the analysis. See Gerlach and Casadevall (1986a) and Kodosky et al. (1991).
Gains of unequilibrated H_2O	3-5	Remove a trial amount of H_2O from analysis, renormalize adjusted analysis, and recalculate CTs. Repeat procedure until all CTs converge. See Gerlach (1980a,b).
Nonequilibrium H_2O loss	4, 6-7	Add a trial amount of H_2O to the original analysis, renormalize adjusted analysis, and recalculate CTs. Repeat procedure until all CTs converge. See Gerlach (1980b), Symonds et al. (1990), and Gerlach (1993b).
Nonequilibrium oxidation of CO to CO_2	6, 8, 9	Convert a trial amount of CO to CO_2 in the original analysis by reversing the reaction: $CO + 1/2O_2 \Rightarrow CO_2$, renormalize the adjusted analysis, and recalculate CTs. Repeat procedure until all CTs converge. See Gerlach and Casadevall (1986a).
Nonequilibrium oxidation of H_2 to H_2O	3, 8, 10	Convert a trial amount of H_2O to H_2 in the original analysis by reversing the reaction: $H_2 + 1/2O_2 \Rightarrow H_2O$, renormalize adjusted analysis, and recalculate CTs. Repeat procedure until all CTs converge. See Le Guern et al. (1982).
Nonequilibrium oxidation of H_2S to SO_2	6, 8, 11	Convert trial amounts of H_2S to SO_2 by reversing the reaction: $H_2S + 3/2O_2 \Rightarrow SO_2 + H_2O$, renormalize adjusted analysis, and recalculate CTs. Repeat procedure until all CTs converge. See Gerlach (1980a).
Gains of unequilibrated H_2	6, 12	If relatively minor, identify and reverse reaction that produces excess H_2, renormalize adjusted analysis, and recalculate CTs. If major, estimate equilibrium gas composition from the mass balances of C, H, and S in the analysis, and from independent estimates of fO_2. See Gerlach (1979. 1980c).

(1) Very low CTs for CH_4 relative to all other species. (2) $\delta^{13}C$ data may indicate a sedimentary source for CH_4. (3) Low CTs for H_2, H_2O, SO_2, and H_2S relative to CTs for CO_2 and CO. (4) Simultaneous samples from the same vent will have widely variable H/C and H/S ratios but relatively constant C/S ratios. (5) δD and $\delta^{18}O$ data for contemporaneous fumarolic condensates may indicate mixing between magmatic and meteoric fluids if the excess H_2O is from a meteoric source. (6) High CTs for H_2, H_2O, SO_2, and H_2S relative to CTs for CO_2 and CO. (7) NaOH solution may have spilled from sampling bottle during collection. (8) Samples may show evidence of air contamination (e.g., >1% N_2, $N_2/Ar \approx$ atmospheric value of 83.6). (9) Simultaneous samples from the same vent may show variable $CO/(CO + CO_2)$ ratios. (10) Simultaneous samples from the same vent may show variable $H_2/(H_2 + H_2O)$ ratios. (11) Simultaneous samples from the same vent may show variable $H_2S/(H_2S + SO_2)$ ratios. (12) Samples probably reacted with Cu, Al, steel, or Ti collection materials.

Gains of H_2. Samples collected prior to 1975 may show disequilibrium from excess H_2 generated by reactions of H_2O and HCl with Cu, Al, or steel sampling materials, as discussed above (Gerlach, 1979, 1980c). Today, samples containing excess H_2 are rare because most are collected with relatively unreactive silica or titanium sampling tubes. However, recent work by Giggenbach and Matsuo (1991) suggests that titanium can react with >400°C volcanic gases to generate H_2 by Reaction (7), especially if the gases contain significant HCl. The symptoms of H_2 gains are anomalously low fO_2 values (Gerlach, 1979) and high CTs for H_2O, H_2, SO_2, and H_2S but low CTs for CO_2 and CO (Table 2).

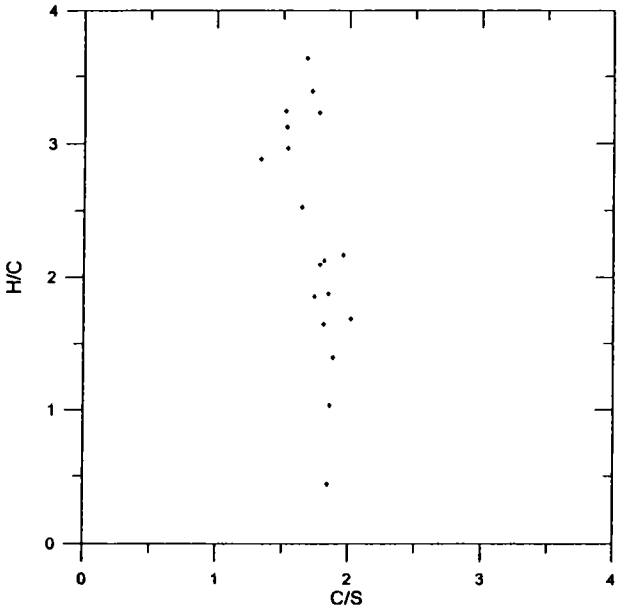

Figure 6. A plot of H/C versus C/S ratios for the 1971 Erta'Ale gas analyses from Giggenbach and Le Guern (1976). All samples were collected from a 1075°C vent over a two-hour period. H_2O errors cause H/C to vary over a wide range but do not affect C/S which is relatively constant (see text).

Retrieval of equilibrium compositions

We assume that high-temperature volcanic-gas samples with quenched equilibrium compositions represent better the volatiles degassed from shallow magma than do samples with disequilibrium compositions. It is therefore desirable to retrieve the initial equilibrium compositions of disequilibrium samples. Retrieval of equilibrium compositions is possible for some disequilibrium samples, but with varying degrees of reliability. If the samples have disequilibrium compositions caused predominantly by a single type of alteration or analytical error, as opposed to multiple or superimposed sources of disequilibrium, their equilibrium compositions often can be restored if the analyses are sufficiently complete (Gerlach and Casadevall, 1986a). Restoration makes no a priori assumptions of an initial equilibrium state but in fact tests the equilibrium hypothesis for high-temperature volcanic gases and yields the last equilibrium composition and temperature. "Restored equilibrium compositions" are considered about as reliable as quenched equilibrium compositions. "Apparent equilibrium compositions" are based on incomplete analyses and the assumption that the gases initially approached a state of chemical equilibrium (Gerlach and Casadevall, 1986a). Analytical data must be complete enough, however, to constrain both the last equilibrium temperature and the concentrations of the undetermined species. Apparent equilibrium compositions are less reliable than restored equilibrium compositions. "Estimated equilibrium compositions" are based on incomplete analyses and the assumption that the gases initially approached a state of chemical equilibrium (Gerlach and Casadevall, 1986a). However, for estimated compositions it is necessary to assume that the gases were in equilibrium at the collection temperature since the analytical data are insufficient for simultaneous determination of both the last equilibrium temperature and concentrations of the undetermined species. Estimated equilibrium compositions are the least reliable of the retrieved equilibrium compositions for high-temperature volcanic gases..

Removal of disequilibrium effects. There is a large body of literature (Gerlach 1979, 1980a-d, 1981, 1993a,b; Le Guern et al., 1982; Gerlach and Casadevall, 1986a; Symonds et al., 1990; Kodosky et al., 1991) that describes computer-based methods (e.g.,

using program SOLVGAS) for removing disequilibrium modifications from volcanic-gas analyses. These restoration procedures involve identifying the sources of disequilibrium, reversing their effects on the analytical data, recalculating the moles of component species, and recomputing the CTs to determine if the adjusted composition is closer to an equilibrium composition (Fig. 4). This process is repeated iteratively until all the CTs converge, or it is determined that a restored equilibrium composition cannot be obtained.

Table 2 summarizes the restoration procedures for the most common disequilibrium modifications of volcanic-gas analyses. For restorable samples that suffer from disequilibrium oxidation of H_2, H_2S, or CO, their restored equilibrium compositions are obtained by reversing Reactions (13), (14), or (15), respectively. For instance, if a sample suffers from disequilibrium oxidation of H_2, its restored equilibrium composition is obtained by converting the gained amount of H_2O to H_2 by reversing Reaction (13). This is done quickly on a computer by converting a trial amount of H_2O to H_2 in the original analysis, discarding the appropriate amount of oxygen, and recomputing the CTs. The procedure is repeated until the CTs converge to within ±10°C. Disequilibrium loss or gain of H_2O is treated in a similar fashion by adding or subtracting trial amounts of H_2O to/from the original analysis, depending on whether H_2O has been lost or gained, and computing CTs for the adjusted analysis. This process is repeated until the equilibrium amount of H_2O is found and the CTs converge.

Some gas analyses have multiple sources of disequilibrium. For instance, the 1974 Erta'Ale samples show evidence of gains or losses of H_2O, loss of sulfur due to reaction with the steel lead-in tubes, and atmospheric oxidation of reduced sulfur species (Gerlach, 1980b). Application of the numerical operations in Table 2 will eliminate only one source of disequilibrium so other methods must be used to remove multiple disequilibrium problems. One common approach is to estimate the last equilibrium composition using the analytical data for unmodified species and assume that the gas was last in equilibrium at the vent temperature (Gerlach, 1980a-c). For instance, Gerlach (1980b) obtains estimated equilibrium compositions for the 1974 Erta'Ale samples, all collected sequentially from the same vent, by the following steps: (1) compute the fO_2 of each sample at the vent temperature from equilibria (15) and analytical data for CO and CO_2, which show consistent CO/CO_2 values; (2) calculate the equilibrium amounts of H_2O for each sample from analytical data for H_2 and the computed fO_2 values; (3) add S to samples with relatively low S/C ratios; and (4) calculate the equilibrium distribution of S species from the computed fO_2 values and the mass balances for C, H, and S in each analysis.

Estimating concentrations of minor and trace species. Many volcanic gas analyses lack data minor and trace species such as COS, S_2, and magmatic O_2 and CH_4). Some of these species may be important in some high-temperature volcanic gases (COS, S_2, CH_4; Gerlach and Nordlie, 1975), and some define petrologically useful intensive parameters (fO_2, fS_2). The equilibrium amounts of COS, S_2, CH_4, and O_2 can be estimated from the following equilibria:

$$CO_2 + H_2S = COS + H_2O \quad (16)$$

$$2\,H_2S = 2\,H_2 + S_2 \quad (17)$$

$$CO_2 + 4\,H_2 = CH_4 + 2\,H_2O \quad (18)$$

$$2\,H_2O = 2\,H_2 + O_2 \quad (19)$$

combined with known equilibrium concentrations of H_2O, H_2, CO_2, and H_2S, and the following equations:

$$n_{COS} = \frac{(\phi_{CO_2} n_{CO_2})(\phi_{H_2S} n_{H_2S}) K_{15}}{\phi_{COS}(\phi_{H_2O} n_{H_2O})} \quad (20)$$

$$n_{S_2} = \frac{N(\phi_{H_2S} n_{H_2S})^2 K_{16}}{\phi_{S_2}(\phi_{H_2} n_{H_2})^2 P} \quad (21)$$

$$n_{CH_4} = \frac{P^2(\phi_{CO_2} n_{CO_2})(\phi_{H_2} n_{H_2})^4 K_{17}}{\phi_{CH_4}(\phi_{H_2O} n_{H_2O})^2 N^2} \quad (22)$$

$$n_{O_2} = \frac{N(\phi_{H_2O} n_{H_2O})^2 K_{18}}{\phi_{O_2}(\phi_{H_2} n_{H_2})^2 P} \quad (23)$$

where n_i is the molar abundance of species i, ϕ_i is the fugacity coefficient of species i, P is the pressure in atmospheres, N is the total moles of gas, and K_{16}, K_{17}, K_{18}, and K_{19} are the equilibrium constants for Reactions (16) through (19), respectively, at pressure P and at the equilibrium temperature of the sample. Since pressure is atmospheric in collection environments (Stevenson, 1993) and the gases can be assumed to be ideal, the P and ϕ_i terms equal unity. For example, to calculate the equilibrium amount of S_2, n_{S_2} is first estimated from (21) with the initial value of N taken as the total moles of gas species (without S_2). The estimate for n_{S_2} is added to the molar amounts of species to calculate an improved value for N, which in turn gives a better estimate of n_{S_2}. This process is repeated until n_{S_2} and N converge. The interactive procedure can be neglected if n_i for the undetermined species is many orders of magnitude smaller than N.

EQUILIBRIUM COMPOSITIONS OF HIGH-TEMPERATURE VOLCANIC GASES

In Tables 3-5, we compile the quenched, restored, apparent, and estimated equilibrium compositions of 136 high-temperature volcanic-gas samples from convergent-plate, divergent-plate, and hot-spot volcanoes (Tables 3-5). The tables include most published and some unpublished equilibrium compositions of >500°C volcanic gases. Table 6 lists additional sources of recent high-quality volcanic-gas data for samples collected at >500°C vents and that undoubtedly contain quenched and retrievable equilibrium compositions. Preliminary interpretation of these additional analyses suggests that they generally support our conclusions on volcanic gases as discussed below. Discussions of studies on <500°C volcanic gases are beyond the scope of this paper, since these low-temperature gases are less likely to contain significant amounts of magmatic volatiles.

Molecular compositions

For each sample in Tables 3-5, we report the 1-bar, mole% concentrations of H_2O, CO_2, SO_2, H_2, H_2S, and CO; many analyses also contain data for HCl and HF, and some include estimated amounts of S_2, COS, and SO. The tables also include the determined values for the equilibrium temperature and fO_2. The tables exclude data for minor amounts of N_2 and Ar that are available for many analyses because these species are often atmospheric in our compiled samples (e.g., Fig. 3).

H_2O, CO_2, and SO_2 are the dominant species in all samples. This is shown clearly in Figure 7 where all samples plot very close to the H_2O-XO_2 mixing line:

$$H_2O = 100 - XO_2 \quad (24)$$

where $XO_2 = SO_2 + CO_2$. Samples departing from the H_2O-XO_2 line have significant concentrations of one or more minor species, including H_2, H_2S, HCl, CO, and S_2. H_2 concentrations range from 0.01 to 3% H_2 (Tables 3-5), and are higher for higher temperatures (Fig. 1) and lower fO_2 values. The concentrations of H_2S and S_2 increase with rising amounts of total S, decreasing fO_2, and with decreasing temperature (Gerlach

Table 3. Equilibrium compositions, temperatures, and log fO_2 values of high-temperature and low-pressure (1 bar) volcanic gases from convergent-plate volcanoes. Concentrations of species reported in mole %; log fO_2 given as log bars.

Magma	Date	Number	T (°C)	log fO_2	H_2O	H_2	CO_2	CO	SO_2	H_2S	S_2	HCl	HF	COS	SO
Mount St. Augustine (Kodosky et al., 1991)															
andesite	7/79	79A3G	648	-17.54	97.23	0.381	1.90	0.0035	0.006	0.057	—	0.365	0.056	—	—
" "	" "	79A4Ga	746	-15.20	97.46	0.568	1.23	0.0053	0.171	0.326	—	0.157	<.003	—	—
" "	" "	79A4Gb	746	-15.37	97.41	0.690	1.12	0.0058	0.111	0.377	—	0.226	<.003	—	—
" "	" "	79A6G	721	-15.77	98.31	0.522	0.74	0.0026	0.045	0.128	—	0.239	<.003	—	—
Mount St. Augustine (Symonds et al., 1990)															
andesite	8/28/87	dome-2	870	-12.45	84.77	0.54	2.27	0.016	6.18	0.68	0.12	5.34	0.086	—	—
" "	" "	dome-3	" "	-12.59	83.91	0.63	2.40	0.020	5.72	1.00	0.20	6.04	0.086	—	—
Mount St. Augustine (Symonds, Gerlach, and Iven, unpublished)															
andesite	7/6/89	Spine-1A	743	-15.20	96.83	0.54	1.49	0.0060	0.22	0.38	—	0.51	0.025	—	—
" "	" "	Spine-1B	764	-14.71	96.80	0.56	1.59	0.0072	0.29	0.32	—	0.41	0.028	—	—
" "	" "	Spine-1C	744	-15.18	96.93	0.54	1.39	0.0056	0.21	0.34	—	0.56	0.034	—	—
" "	" "	Spine-1D	775	-14.46	96.73	0.56	1.50	0.0072	0.33	0.29	—	0.55	0.030	—	—
" "	" "	Spine-1E	752	-14.99	96.94	0.54	1.45	0.0061	0.25	0.34	—	0.45	0.030	—	—
Mount Etna (Huntingdon, 1973; Gerlach, 1979)															
hawaiite	7/12/70	horn. 1 #11	1075	-9.47	27.71	0.30	22.76	0.48	47.70	0.22	0.76	—	—	—	0.06
" "	7/12/70	" " #16A	" "	" "	47.10	0.51	23.42	0.49	27.96	0.22	0.26	—	—	—	0.04
" "	7/13/70	" " #8	" "	" "	46.91	0.50	22.87	0.48	28.70	0.22	0.28	—	—	—	0.04
" "	7/14/70	" " #13	" "	" "	44.59	0.48	22.23	0.46	31.61	0.24	0.33	—	—	—	0.04
" "	7/12/70	horn. 2 #10	" "	" "	47.26	0.51	26.06	0.54	25.18	0.20	0.21	—	—	—	0.03
" "	7/12/70	" " #17	" "	" "	46.80	0.50	24.55	0.51	27.14	0.21	0.25	—	—	—	0.03
" "	7/12/70	" " #14A	" "	" "	49.88	0.54	21.69	0.45	26.93	0.22	0.24	—	—	—	0.03
" "	7/12/70	" " #12A	" "	" "	53.69	0.57	20.00	0.42	24.85	0.22	0.21	—	—	—	0.03
" "	7/13/70	" " #5	" "	" "	49.33	0.53	24.32	0.51	24.86	0.20	0.21	—	—	—	0.03
" "	7/13/70	" " #7	" "	" "	43.09	0.46	24.00	0.50	31.34	0.23	0.33	—	—	—	0.04
" "	7/13/70	" " #6	" "	" "	49.91	0.54	23.56	0.49	25.05	0.21	0.21	—	—	—	0.03
" "	7/13/70	" " #9	" "	" "	48.27	0.52	19.71	0.41	30.48	0.25	0.31	—	—	—	0.04
" "	7/14/70	" " #15	" "	" "	47.82	0.51	17.08	0.36	33.54	0.27	0.38	—	—	—	0.04
" "	7/13/70	horn. 3 #1	" "	" "	49.50	0.53	33.58	0.70	15.45	0.13	0.08	—	—	—	0.02
" "	7/13/70	" " #4	" "	" "	49.91	0.54	33.93	0.71	14.69	0.12	0.07	—	—	—	0.02

Table 3 (continued)

Magma	Date	Number	T (°C)	log fO_2	H_2O	H_2	CO_2	CO	SO_2	H_2S	S_2	HCl	HF	COS	SO
Gunung Merapi (Le Guern et al., 1982)															
andesite	1978	Mer 78-1	826	-13.70	95.30	0.87	3.31	0.03	0.25	0.24	0.003	—	—	—	—
" "	" "	Mer 78-2	806	-14.01	94.53	0.74	4.08	0.03	0.31	0.30	0.004	—	—	—	—
" "	" "	Mer 78-3	820	-13.79	93.64	0.81	4.54	0.04	0.50	0.46	0.010	—	—	—	—
" "	" "	Mer 78-4	900	-12.69	91.04	1.44	5.19	0.10	1.07	1.08	0.070	—	—	—	—
" "	" "	Mer 78-5	767	-14.86	95.83	0.71	3.26	0.02	0.06	0.12	0.0003	—	—	—	—
" "	1979	Mer 79-1	895	-12.77	88.53	1.37	7.56	0.15	1.14	1.16	0.08	0.59	0.04	—	—
" "	" "	Mer 79-2	915	-12.49	88.87	1.54	7.07	0.16	1.15	1.12	0.08	0.59	0.04	—	—
Momotombo (Bernard, 1985)															
thol. basalt	12/80	MoMo-1	820	-13.55	97.11	0.70	1.44	0.0096	0.50	0.23	0.0003	2.89	0.259	—	—
" "	" "	MoMo-2	658	-16.52	97.90	0.17	1.47	0.0015	0.30	0.16	0.0009	2.68	0.240	—	—
" "	" "	MoMo-3	777	-14.35	97.30	0.50	1.44	0.0063	0.45	0.29	0.0040	2.86	0.256	—	—
Mount St Helens (Gerlach and Casadevall, 1986a)															
dacite	9/25/80	800925-710	802	-14.25	91.58	0.8542	6.942	0.06	0.2089	0.3553	0.0039	—	—	0.0008	—
" "	9/16/81	CNRS	663	-16.76	98.52	0.269	0.913	0.0013	0.073	0.137	0.0003	0.089	—	0.00002	—
" "	9/17/81	CNR	710	-15.77	98.6	0.39	0.886	0.0023	0.067	0.099	0.0002	0.076	0.03	1.8E-05	—
Poas (Delorme, 1983, Barquero, unpublished; Rowe, 1991)															
thol. basalt	6/17/81	P31	1002	-10.11	95.59	0.5997	0.8170	0.0083	1.877	0.0198	—	0.974	0.011	1.2E-06	—
" "	6/18/81	P35	1010	-9.96	96.12	0.5889	0.7042	0.0071	1.622	0.0140	—	0.814	0.098	7.3E-08	—
" "	6/18/81	P39	971	-10.53	96.04	0.5433	0.7289	0.0062	1.681	0.0224	—	0.874	0.102	1.1E-07	—
" "	6/19/81	P44	989	-10.20	96.29	0.5240	0.7768	0.0066	1.511	0.0131	—	0.784	0.091	7.1E-08	—
" "	6/28/81	P52	1007	-9.99	95.28	0.5639	0.9607	0.0093	2.004	0.0163	—	1.039	0.121	1.2E-07	—
" "	6/28/81	P53	991	-10.25	95.86	0.5776	0.8097	0.0077	1.721	0.0194	—	0.894	0.104	1.1E-07	—
" "	7/9/81	P60	965	-10.82	96.14	0.6659	0.7130	0.0073	1.535	0.4199	—	0.804	0.094	2.0E-07	—
" "	8/13/81	P61	1044	-9.46	96.54	0.6030	0.8930	0.0099	1.232	0.0065	—	0.638	0.074	4.6E-08	—
" "	8/13/81	P62	1045	-9.35	96.16	0.5416	0.9983	0.0100	1.450	0.0055	—	0.750	0.087	4.4E-08	—
" "	10/83	P10-83	960	-10.42	97.08	0.3859	0.5281	0.0031	1.988	0.0113	—	—	—	3.9E-08	—

Table 3 (continued)

Magma	Date	Number	T (°C)	log fO_2	H_2O	H_2	CO_2	CO	SO_2	H_2S	S_2	HCl	HF	COS	SO
Showa-Shinzan (Nemoto et al., 1957; Mizutani, 1962a; Mizutani and Sugiura, 1982; Symonds and Mizutani, in prep.)															
dacite	9/8/54	A-1 vent	1015	-9.93	98.04	0.63	1.2	0.0129	0.043	0.0004	2.6E-07	0.053	0.024	—	—
" "	8/7/57	" "	791	-13.17	99.32	0.2	0.39	0.00068	0.021	0.0005	1.2E-07	0.047	0.022	—	—
" "	8/13/58	" "	720	-14.72	99.39	0.16	0.38	0.0004	0.01	0.0008	1.0E-07	0.044	0.019	—	—
" "	7/7/59	" "	750	-14.06	99.28	0.18	0.47	0.00065	0.012	0.0007	9.2E-08	0.039	0.02	—	—
" "	8/11/60	" "	735	-14.38	99.41	0.17	0.34	0.0004	0.014	0.0008	1.5E-07	0.042	0.019	—	—
" "	8/5/61	" "	811	-12.89	99.37	0.24	0.24	0.00056	0.02	0.0006	1.4E-07	0.088	0.03	—	—
" "	8/7/62	" "	718	-14.82	99.58	0.17	0.12	0.00013	0.016	0.0014	3.4E-07	0.089	0.028	—	—
" "	8/7/63	" "	701	-15.22	99.59	0.16	0.12	0.00012	0.0082	0.0011	1.3E-07	0.092	0.029	—	—
" "	9/23/64	" "	728	-14.56	99.67	0.17	0.056	0.000065	0.0093	0.0007	8.4E-08	0.062	0.027	—	—
" "	10/5/73	" "	698	-14.98	99.81	0.11	0.019	0.000013	0.0084	0.0004	3.2E-08	0.036	0.016	—	—
" "	9/1/74	" "	645	-16.27	99.83	0.083	0.032	0.000012	0.008	0.0008	6.4E-08	0.035	0.014	—	—
" "	8/28/77	" "	799	-13.75	99.46	0.48	0.013	0.000056	0.008	0.0023	4.7E-07	0.027	0.011	—	—
" "	11/21/77	" "	619	-17.11	99.86	0.085	0.014	0.000005	0.0049	0.0012	7.2E-08	0.021	0.012	—	—
" "	10/8/78	" "	588	-17.85	99.88	0.06	0.022	0.000005	0.0055	0.0014	8.1E-08	0.019	0.01	—	—
" "	7/9/59	A-6A vent	656	-16.45	99.41	0.15	0.36	0.00027	0.0089	0.0037	5.6E-07	0.051	0.021	—	—
" "	8/13/60	" "	694	-15.24	99.49	0.13	0.29	0.00023	0.01	0.0009	1.1E-07	0.06	0.02	—	—
" "	8/5/57	C-2 vent	759	-14.1	99.11	0.24	0.5	0.00096	0.033	0.0033	1.7E-06	0.078	0.031	—	—
" "	8/10/58	" "	663	-16.12	99.49	0.13	0.3	0.0002	0.011	0.0024	3.8E-07	0.047	0.018	—	—
" "	7/1/59	" "	650	-16.58	99.33	0.14	0.43	0.00029	0.01	0.0043	7.5E-07	0.057	0.023	—	—
" "	8/9/60	" "	630	-17.41	99.24	0.18	0.44	0.00035	0.0065	0.0109	1.7E-06	0.09	0.028	—	—
" "	8/5/61	" "	640	-16.82	99.64	0.13	0.15	0.000089	0.0077	0.0035	4.4E-07	0.047	0.018	—	—
" "	8/5/62	" "	601	-18.09	99.7	0.13	0.1	0.000052	0.0046	0.01	1.1E-06	0.032	0.019	—	—
Usu (Matsuo et al., 1982; Gerlach, unpublished)															
dacite	9/1/79	11	659	-16.92	95.8	0.273	3.024	0.00440	0.258	0.609	0.0052	0.0241	0.0116	0.00032	—
" "	9/1/79	12	676	-16.58	96.1	0.329	2.641	0.00501	0.219	0.537	0.0042	0.160	0.0332	0.00026	—
" "	9/28/79	16	656	-17.20	96.1	0.342	2.613	0.00468	0.142	0.714	0.0042	0.105	0.0208	0.00031	—
" "	1/28/80	26	678	-16.45	97.3	0.303	1.696	0.0029	0.200	0.350	0.0022	0.160	—	0.00011	—
" "	1/28/80	27	667	-16.70	97.0	0.285	1.864	0.0029	0.226	0.461	0.0033	0.126	—	0.00015	—

--- not determined or below detection

Table 4. Equilibrium compositions, temperatures, and log fO_2 values of high-temperature and low-pressure (1 bar) volcanic gases from divergent-plate volcanoes.
Concentrations of species reported in mole %; log fO_2 given as log bars.

Magma	Date	Sample	T (°C)	log fO_2	H_2O	H_2	CO_2	CO	SO_2	H_2S	S_2	HCl	COS
Ardoukoba (Allard et al., 1979; Gerlach, 1981)													
thol. basalt	11/13/78	A89	1070	-10.17	78.71	1.73	3.78	0.16	12.94	1.57	1.07	—	—
" "	" "	A92	" "	" "	77.75	1.71	4.02	0.17	13.52	1.62	1.17	—	—
" "	" "	G82	" "	" "	76.05	1.68	3.39	0.14	15.38	1.80	1.51	—	—
Erta'Ale (Tazieff et al., 1972; Giggenbach and Le Guern, 1976; Gerlach, 1980b)													
thol. basalt	12/3/71	1032	1075	-10.12	69.41	1.57	17.16	0.75	9.46	1.02	0.59	—	0.02
" "	" "	1130	" "	" "	69.41	1.57	17.12	0.75	9.49	1.03	0.59	—	0.02
" "	" "	1131	" "	" "	69.45	1.57	17.92	0.79	8.77	0.95	0.50	—	0.02
" "	" "	1132	" "	" "	69.59	1.57	16.13	0.71	10.17	1.10	0.68	—	0.02
" "	" "	1133	" "	" "	69.60	1.57	17.58	0.77	8.93	0.97	0.52	—	0.02
" "	" "	1150	" "	" "	70.16	1.59	17.11	0.75	8.86	0.97	0.52	—	0.02
" "	" "	1151	" "	" "	68.36	1.55	18.88	0.83	8.87	0.94	0.52	—	0.02
" "	" "	1152	" "	" "	68.83	1.56	18.22	0.80	9.04	0.97	0.54	—	0.02
" "	" "	1153	" "	" "	70.88	1.60	17.47	0.77	7.95	0.88	0.41	—	0.01
" "	" "	1154	" "	" "	69.43	1.57	18.06	0.79	8.67	0.94	0.49	—	0.02
" "	" "	1155	" "	" "	68.72	1.55	18.81	0.83	8.63	0.92	0.49	—	0.02
" "	" "	1157	" "	" "	71.65	1.62	16.61	0.73	8.03	0.90	0.42	—	0.01
" "	" "	1214	" "	" "	69.55	1.57	18.10	0.80	8.53	0.92	0.48	—	0.01
" "	" "	1216	" "	" "	69.27	1.56	18.38	0.81	8.53	0.92	0.48	—	0.02
" "	" "	1224	" "	" "	69.99	1.58	17.93	0.79	8.31	0.91	0.45	—	0.02
" "	" "	1225	" "	" "	70.21	1.59	18.30	0.81	7.80	0.85	0.40	—	0.02
" "	" "	1226	" "	" "	66.99	1.51	18.57	0.82	10.29	1.07	0.70	—	0.02
" "	" "	1227	" "	" "	70.40	1.59	18.00	0.79	7.89	0.87	0.41	—	0.01
" "	1/23/74	910	1130	-9.16	77.24	1.39	11.26	0.44	8.34	0.68	0.21	0.42	—
" "	" "	911	" "	-9.29	76.05	1.57	12.52	0.56	7.59	0.93	0.31	" "	—
" "	" "	916	" "	-9.31	75.06	1.59	13.08	0.60	7.84	1.01	0.36	" "	—
" "	" "	920	" "	-9.21	78.28	1.48	10.92	0.45	7.51	0.72	0.21	" "	—
" "	" "	931	" "	-9.32	77.52	1.68	11.36	0.53	7.12	1.01	0.32	" "	—
" "	" "	932	" "	-9.32	76.52	1.66	11.94	0.56	7.46	1.05	0.35	" "	—
" "	" "	933	" "	-9.29	77.87	1.61	11.38	0.51	7.02	0.88	0.26	" "	—
" "	" "	934	" "	-9.25	77.47	1.53	11.51	0.49	7.47	0.82	0.25	" "	—
" "	" "	935	" "	-9.27	77.45	1.57	11.53	0.51	7.37	0.86	0.26	" "	—
" "	" "	936	" "	-9.36	78.19	1.76	11.22	0.55	6.46	1.05	0.31	" "	—
" "	" "	937	" "	-9.34	76.76	1.70	11.93	0.57	7.16	1.08	0.35	" "	—
Nyiragongo (Chaigneau et al., 1960; Gerlach, 1980d)													
nephelinite	1959	2	970	-12.0	43.50	1.29	48.55	2.20	2.02	1.72	0.62	—	0.09
" "	" "	12	1020	-11.3	45.90	1.59	45.44	2.72	2.30	1.41	0.55	—	0.08
" "	" "	13	960	-12.4	55.62	2.18	36.35	2.13	0.81	2.45	0.38	—	0.08
Surtsey (Sigvaldason and Elisson, 1968; Gerlach, 1980c)													
alk. basalt	10/15/64	12	1125	-9.80	81.13	2.80	9.29	0.69	4.12	0.89	0.25	—	—
" "	" "	13	" "	-9.78	81.98	2.77	9.79	0.71	3.15	0.64	0.13	—	—
" "	2/21/65	17	" "	-9.82	87.88	3.12	5.01	0.38	2.46	0.63	0.10	—	—
" "	" "	22	" "	-9.55	87.83	2.27	6.43	0.36	2.43	0.24	0.03	—	—
" "	" "	24	" "	-9.75	87.40	2.86	5.54	0.39	2.72	0.54	0.09	—	—
" "	3/31/67	29	" "	-9.11	91.11	1.42	3.31	0.11	2.81	0.06	0.01	—	—
" "	" "	30	" "	-9.30	92.47	1.79	1.21	0.05	3.27	0.14	0.02	—	—
" "	" "	31	" "	-9.27	92.46	1.74	1.31	0.05	3.74	0.15	0.02	—	—

--- not determined or below detection; HF and SO not determined in all samples

Table 5. Equilibrium compositions, temperatures, and log fO_2 values of high-temperature and low-pressure (1 bar) volcanic gases from hot-spot volcanoes. Concentrations of species reported in mole %; log fO_2 given aslog bars.

Magma	Date	Sample	T (°C)	log fO_2	H_2O	H_2	CO_2	CO	SO_2	H_2S	S_2	HCl	HF	COS
Kilauea Summit Lava Lake (Shepherd, 1921; Jaggar, 1940; Gerlach, 1980a)														
thol. basalt	3/25/18	J8	1170	-8.38	37.09	0.49	48.90	1.51	11.84	0.04	0.02	0.08	—	—
" "	3/13/19	J11	1100	-9.33	40.14	0.55	36.69	1.03	21.06	0.20	0.25	0.00	—	—
" "	3/15/19	J13	1175	-8.40	69.29	1.01	17.82	0.62	10.93	0.08	0.03	0.21	—	—
" "	3/16/19	J14	1100	-9.30	35.09	0.54	47.41	1.52	15.06	0.15	0.17	0.00	—	—
" "	3/17/19	J16	1140	-8.84	60.42	0.87	23.21	0.74	14.31	0.14	0.07	0.21	—	—
" "	" "	J17	1085	-9.65	65.95	1.02	20.27	0.62	11.44	0.32	0.16	0.17	—	—
" "	" "	J18	1185	-8.45	58.14	1.03	21.76	0.93	17.46	0.17	0.13	0.32	—	—
Kilauea East Rift Zone (Gerlach, 1993a)														
thol. basalt	1/14/83	Pele 9	1010	-10.49	79.8	0.9025	3.15	0.0592	14.9	0.622	0.309	0.1	0.19	0.0013
" "	" "	Pele 4	997	-10.76	81.6	0.9929	3.80	0.0702	12.0	0.761	0.358	0.171	0.20	0.0016
" "	" "	Pele 6	1016	-10.54	80.0	1.059	3.55	0.0804	13.7	0.875	0.445	0.153	0.12	0.0022
" "	1/15/83	Pele 12	935	-11.91	78.7	1.065	3.17	0.0584	11.5	3.21	1.89	0.167	0.20	0.0054
" "	" "	Pele 2	948	-11.55	78.5	0.9272	3.89	0.0594	13.4	1.70	1.12	0.148	0.19	0.0032
" "	" "	Pele 3	952	-11.41	80.7	0.8429	3.78	0.0617	12.5	1.32	0.540	0.162	0.17	0.0032
" "	" "	Pele 5	1003	-10.61	82.5	0.9370	3.56	0.0649	11.8	0.587	0.232	0.151	0.15	0.0013
" "	" "	Pele 7	1032	-10.19	80.4	0.9289	3.52	0.0784	14.0	0.511	0.197	0.174	0.19	0.0014
" "	1/16/83	Pele 8	979	-11.00	76.2	0.8655	3.35	0.0587	17.2	1.22	0.808	0.169	0.18	0.0026
" "	" "	Pele 10	980	-10.92	78.8	0.8246	3.00	0.0496	15.6	0.902	0.469	0.173	0.17	0.0017

— not determined or below detection; SO not determined in all samples.

Table 6. Sources of high-quality volcanic-gas analyses from >500°C vents not listed in Tables 3-5.

Volcano	*Tectonic setting*	*Date(s)*	*Reference*
Kilauea	Hot Spot	1960	Heald et al. (1963)
" "	" "	1980-83	Greenland (1987a)
Klyuchevskoy	Convergent Plate	1988	Taran et al. (1991)
Mauna Loa	Hot Spot	1984	Greenland (1987b)
Momotombo	Convergent Plate	1982-85	Menyailov et al. (1986)
Satsuma-Iwojima	Convergent Plate	1962-67	Matsuo et al. (1974)
" "	" "	1990	Shinohara et al. (1993)
Tolbachik	Convergent Plate	1975-76	Menyailov & Nikitina (1980)
Usu	Convergent Plate	1978-80	Matsuo et al. (1982)
" "	" "	1985	Giggenbach & Matsuo (1991)
White Island	Convergent Plate	1971-88	Giggenbach (1987); Giggenbach & Shepard (1989); Giggenbach & Matsuo (1991)

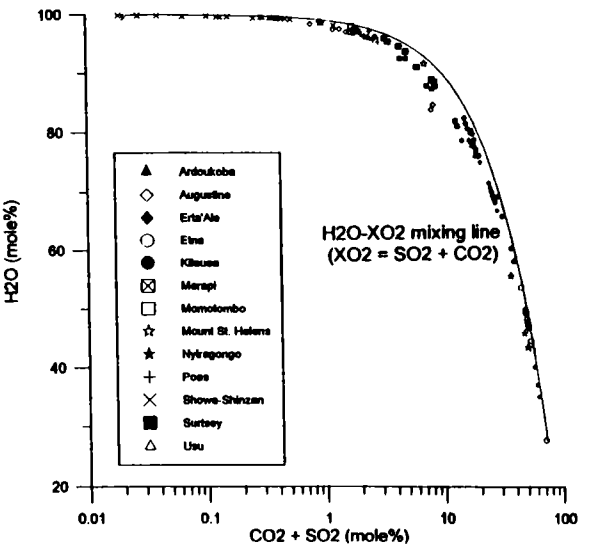

Figure 7. Concentrations of H_2O versus CO_2 + SO_2 for selected equilibrium volcanic–gas compositions. Most data lie close to the H_2O-XO_2 (XO_2 = CO_2 + SO_2) mixing line. Data from Tables 3,4,5. Filled symbols represent gases from divergent-plate and hot-spot volcanoes; others mark gases from convergent-plate volcanoes.

and Nordlie, 1975; Symonds et al., 1992), and are generally highest in samples from basalt (Tables 3-5). CO increases with temperature (Fig. 1) and total C (Gerlach and Nordlie, 1975), and is higher in samples from basalt (Tables 3-5). Samples from convergent plate volcanoes contain up to 6% HCl (e.g., Mount St. Augustine; Symonds et al., 1990; Kodosky et al., 1991).

Elemental compositions

Elemental compositions are calculated from the molar compositions in Tables 3-5 using the following equation (from Gerlach and Casadevall, 1986b):

$$e_j = \sum_{i=1}^{N} a_{ij} n_i \qquad (23)$$

where e_j is the total moles of element j per 100 moles of sample, a_{ij} is the number of moles of element j in a mole of species i, n_i is the mole% concentration of species i (Tables 3-5), and N is the total number of species. For example, 100 moles of Kilauea sample J8 (Table 5) contains 75.32 moles H, 160.08 moles O, 50.41 moles C, 11.92 moles S, and 0.08 moles Cl. The elemental compositions provide a data base for graphical comparison of all samples in Tables 3-5, as shown in Figures 8 to 12.

Figure 8 shows a H-C-S ternary plot based on the equilibrium compositions of samples in Tables 3-5. In general, samples from convergent-plate volcanoes have proportionally more H than samples from divergent-plate and hot-spot systems (Fig. 8) and consequently have higher H/S and H/C ratios than samples from divergent-plate and hot-spot volcanoes (Fig. 9). These characteristics reflect much higher H_2O concentrations in convergent-plate samples.

C and S are most enriched in samples from divergent-plate and hot-spot volcanoes and least enriched in samples from convergent-plate volcanoes (Fig. 8). Mount Etna, an enigmatic convergent-plate volcano, also discharges C- and S-rich gases, probably because its alkaline basalt magma comes from a gas-rich source. The most C-rich samples come from the 1959 Nyiragongo and 1918-19 Kilauea summit lava lakes, whereas the most

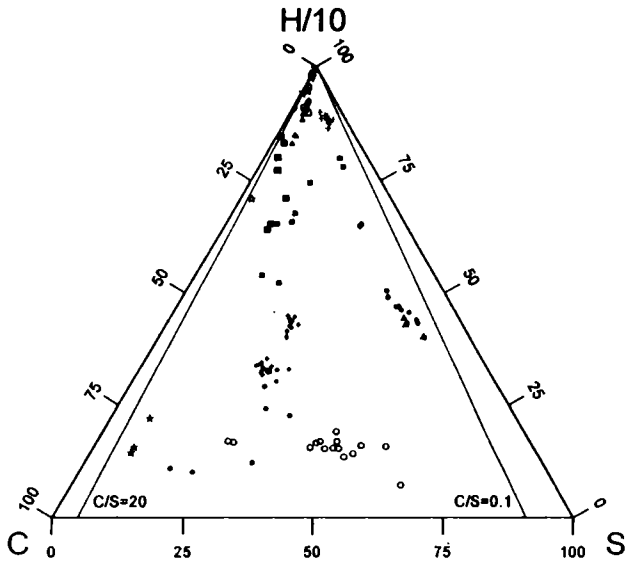

Figure 8. Ternary plot of atomic H/10, C, and S for equilibrium volcanic-gas compositions. Solid lines mark C/S ratios of 0.1 and 20. Symbol legends and data sources are listed in Figure 7.

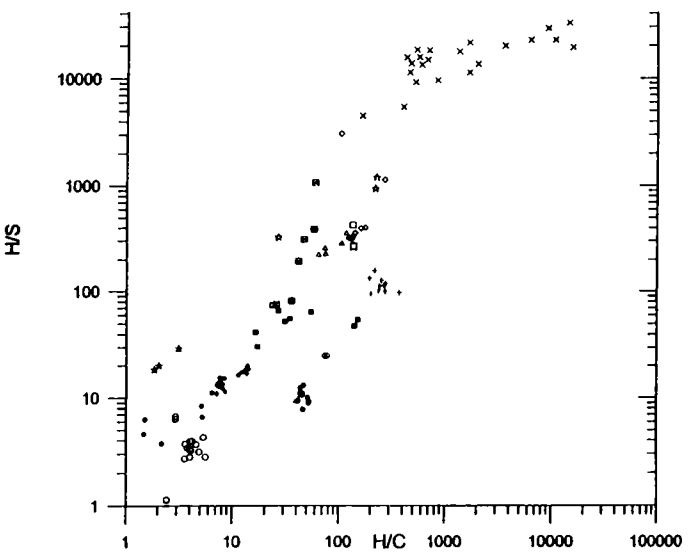

Figure 9. Atomic H/S versus H/C for selected equilibrium gas compositions. Symbols and data sources in Figure 7.

S-rich samples come from flank lava flows at Mount Etna and from the east rift of Kilauea (Fig. 8). The C/S ratios of samples from convergent-plate volcanoes and divergent-plate and hot-spot volcanoes are roughly similar (Fig. 10). C/S ratios of volcanic gases depend largely on the extent of degassing of the magma. For instance, at Kilauea the C/S ratios decrease from 4 for samples from relatively undegassed summit lava lakes to about 0.15 for samples from partially degassed lavas of a flank eruption along the east rift zone.

Compared to samples from divergent-plate and hot-spot volcanoes, samples from convergent-plate volcanoes contain higher proportion of Cl in the C-S-Cl system (Fig. 11). Cl/S is clearly much higher in samples from convergent-plate volcanoes where it ranges from 0.03 to 10 than in samples from divergent-plate and hot-spot volcanoes where it

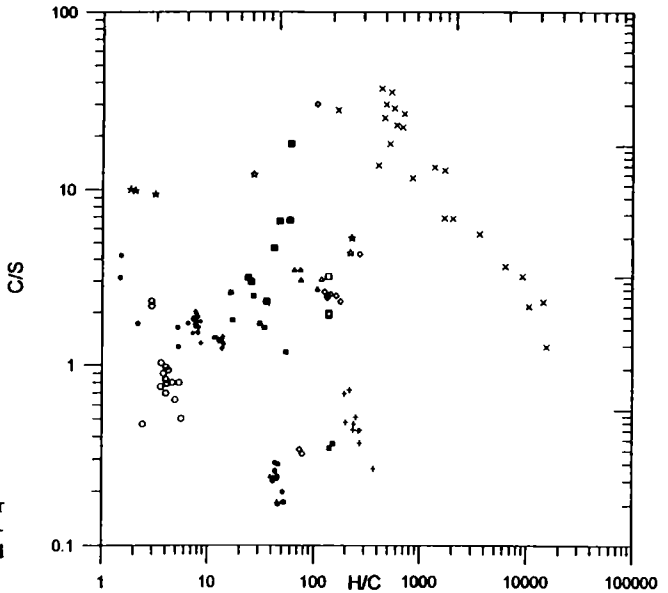

Figure 10. C/S versus H/C for selected equilibrium gas compositions. Symbol legends and data sources listed in Figure 7.

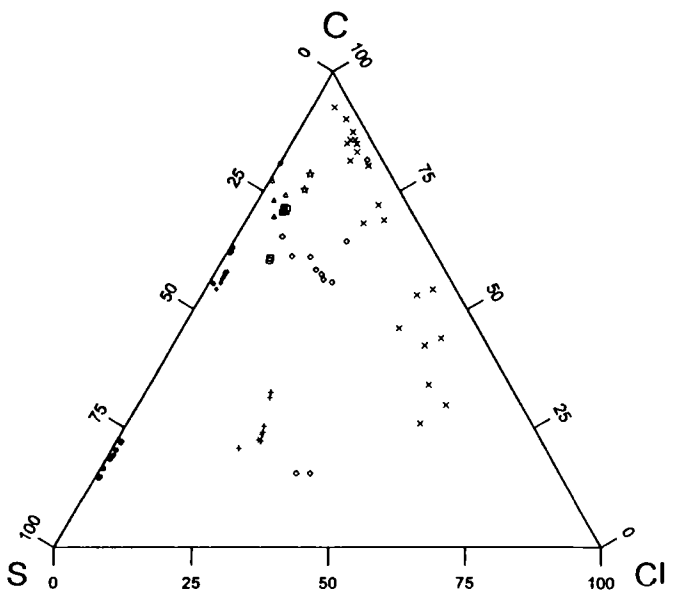

Figure 11. Ternary plot of atomic C, S, and Cl for equilibrium volcanic-gas compositions. Symbol legends, data sources listed in Figure 7.

ranges from 0.006 to 0.05. However, the Cl concentrations of divergent-plate and hot-spot volcanic gases are within the range of those for convergent plate volcanoes (Fig. 12).

The most likely explanation for the H_2O and Cl enrichments in convergent-plate gases (Figs. 8 and 11) is that their magmas are enriched in H_2O and Cl relative to hot-spot and divergent-plate magmas. This explanation accounts for the H_2O and Cl enrichments in convergent-plate gases for all magma types, it is consistent with the H_2O and Cl enrichments of subduction zone magmas, and it fits the modern conceptual tectonic

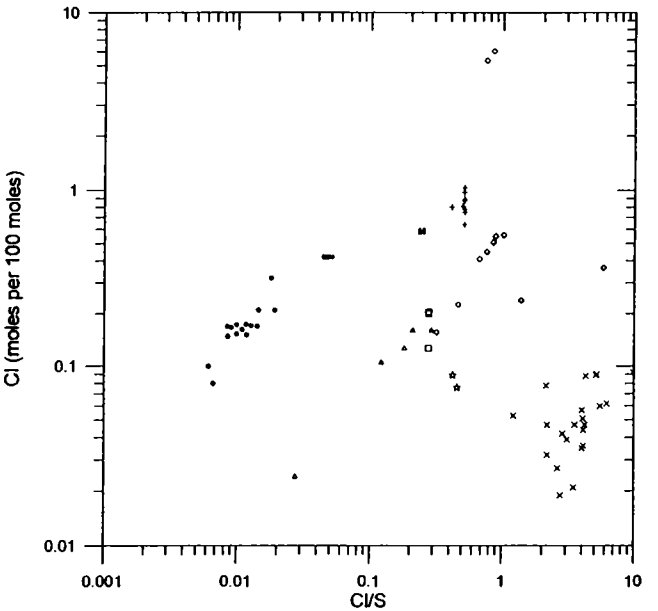

Figure 12. Atomic Cl versus Cl/S for selected equilibrium gas compositions. Symbol legends, data sources listed in Figure 7.

framework. Allard (1983) originally suggested that high-temperature gases from hot-spot and divergent-plate volcanoes contain mostly mantle-derived volatiles, whereas convergent-plate volcanoes discharge gases containing crustal and mantle components. Giggenbach (1992) used δD and $\delta^{18}O$ data of fumarolic condensates to argue that gas discharges from convergent-plate andesites contain subducted seawater. These observations are consistent with previous work (e.g., Gill, 1981; Ito et al., 1983; Stolper and Newman, 1994) which shows that magmas from convergent-plate volcanoes have higher pre-eruption H_2O and Cl contents (see Chapter 8). Subduction of hydrothermally altered oceanic slabs and sediments (e.g., Ito et al., 1983; Alt, 1994) beneath convergent-plate volcanoes is implicit in plate tectonic theory, and the subducted material provides an important source for volatiles associated with arc magmatism. Prograde metamorphic reactions in the oceanic crust and dewatering of the marine sediments drive H_2O, Cl, and other volatiles from the subducted slab into the overlying mantle wedge (e.g., Peacock, 1990), and these recycled volatiles enrich subduction zone magmas and their gas discharges (see Chapter 12 regarding volatile recycling).

Oxygen fugacities

The equilibrium fO_2 values of the samples are reported in Tables 3-5 and plotted as a function of inverse temperature in Figure 13. For comparison, Figure 13 shows that the calculated fO_2 values for the Mount St. Helens compositions (Table 3) are in excellent agreement with simultaneous in situ fO_2 measurements (Gerlach and Casadevall, 1986a). Similar agreement exists between equilibrium fO_2 values and simultaneous in situ fO_2 measurements at Merapi and Momotombo (Bernard, 1985). Simultaneous in situ fO_2 measurements are not available for samples from the other volcanoes.

Figure 13 shows that the fO_2 values lie between one log unit below quartz-fayalite-magnetite (QFM) to two log units above Ni-NiO (NNO), within the range expected for basic to silicic volcanic rocks (Carmichael, 1991). In general, the fO_2 values are broadly

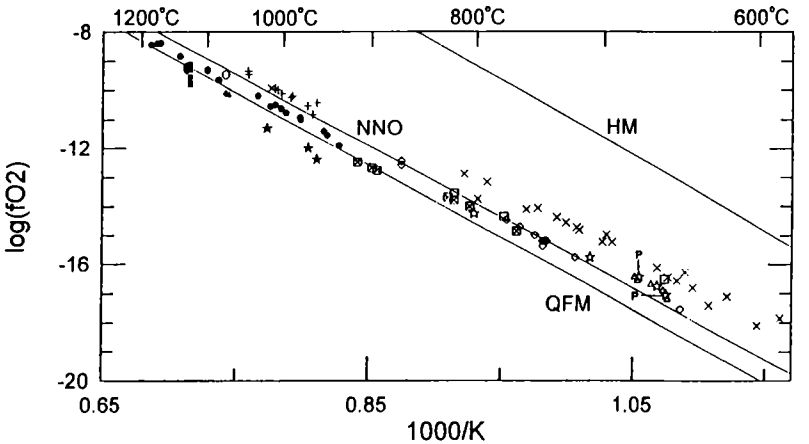

Figure 13. Plot of log fO_2 versus inverse temperature for selected equilibrium gas compositions (Tables 3-5). The quartz-fayalite-magnetite (QFM), Ni-NiO (NNO), and hematite-magnetite (HM) oxygen buffers are shown for reference. Symbol legends and data sources are listed in Figure 7. The plot also shows the September 16, 1981 oxygen fugacity probe data (P) for Mount St. Helens (Gerlach and Casadevall, 1986a).

similar to those expected for their respective lavas. For example, the fO_2's for Kilauea are within the range for Kilauea lavas (>1 log unit below to < 1 log unit above QFM; Carmichael, 1991); the fO_2's for Ardoukoba, Erta'Ale, and Surtsey, all divergent-plate basalts, are up to 1 log unit higher than the range for oceanic basalts (3 to <1 log units below QFM; Carmichael, 1991); the fO_2's for Merapi, Momotombo, and Poás are similar to those for other basaltic andesites (<1 log unit below to 1 log unit above NNO; Carmichael, 1991); the fO_2's for Augustine, Showa-Shinzan, and Usu are similar to other orthopyroxene-bearing silicic lavas (<1 log unit below to 1 log unit above NNO; Carmichael, 1991); and the fO_2's for Mount St. Helens are about 1 log unit below those for its hornblende-bearing dacite (Gerlach and Casadevall, 1986b). The general similarities between the fO_2's of the gases and their respective lava types suggests that lavas buffer fO_2 in high-temperature volcanic gases, although this has only been demonstrated at Kilauea (Gerlach, 1993a).

Pressure effects

To indicate the effects of pressure on gas compositions, we show the calculated equilibrium distribution of species from 1 to 100 bars for two gas samples: (1) sample 800925-710 from Mount St. Helens (Table 3) to represent SO_2-poor gases and (2) sample J8 from Kilauea (Table 5) to represent SO_2-rich gases. The calculations are done with program GASWORKS (Symonds and Reed, 1993) at the approximate magmatic temperatures of 1000° and 1170°C for Mount St. Helens and Kilauea, respectively (Gerlach and Casadevall, 1986b; Gerlach, 1980a). We treat the gases as ideal, which is reasonable for >600°C gas mixtures at < 500 bars (Holloway, 1977; Spycher and Reed, 1988), and consider only reactions between the most abundant species in the H-C-O-S system (H_2O, CO_2, H_2, SO_2, H_2S, CO, S_2, and COS); minor amounts of HCl and HF in these samples are neglected. The general effect of higher pressure is to increase H_2S, COS, and S_2, and to decrease SO_2, H_2, and CO (Fig. 14). The crossover between H_2S and SO_2 is at 18 bars for the Mount St. Helens case. A similar increase in H_2S is observed for the Kilauea case, but H_2 is not abundant enough in the J8 sample to cause H_2S to supersede SO_2 via Reaction (26). These pressure changes occur mostly in the first 50 bars and are the result

or volume effects that favor fewer moles of products than reactants in the following reactions (Gerlach and Casadevall, 1986b):

$$SO_2 + 3\ H_2 \Rightarrow H_2S + 2\ H_2O, \quad (26)$$

$$2\ H_2 + CO + SO_2 \Rightarrow 2\ H_2O + COS, \quad (27)$$

$$2\ H_2 + SO_2 \Rightarrow 2\ H_2O + 1/2\ S_2. \quad (28)$$

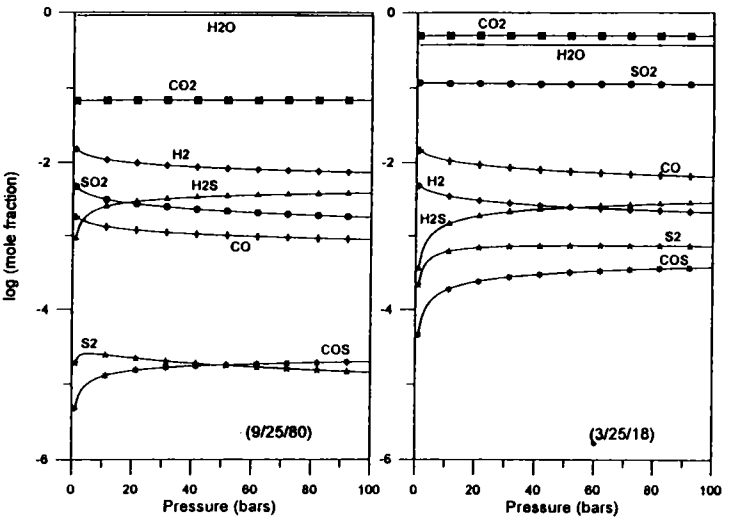

Figure 14. Calculated distribution of the most abundant species of H, O, C, and S as a function of pressure for (A) Mount St. Helens sample 800925-710 at 1000°C and (B) Kilauea sample J8 at 1170°C. Starting compositions at 1 bar pressure are tabulated in Tables 3-5.

SHALLOW MAGMA DEGASSING PROCESSES

Degassing at hot-spot and divergent-plate volcanoes

Kilauea volcano. Studies of high-temperature volcanic gases have contributed to understanding magma degassing processes at Kilauea volcano (Gerlach, 1980a, 1986, 1993a; Gerlach and Graeber, 1985; Greenland et al., 1985; Gerlach and Taylor, 1990). Sustained summit lava lake eruptions persisted at Kilauea during most of the previous century and on into the early 1920's and for brief periods in 1952 and 1967-1968. In essence, the roof of the summit magma chamber rose to the surface and a continuous resupply of magma sustained a lava lake at these times. Sustained summit lava lake eruptions emit relatively CO_2-rich, Type I volcanic gases (J series samples, Table 5, Fig. 15) directly to the atmosphere in a one-stage degassing process (Fig. 16a). The Type I gas samples (Table 5) plotted in Figure 15 include CO_2-rich samples like J-8, which was collected from a crack in a spatter cone adjacent to upwelling resupply magma, and several samples poorer in CO_2 that were emitted by partially degassed resupply magma at the margins of a summit lava lake.

Sustained summit lava lake eruptions have been comparatively uncommon in this century, when most eruptions have occurred along rift zones. The magma of rift zone eruptions is temporarily stored in the summit chamber prior to being discharged into the rift

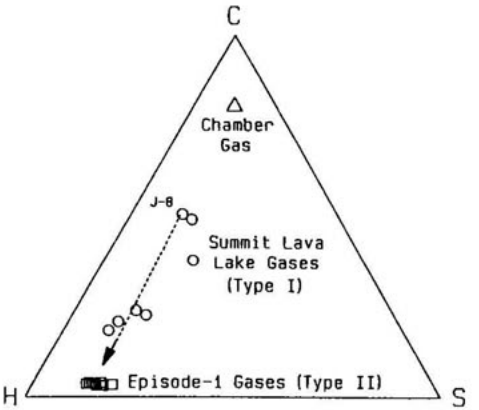

Figure 15. Ternary plot of C, H, and S for Type I volcanic gases (circles) from the 1918-19 summit lava lake (J-series samples in Table 5), Type II volcanic gases (squares) collected in 1983 from the east rift zone of Kilauea (Pele samples in Table 5), and the CO_2-rich summit Chamber Gas composition (triangle). The degassing vector originating at J-8 (Table 5) illustrates that the CO_2-depleted, Type II gases lie on a continuation of the trend formed by Type I gases from partially degassed summit lava lake resupply magma. [By permission of the editor of Geochimica et Cosmochimica Acta; Gerlach (1993a), Fig. 3, p. 799.

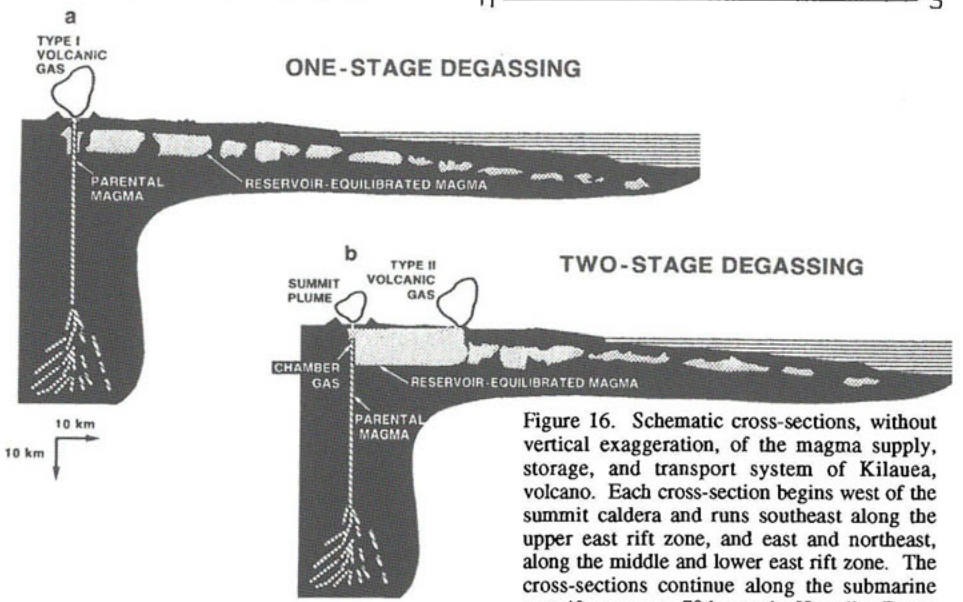

Figure 16. Schematic cross-sections, without vertical exaggeration, of the magma supply, storage, and transport system of Kilauea, volcano. Each cross-section begins west of the summit caldera and runs southeast along the upper east rift zone, and east and northeast, along the middle and lower east rift zone. The cross-sections continue along the submarine east rift zone out ~70 km to the Hawaiian Deep. For purposes of clarity the thickness of the feeder conduit for parental magma is greatly exaggerated and the summit chamber is somewhat enlarged. A plexus of dikes, sheets, and conduits is believed to constitute the summit chamber and east rift zone storage reservoirs shown schematically here as regions with high melt-to-rock ratios. (a) A one-stage degassing process during a continuously supplied summit lava lake eruption emitting Type I volcanic gases (J-series samples, Table 5, Fig. 15) derived from lava lake resupply magma. (b) A two-stage degassing process involving CO_2-rich chamber gas (Fig. 15) venting from new magma equilibrating in the summit reservoir and a rift zone eruption emitting type II volcanic gases (Pele samples, Table 5, Fig. 15) derived from summit reservoir-equilibrated magma. The chamber gas supplies volatiles to the summit hydrothermal system and to the summit fumaroles and plume. Eruptions of reservoir-equilibrated magma occur in the summit region and along the rift zone at subaerial and submarine sites. From Gerlach (1986).

zone complex (Fig. 16b). Equilibration and evolution of new magma injected into and temporarily stored in the summit chamber result in degassing of excess gas, which leads to the emission of a Chamber Gas containing >90% CO_2 (Fig. 15). Summit chamber degassing acts on all magma discharged into the reservoir system of the rift zone complex, and it is the first stage of a two-stage degassing process for magma that is subsequently erupted from the rift zone (Fig. 16b); the second stage occurs during the rift zone eruption

itself (Fig. 16b). Summit chamber degassing removes so much CO_2 that, compared to Type I gases, rift zone eruptions produce distinctly CO_2-depleted, Type II volcanic gases, such as the Pele samples (Table 5, Fig. 15). The compositions of Chamber, Type I, and Type II gases plotted in Figure 15 show that Type I and Type II gases differ from each other mainly by their CO_2 content, and that the latter gases lie on a continuation of the trend formed by Type I gases from the partially degassed resupply magma of a summit lava lake (Fig. 15).

Divergent-plate volcanoes. Similar degassing processes may be common at divergent-plate volcanoes (Gerlach, 1989a, 1989b). For instance, in the axial volcanic fields of the Afar depression, there are similar differences in the compositions of gas samples from the sustained summit lava lake of Erta'Ale volcano and samples from a fissure eruption at Ardoukoba on the Asal Rift in 1978 (Table 4, Fig. 8). In this case also, the summit lava lake and rift zone volcanic gases differ from each other mainly by their CO_2 content, which is higher in the summit lava lake gases (Type I) compared to the rift zone eruption gases (Type II) (Table 4, Fig. 8), suggesting again that the magma of the rift eruption at Ardoukoba underwent a two-stage degassing process with the first stage consisting of CO_2-rich chamber degassing during prior storage in a crustal magma reservoir. Finally, there is evidence to suggest that mid-oceanic ridge basalts undergo an analogous two-stage degassing process in which the first stage of degassing is the release of CO_2-rich gas from the ridge magma reservoirs that overlie the principal mantle sources of partial melt (Gerlach, 1989b).

Generalizations. Chamber degassing fractionates the volatiles in the magma supplied from the mantle to hot-spot and divergent-plate crustal magma chambers. In general, it probably operates largely on the basis of volatile solubility in basaltic melts, removing most of the CO_2 and heavier rare gases (Ar, Kr, Xe, Rn), much of the He and Ne, some sulfur, and minor amounts of water and halogens (see also Chapters 6, 7 and 8). Chamber degassing also may be an effective mechanism for fractionating stable isotopes of volatile elements — e.g., carbon isotopes (Gerlach and Taylor, 1990). Therefore, Type I volcanic gases better represent the volatiles of new magma from the mantle, whereas Type II gases reflect fractionation by chamber degassing during crustal storage. Chamber degassing of CO_2-rich gas is responsible for the tendency of volcanic gases from hot-spot and divergent-plate basalts to separate into a high C/S group and a low C/S group (Fig. 8). The high C/S group consists of Type I gases and show somewhat variable C/S (~1-4), possibly reflecting different mantle sources. The low C/S group includes the Type II gases, which have comparatively restricted C/S values near 0.3, perhaps reflecting equilibration to similar low pressure conditions in crustal magma chambers.

Degassing at convergent-plate volcanoes

There are several examples of time-series studies of the degassing of magma-hydrothermal systems at convergent-plate volcanoes. In addition to those considered below for Showa-Shinzan, Mount St. Helens, and White Island volcanoes, there are studies of time-series gas sampling available for Momotombo volcano, Nicaragua (Menyailov et al., 1986) and Vulcano, Italy (Tedesco et al., 1991; Magro and Pennisi, 1991).

Showa-Shinzan dome, Japan. The 31 years of gas data from Showa-Shinzan is currently the longest set of time-series data on high-temperature fumarolic emissions (Mizutani, 1962b, 1978; Mizutani and Sugiura, 1982; Symonds and Mizutani, in prep.). Showa-Shinzan is a dacitic lava dome that formed during the 1943-45 eruption of Usu volcano, Japan. High-temperature fumaroles on the dome were sampled from 1954 to

1985, during which the dome degassed, cooled, and was invaded by meteoric vapor. Samples collected from the A-1 fumarole, the hottest vent, in 1954-78 (Table 3) and in 1985 (Symonds and Mizutani, in prep.) best represent the temporal evolution of the discharged volatiles during the 31-year period.

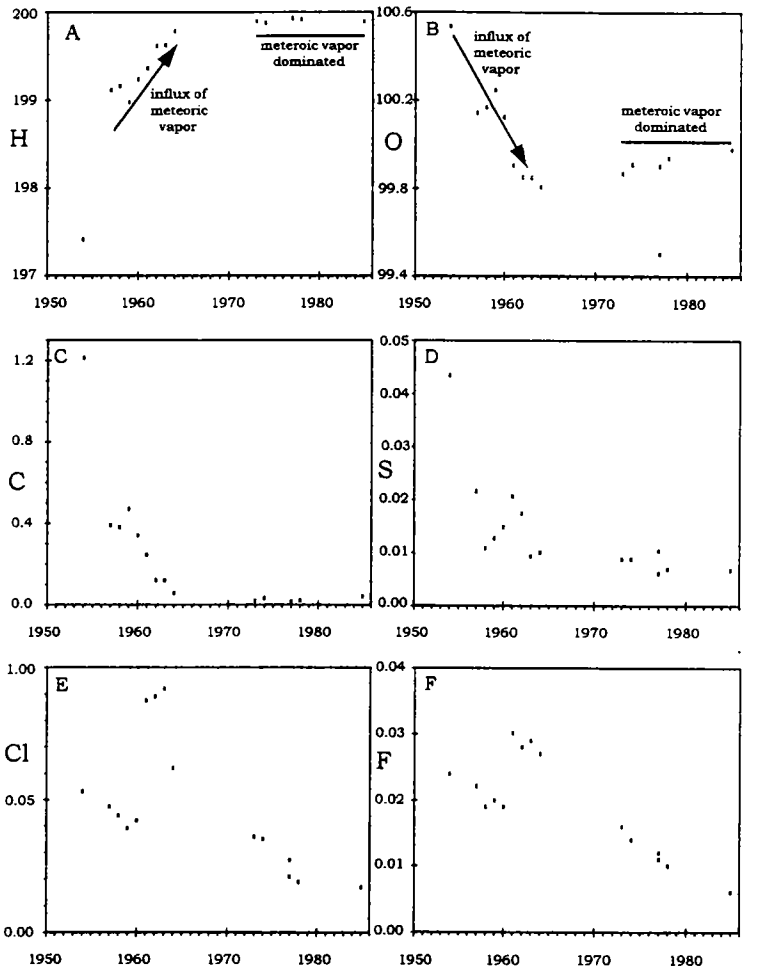

Figure 17. Plot showing moles of elemental hydrogen (A), oxygen (B), carbon (C), sulfur (D), chlorine (E), and fluorine (F) per 100 moles of gas for samples collected from the A-1 fumarole on Showa-Shinzan between 1954 and 1985 (Table 3). Arrows in (A-B) show schematically the inferred influx of meteoric H_2O into the A-1 gases from 1954 to 1964, whereas the solid lines in (A-B) mark the period from 1973 to 1985 when the A-1 gases were dominated by meteoric vapor.

Figure 17 shows the temporal evolution of elemental H, O, C, S, Cl, and F in the A-1 fumarole gases from 1954 to 1985. During this period, the equilibrium temperatures of the A-1 gases dropped from 1015 to 518°C. From 1954 to 1964 the A-1 gases became increasingly enriched in H but depleted in O, C, and S (Fig. 17A-D). After 1972, most samples contained >99.8% H_2O and contained nearly constant levels of H, O, C,

and S (Fig. 17A-D). As suggested by Mizutani and Sugiura (1982), these trends reflect the escalating amounts of meteoric H_2O in these samples, which is especially pronounced from 1954 to 1964. After 1964, the A-1 fumarole gases were dominated by meteoric vapor. In contrast, concentrations of atomic Cl and F generally decreased from 1954 to 1960, increased sharply between 1961 and 1964, and decreased after 1964 (Fig. 17E-F). The general decrease in Cl and F from 1954 to 1985 represents the overall meteoric-water-dilution trend. However, the sharp increase in Cl and F between 1961 and 1964 may represent a late-stage halogen release from the magma. In essence, Cl and F partition from the magma much later than C and S, and these late-stage halogens overprint the overall meteoric-water-dilution trend during the 1961-64 period. Figure 18B shows that the Cl/S ratio increased five-fold from 1954 to 1964. Over the same interval, the C/S ratio decreased by a factor of five (Fig. 18A). In contrast, the 1954-64 Cl/F ratios were relatively constant (Fig. 18C).

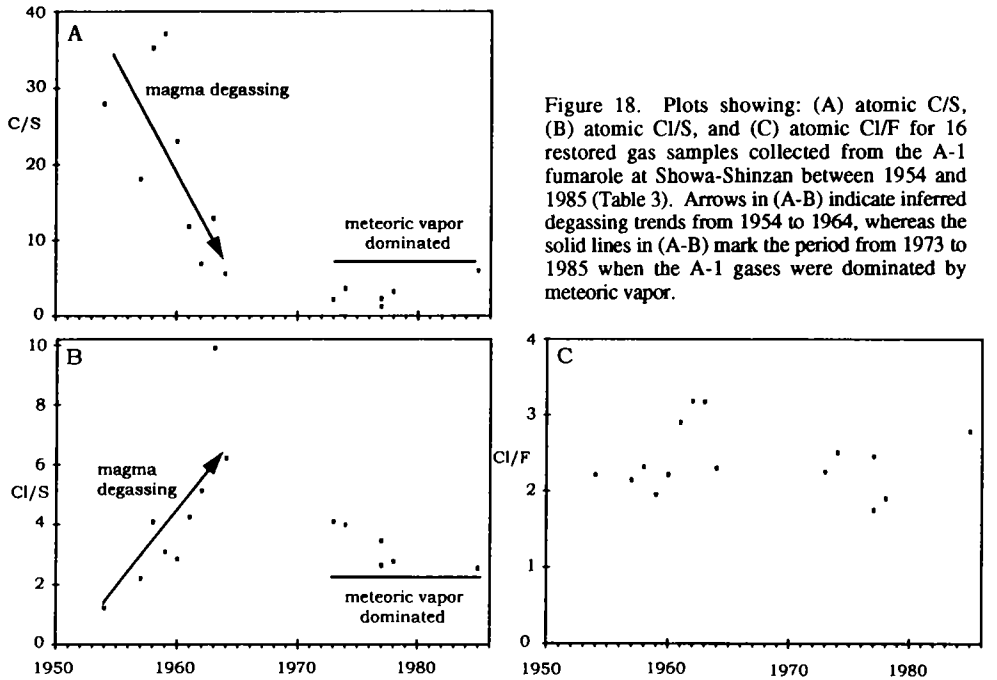

Figure 18. Plots showing: (A) atomic C/S, (B) atomic Cl/S, and (C) atomic Cl/F for 16 restored gas samples collected from the A-1 fumarole at Showa-Shinzan between 1954 and 1985 (Table 3). Arrows in (A-B) indicate inferred degassing trends from 1954 to 1964, whereas the solid lines in (A-B) mark the period from 1973 to 1985 when the A-1 gases were dominated by meteoric vapor.

The 1015° to 518°C temperature drop of the equilibrium A-1 gases from 1954 to 1985 caused ratios of H_2O/H_2, CO_2/CO, and H_2S/SO_2 to increase (Fig. 19), chiefly because the equilibrium amounts of H_2S increased while those of H_2, SO_2, and CO decreased (Fig. 1). These temperature-induced changes reflect right shifts in Reaction (26) and this reaction:

$$SO_2 + 3\,CO + H_2O = H_2S + CO_2 \qquad (29)$$

Mount St. Helens, U.S.A. The 1980-86 eruptions of Mount St. Helens provided an opportunity to study the evolution of gases discharging from a magma-hydrothermal system (Gerlach and Casadevall, 1986a,b). The volcano erupted explosively on 18 May 1980, followed by five smaller explosive eruptions in the summer of 1980 and the extrusion of a lava dome after the October 1980 explosive eruption. The dome grew by episodic exogenous and endogenous growth until 1986. Gases were collected from fumaroles on the crater floor and on the dome from September 1980 to September 1981 (Table 3; additional data in Gerlach and Casadevall, 1986a). Over this period, the H content of the

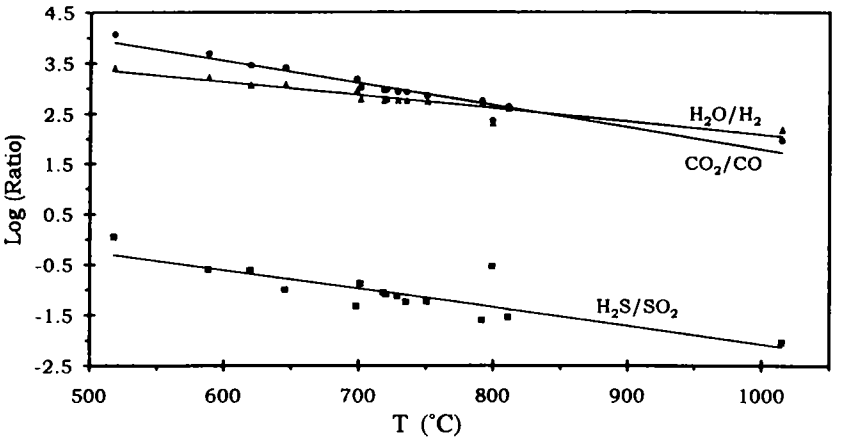

Figure 19. Plot showing ratios of H_2O/H_2 (triangles), CO_2/CO (circles), and H_2S/SO_2 (squares) as a function of temperature for the A-1 fumarole Showa-Shinzan gas samples (Table 3). Solid lines represent linear regression fits of the data. All correlation coefficients are significant at the 99% confidence level.

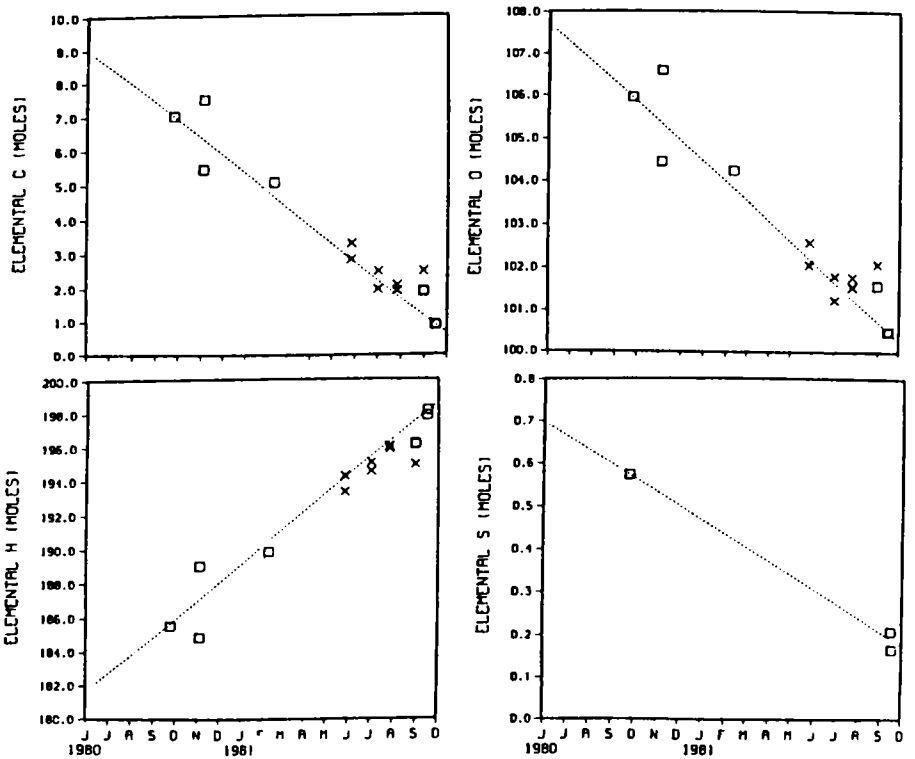

Figure 20. Elemental C, O, H, and S in moles per 100 moles of gas for 16 samples collected from Mount St. Helens, September 1980 to September 1981. The squares represent highest-quality restored and apparent compositions (Table 3) and Xs mark estimated compositions determined by Gerlach and Casadevall (1986a). The dashed line is the compositional trend for the 3 best samples reported in Table 3. [By permission of the editor of Journal of Volcanology and Geothermal Research; Gerlach and Casadevall (1986b), p. 150.]

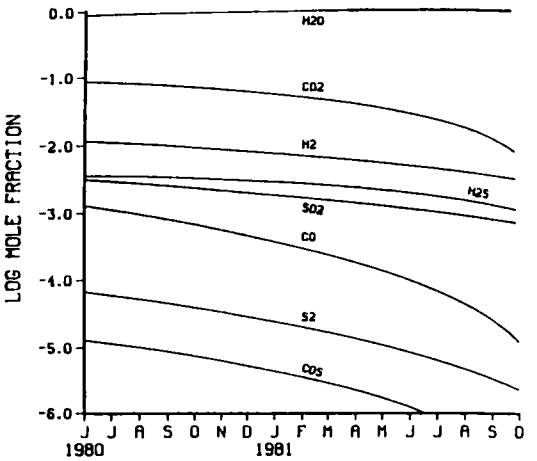

Figure 21. Equilibrium model of 1-atm fumarole gas compositions for Mount St. Helens between June 1980 and October 1981. [Used by permission of the editor of Journal of Volcanology and Geothermal Research, from Gerlach and Casadevall (1986b), Fig. 2, p. 152.]

gases increased linearly while the concentrations of C, O, and S decreased, also in a linear fashion (Fig. 20). These trends reflect the steady dilution of the magmatic gases by hydrothermal vapor over this time period. Estimates of the proportion of hydrothermal vapor in the Mount St. Helens gases range from 20 to 40% in June 1980 to 50 to 100% by October 1981. Like Showa-Shinzan, there are also temperature-related changes in the ratios of gas species. Linear changes in vent temperature and atomic compositions of fumarolic gases between September 1980 and September 1981 were used to constrain a 1-atm equilibrium model of the gases between June 1980 and October 1981 (Fig. 21).

White Island, New Zealand. White Island, an active andesitic-dacitiv volcano at the northeastern end of the Taupo volcanic zone, has emitted fumarolic gases for at least the past 150 years (Cole and Nairn, 1975). Regular fumarole gas sampling (about 2 samples per year from 6 to 10 fumaroles) commenced in 1971 and continues to the present day (Giggenbach and Sheppard, 1989). Over this time period, eruptions occurred in July 1971, between December 1976 and January 1982, and between December 1983 and February 1984. Between 1971 and 1984, samples from the Donald Mound fumarole, consistently the hottest vent, display cyclical variations in concentrations of HCl, H_2, SO_2, and H_2S that increase and decrease with fumarole temperature, although the decreases in H_2S during periods of lower temperatures are much larger than the corresponding decreases in SO_2 (Fig. 22). The concentration of CO_2 also varies with temperature, but somewhat less than the other gases (Fig. 22). Giggenbach and Sheppard (1989) suggest that fluctuating inputs of magmatic gas into the subvolcanic system trigger movements in the inferred subsurface brines (Fig. 23) that may account for the variations in gas compositions from the Donald Mound fumaroles. During periods of high magmatic-gas output between late 1982 until early 1983, magmatic gases vented freely from the magma to the Donald Mound fumaroles (Fig. 23). However, during periods of low magmatic gas flux, brines, inferred from the intermittent occurrence of highly mineralized acidic springs, invade the vapor-only zone (Fig. 23) and absorb HCl, SO_2, and other condensable gases. H_2S also decreases during the low-temperature periods, probably a consequence of subsurface precipitation and loss of native S. Subsequent reheating evaporates the brines and deposits sulfur, releasing some of the previously absorbed volatiles and sometimes producing higher-than-magmatic concentrations of HCl and total S. CO_2 probably fluctuates less than the HCl and SO_2 because it is less soluble in the brine (see below).

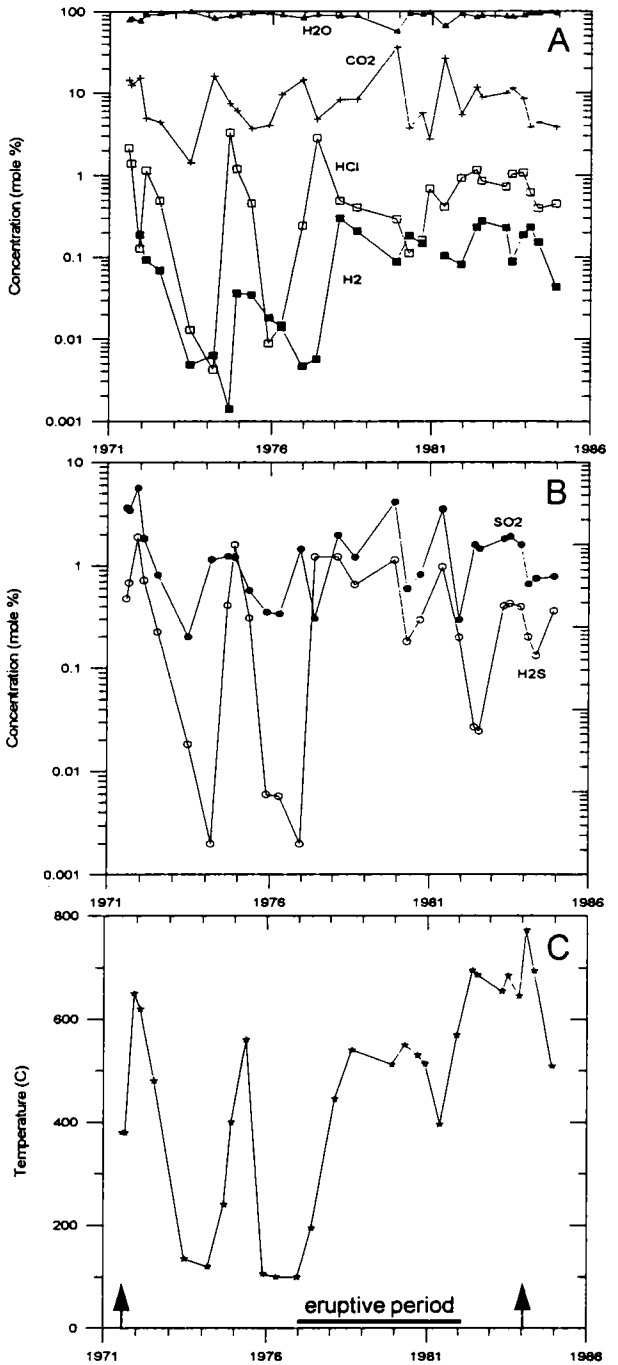

Figure 22. Temporal evolution of discharges from the hottest Donald Mound fumarole on White Island volcano from 1971 to 1984. Diagram shows the temporal evolution of

(A) H_2O, CO_2, HCl, and H_2;

(B) SO_2 and H_2S; and

(C) temperature.

Arrows mark short eruptive episodes in July 1971 and between December 1983 and February 1984; bar marks December 1976 to January 1982 eruptive period. All data from Giggenbach and Sheppard (1989). Total S and its oxidation state, n, recalculated as SO_2 and H_2S, assuming they are the dominant species, using the equations described by Giggenbach and Goguel (1989; p. 49); when n exceeded 4.0, we assigned an arbitrary value of 0.002 mole % for the concentration of H_2S. H_2 data unavailable for samples collected on July 29 and August 26, 1971, and on December 2, 1980.

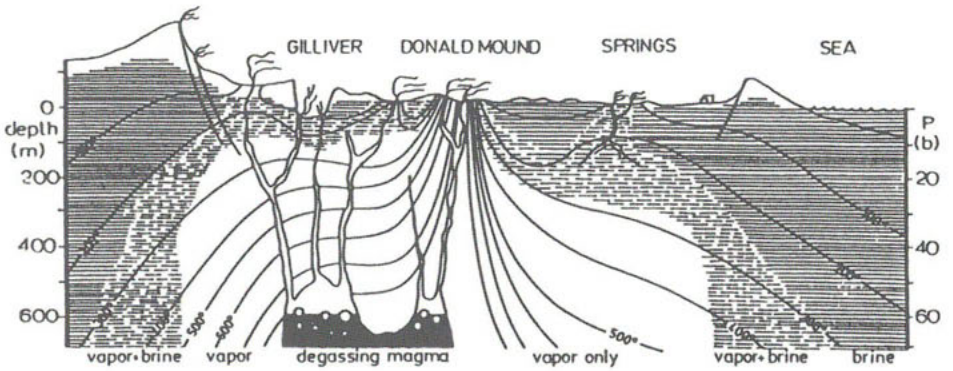

Figure 23. Schematic cross-section across the White Island crater showing inferred locations, relative to Donald Mound, of degassing magma, vapor-only zone, vapor-plus-brine zone, and brine-only zone for the high-temperature periods in 1972 and 1975. Diagram from Giggenbach and Sheppard (1989).

Gas/lava interactions during degassing

It is commonly assumed that, after discharging from magma, volcanic gases maintain homogeneous equilibrium with falling temperature until they quench. A test of this assumption with ten high-temperature gas samples (Pele samples, Table 5) reveals a more complex process for gases emitted from an erupting fissure in 1983 on the east rift zone of Kilauea (Gerlach, 1993a). The Pele analyses have log fO_2 values that fall on a tight linear trend ($r^2 = 0.982$) as a function of reciprocal (last equilibrium) temperature (Fig. 24a). Regression of the data yields the following equation:

$$\log fO_2 = -26{,}410\ (1/T) + 10.06 \qquad (29)$$

where fO_2 is in bars and T is in Kelvin; the equation is valid from 935 to 1032°C. Values of log fH_2, log fCO, log fS_2, log fH_2S, log fCl_2, and log fF_2 also follow linear trends as a function of reciprocal (last equilibrium) temperature (Fig. 24b-g). It can be shown that these linear trends do not represent the intrinsic closed-system trends expected if the gases maintained homogeneous equilibrium during cooling. Numerical simulation of closed-system (homogeneous equilibrium) cooling of each sample from high temperature to the last equilibrium temperature produces trends that depart from the observed linear trends for all species, except for F_2 (Fig. 24a-g). Open-system cooling involving oxygen transfer between the major gas species (H_2O, CO_2, SO_2) and lava, however, is consistent with the observed linear log fO_2-versus-reciprocal-temperature trend. Numerical simulations show, moreover, that the gas/lava oxygen transfer required to constrain log fO_2 by equation (29) during open-system cooling also produces the observed linear trends of all minor and trace species (Fig. 24a-g). Mass balance calculations suggest that redox reactions between the gas and ferrous/ferric iron in the lava are plausible mechanisms for the oxygen transfer. Oxygen transfer during cooling is variable—probably reflecting fluctuating rates of gas flow. Higher flow rates reduce the time available for gas/lava oxygen exchange and result in gases with higher last equilibrium temperatures; lower flow rates favor oxygen transfer down to lower temperatures. Gas/lava exchanges of other components (C,H,S) apparently are relatively insignificant during cooling; thus, multicomponent gas/lava heterogeneous equilibrium is not realized. Samples of higher-temperature—up to 1185°C—CO_2-rich volcanic gases from sustained summit lava lake eruptions (J-series samples, Table 5) also show buffering by gas/lava oxygen transfer. The two data sets give a tightly constrained log fO_2—relative to the nickel-nickel oxide (NNO) buffer—of NNO - 0.5(±0.05) for subaerially erupted Kilauea basalt from liquidus to solidus temperatures (Fig. 13). Thus,

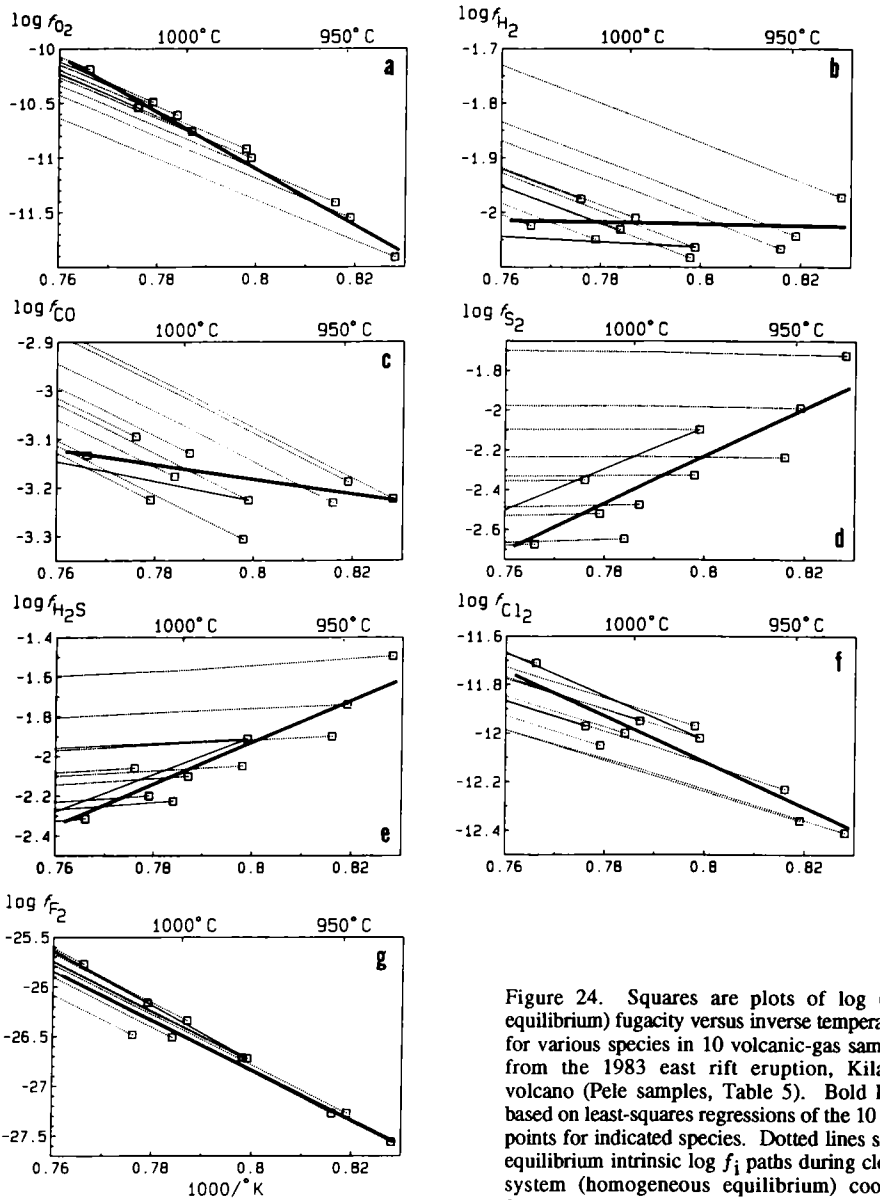

Figure 24. Squares are plots of log (last equilibrium) fugacity versus inverse temperature for various species in 10 volcanic-gas samples from the 1983 east rift eruption, Kilauea volcano (Pele samples, Table 5). Bold lines based on least-squares regressions of the 10 data points for indicated species. Dotted lines show equilibrium intrinsic log f_i paths during closed system (homogeneous equilibrium) cooling from high temperatures to the last equilibrium temperatures. Solid lines in b-g show examples based on Pele 8 of log f_i paths during open system (heterogeneous equilibrium) cooling with gas/lava oxygen transfer to constrain fO_2 by equation (29). All other samples also give open system curves parallel to the bold regression curves; to keep b-g legible, only the Pele 8 open system curve is shown. [Used by permission of the editor of Geochimica et Cosmochimica Acta, from Gerlach (1993a), Fig. 4, p. 800.]

the chemical equilibrium preserved in the Kilauea gas samples is a heterogeneous equilibrium involving gas/lava exchange of only oxygen, and the last equilibrium temperature is the temperature at which this exchange ceased. Preservation of this last

equilibrium in the samples suggests that homogeneous reaction rates within the gas phase were slow compared to the time it took the gases to move from the last site of gas/lava equilibration to the site of collection. These findings contrast with the commonly held assumption that volcanic gases are released from lava in a state of chemical equilibrium and then continue equilibrating homogeneously with falling temperature until they quench. Although volcanic gases may often reflect closed-system equilibrium during cooling (Giggenbach, 1987), open system gas/lava equilibration may not be uncommon.

Trace-element vapor transport and deposition during degassing

Another use of high-temperature equilibrium compositions of volcanic gases is to constrain thermochemical models of the origin, transport, and deposition of trace elements in volcanic gases. In addition to H_2O, CO_2, SO_2, H_2, H_2S, HCl, HF, CO, S_2, and COS, high-temperature volcanic gases contain myriad trace elements (e.g., Na, Cu) that are transported as volatile species (e.g., NaCl, CuCl) or eroded-rock aerosols (Symonds et al., 1987, 1992; Quisefit et al., 1989). The volatile trace elements are of considerable interest for their atmospheric impacts (Buat-Ménard and Arnold, 1978), the origin of incrustations (colorful deposits that include both sublimates, precipitated directly from the gas, and solids that form by other processes) around volcanic vents (Stoiber and Rose, 1974), and their implications for the origin of some types of ore deposits (Krauskopf, 1957, 1964; Symonds et al., 1987; Bernard et al., 1990). Multicomponent chemical equilibrium calculations can help unravel the origin and transport of these trace elements, and help determine the origin of fumarolic incrustations. Central to this approach are tests for equilibrium between the volcanic gases (major and minor gases, trace elements) and the magma, sublimates, incrustations, and aerosols. Evidence for equilibrium among the major gases lends credence to thermochemical equilibrium calculations for trace elements.

Model results suggest that most trace elements in volcanic gases are degassed from magma as simple chlorides (e.g., $ZnCl_2$, KCl, AgCl) and other species (e.g., AsS, Hg, H_2MoO_4, H_2BO_3, H_2Se), and that the speciation of each volatile element depends on the bulk gas composition (Symonds et al., 1987, 1992; Quisefit et al., 1989; Symonds and Reed, 1993). The models also predict that Al, Ca, Mg, and other non-volatile rock-forming elements exist primarily as eroded-rock aerosols rather than volatile species in volcanic gases (Quisifit et al., 1989; Symonds et al., 1992; Symonds and Reed, 1993). A third result is that volcanic sublimates generally precipitate in the order of their equilibrium saturation temperatures, which explains the overall zoning of sublimates in volcanic fumaroles (Symonds et al., 1987; Quisefit et al., 1989; Symonds and Reed, 1993). However, textures of volcanic sublimates indicate that this is a quasi-equilibrium process, whereby the gas starts precipitating sublimates at their equilibrium saturation temperature but fails to maintain equilibrium with the precipitating sublimates at cooler temperatures (Symonds, 1993). A final result is that volcanic incrustations form by complex processes involving direct precipitation of sublimates from cooling volcanic gases, and reactions between volcanic gases, wall rock, and air (Getahun et al., 1994).

REMOTE SENSING OF GAS EMISSIONS

In addition to direct sampling, volcanic gases can be studied remotely by airborne and ground-based instruments and by satellite. Remote sensing offers great advantages in volcanic-gas work: 1. *Safety*, a point that cannot be overemphasized since the tragedy at Galeras, which occurred during attempts by scientists to collect direct gas samples at a central vent (Williams, 1993). Erebus Volcano in the Antarctic is another example of a volcano which has an open vent and plenty of active surficial degassing, but direct

sampling is apparently impossible because of human-safety concerns. 2. *Expediency.* In other cases sampling is not done because suitable sites cannot be found free of substantial contamination of the gas by groundwater or the atmosphere. In these cases remote sensing measurements can often produce useful data. 3. *Gives flux data.* Remote sensing can determine fluxes of species whereas direct gas sampling alone cannot (see Chapter 12). 4. *Instantaneous analysis.* Remote sensing can determine concentrations or fluxes instantaneously in situ, rather than requiring transport (and reaction) of the samples between the sampling point and the laboratory. 5. *Potential economic advantages.* The opportunity for repetitive measurements of gas emissions at many or most volcanoes from satellite platforms exists as more extensive satellite based systems are developed. Since a satellite platform can potentially service many volcanoes, it could become a cost effective way to monitor volcanoes regularly and economically. 6. *Broad potential capability for many gas species.* It can in theory at least be applied to many gas species, and also to various types of particles or aerosols. This advantage is far from realized, however.

In spite of these advantages, remote sensing techniques have not been applied very widely at volcanoes. This is because of limited knowledge of the appropriate techniques, limited budgets for fieldwork at volcanoes, a lack of equipment suited for field work under the rugged field conditions, and the operational difficulties associated with the volcano/atmosphere interface.

Table 7. The ten most common volcanic gas species in volcanic plumes.

Column 1	Column 2	Column 3	Column 4
Species	*Estimated volcanic contribution to highly diluted plume*	*Ambient tropospheric concentration*	*Mixed plume concentration*
H_2O	10 - 20 ppm	40 - 40,000 ppm	40 - 40,000 ppm
CO_2	0.5 - 10 ppm	~ 300 ppm	301 - 310 ppm
SO_2	1 - 2 ppm	0.1 - 70 ppb	1 - 2 ppm
HCl	0.1 - 2 ppm	~ 1 ppb	0.1 - 2 ppm
H_2S	100 - 500 ppb	0.08 - 24 ppb	100 - 500 ppb
S_2	10 - 80 ppb	?	?
H_2	5 - 40 ppb	540 - 810 ppb	545 - 850 ppb
HF	5 - 40 ppb	?	?
CO	1 - 20 ppb	0.05 - 0.2 ppm	51 - 220 ppb
SiF_4	1 - 5 ppb	?	?

Data are based upon homogeneous gas calculations (Symonds and Reed, 1993) and direct gas sampling at high temperature fumaroles. Dilution factors are constrained by direct data (Lazrus et al., 1979; Rose et al, 1980; Friend et al., 1982; Casadevall et al., 1984; Rose et al., 1985, 1988) which demonstrate factors of 10^4 to 10^5. Near vent concentrations may be higher due to lower dilution ratios. Plumes are assumed to have an SO_2 concentration of 1 to 2 ppm (Casadevall et al., 1981; Harris et al., 1981; Rose et al., 1985) for comparison with other species. Species ambient atmospheric levels are from Graedel (1978) and Schidlowski (1986). Column 4 = Column 2 + Column 3. From Andres and Rose (1994).

One way of describing the volcano/atmosphere interface is to compare the concentrations of various chemical species in volcanic gases with the background concentrations in the atmosphere (Table 7). Remote sensing is done from a distance and requires looking through the atmosphere at a gas emission plume. It is obviously more advantageous to make measurements when the concentration of the constituent in question is significantly above the background atmospheric concentrations. The two most abundant gas species in volcanic gases, H_2O and CO_2, are also found in the ambient atmosphere at

significant concentrations. This partly explains why remote sensing of volcanoes is at a primitive level. The remote sensing of CO_2, for example, requires detecting and mapping a 1 to 5 ppm anomaly in a 300 ppm background, and doing it through a background that is usually many times the width of the plume. The lack of contrast between the plume and the atmosphere is influenced by the dilution of the volcanic plume by the atmosphere, generally by factors of 1000 to 100,000 or more (Rose et al., 1980), by the time that the remote sensor is applied. This happens within the first seconds of emission to the atmosphere, and means that volcanic plumes ingest large amounts of air and transport it upward. Only volcanic-gas species such as SO_2, which has a very low atmospheric background concentration, can be easily outlined in a plume by remote sensing. Examples of plume-concentration anomalies of SO_2 are shown in Figure 25.

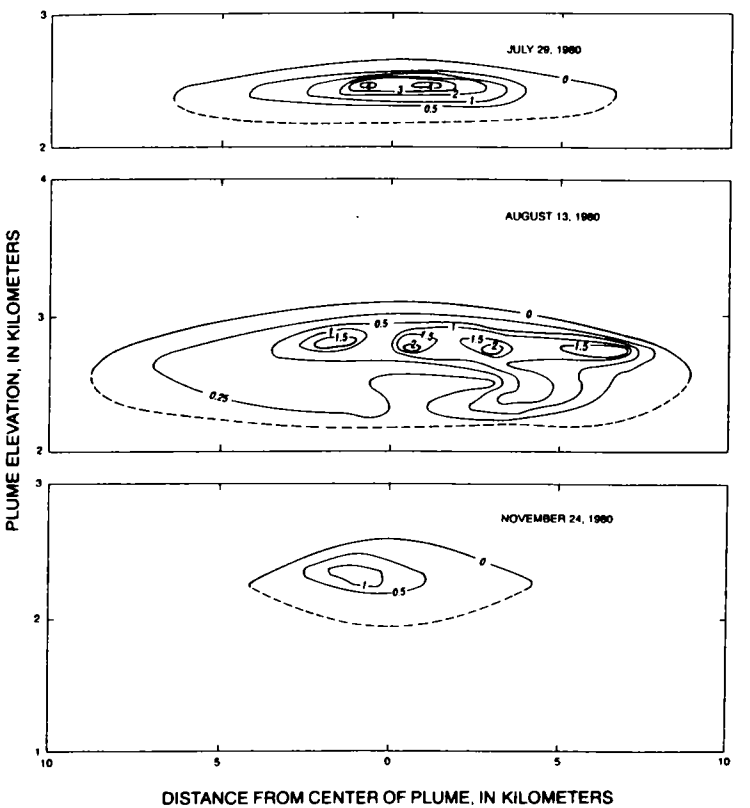

Figure 25. Interpretive cross-sections of SO_2 concentrations (ppm by volume) for three plumes from Mount St. Helens in 1980. Based on COSPEC traverses at 5 to 7 different altitudes in a fixed-wing aircraft. These demonstrate the relatively dilute nature of volcanic plumes. For comparison, undiluted gas leaving the magma in June 1980 contained ~0.3 mole % SO_2 (Gerlach and Casadevall, 1986b), so the plumes shown are diluted by factors of ~1000 to 12,000 at ambient pressures. [Used by permission of the editor of Journal of Volcanology and Geothermal Research; McGee (1992), Fig. 8, p. 280.]

The concentration of any volcanic-gas constituent can easily be overwhelmed by the atmosphere unless its abundance in volcanic gases greatly exceeds its ambient atmospheric concentration. Also if there is a gradient of concentration of some species in the atmosphere such that it decreases in concentration with altitude, a common situation for H_2O and CO_2, then ingestion of air at the base of the plume will result in a contrast

between the plume and the surrounding atmosphere that will overwhelm and mask the volcanic component. On a typical summer day in temperate climates there is a higher H_2O content in air closer to the Earth's surface. Because a rising volcanic plume ingests large amounts of air at its base, the plume will be full of water vapor from the atmosphere. Any volcanic H_2O is swamped by atmospheric water vapor. Ingestion of lower altitude air can thus greatly complicate the utility of remote sensing, whether it is ground based or from an airborne or satellite platform. (see also Woods, 1993).

CORRELATION SPECTROMETER DETERMINATION OF SO_2 EMISSIONS

Instrumentation and methods

Of the three most abundant species in volcanic gases, H_2O, CO_2 and SO_2 , the remote determination of SO_2 has enjoyed the greatest progress, mainly because of atmospheric problems discussed above with respect to H_2O and CO_2. Beginning in about 1971, an ultraviolet correlation spectrometer (COSPEC, made by Barringer, of Canada), which uses skylight as an ultraviolet source (Millán and Hoff, 1978) has been used at many volcanoes to measure the flux of SO_2 (Stoiber and Jepsen, 1973). This instrument has become a standard tool to make measurements at open-vent volcanoes (Stoiber et al., 1983), and a growing list of data sets has accumulated (see Andres et al., 1993; 1994). In all, the instrument has been used at approximately 50 volcanoes, far more than any similar measurement, and has been used as a tool to estimate the total SO_2 degassing to Earth's atmosphere from volcanoes (Berresheim and Jaschke, 1983; Stoiber et al., 1987). The COSPEC can be used in a number of ways. It can operate in an airplane, from an automobile or a boat, and also from a fixed point on a tripod. In general it works best when it is within a kilometer or two of the gas plume, because attenuation from a long path (>5 km) or from dust or aerosol is significant (Rose et al., 1985). At many volcanoes, aircraft measurements are the highest quality, but the cost of aircraft platforms is frequently too high to allow continuous measurements. The environmental conditions of each volcano (location of the active vent with respect to roads, atmospheric clarity, wind patterns, interfering SO_2 sources) dictate the way the COSPEC is used at each volcano, and the frequency of measurements reflects these as well as the resources of the local volcano observatory. The instrument cannot be used in low-light conditions (night, early morning or late evening in the tropics, anytime during high latitude winters). There are typically significant concentrations of aerosols in volcanic plumes (Fig. 26) and the attenuation effects of these aerosols on the COSPEC results are not well known. Also the signal can be saturated by thick plumes with high SO_2 burdens (Casadevall, 1985). The variety of possible styles of data collection (Fig. 27) reflect the environmental conditions as well as the scientific objectives of the measurements and the type of platform used. Sometimes, especially in aircraft surveys, only a few scans of the plume are made, whereas in other cases hundreds of data scans at intervals of minutes or even seconds are made (see Fig. 27H). There is interest in the interpretation of both long-term and short-term data sequences which measure fluxes of SO_2 at volcanoes (Table 8).

An important factor that influences the quality of data collected by COSPECs is the necessity of measuring the wind speed that is moving the plume or the rise speed of the plume. This is true because the COSPEC looks at a single angular path and is generally used to measure a transect across the plume, either horizontal or vertical, and this burden must be multiplied by a plume movement speed to get a flux (Stoiber et al., 1983). It has been shown by COSPEC users that uncertainty in the plume movement speed is usually the largest source of error in individual flux measurements, and that the high uncertainties (usually 20 to 50%) associated with COSPEC-determined fluxes are largely due to

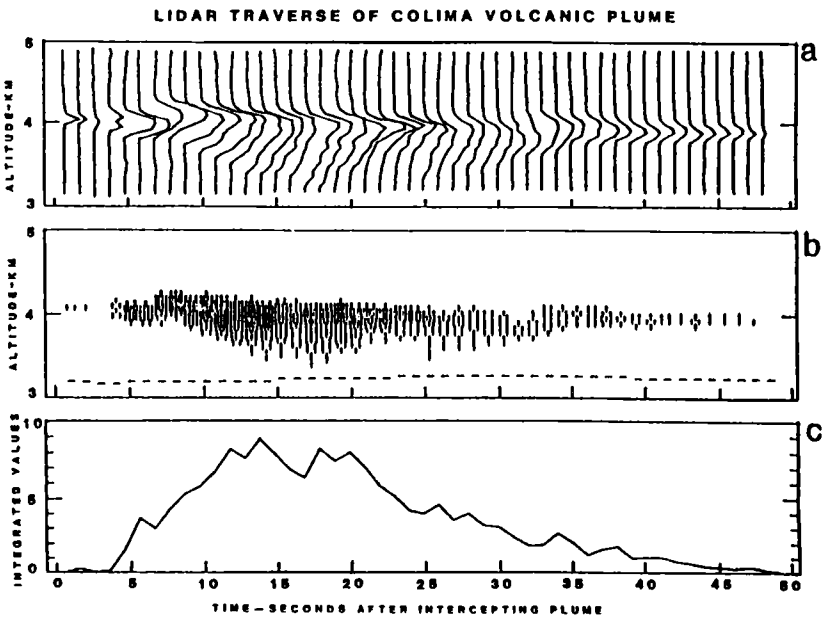

Figure 26. Lidar data collected on a traverse of a plume from Colima Volcano in February 1982 (Casadevall et al., 1984). This aircraft survey also did a COSPEC-based plume flux determination of 320 t/d, and the SO_2 absorption signal matched the lidar record in the traverses, which showed that aerosols in the plume tracked with the SO_2 in this case.

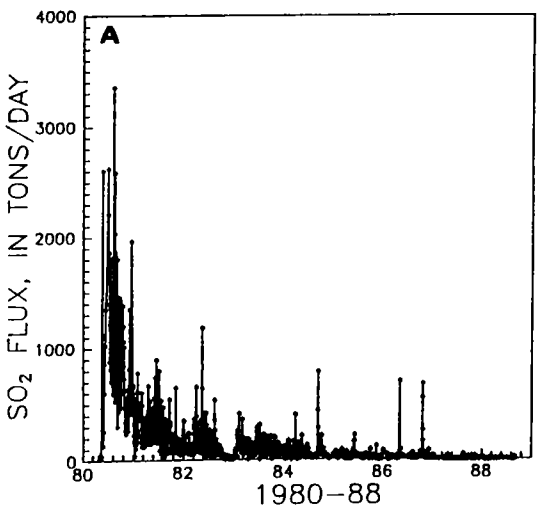

Figure 27. Examples of time dependent COSPEC data sets collected at volcanoes—see text for discussion of potential errors.

(A) Mount St. Helens, 1980-88. This is the most extensive data set of its kind, and shows a long term exponential decay since May 18, 1980. [By permission of the editor, Journal of Volcanology and Geothermal Research; McGee (1992), Fig.2, p. 271.]

imperfect wind speed measurements. Because aircraft have devices that can aid in active windspeed determinations, and because aircraft platforms allow easy adjustments of measurement distance and geometry of the transect, airborne COSPEC surveys are generally considered to be of higher quality. Their expense is higher, however, and this often means that various types of ground-based surveys are used instead. The principal

Table 8. Some examples of use of COSPEC data from the volcanological literature.

Volcano, date	*Application*	*Reference*
Fuego, 1978	COSPEC with particle and gas samplers	Lazrus et al. (1979)
Etna, 1978	SO_2 emissions and forecasting activity	Malinconico (1979)
St Helens, 1980	Low SO_2 before eruption	Stoiber et al. (1980)
Fuego, 1974-7	Excess SO_2 released	Rose et al. (1982)
Galunggung, 1982	SO_2 emissions and activity	Baddrudin (1983)
St Helens, 1980-2	Long term SO_2 and magmatic processes	Casadevall et al. (1983)
Colima, 1984	COSPEC with lidar data for particles	Casadevall et al. (1984)
Kilauea 1984-5	Summit versus rift SO_2	Greenland et al. (1985)
White Island 1984-5	COSPEC paired with direct gas data	Rose et al. (1986)
Masaya, 1980-2	Environmental hazards of plumes	Stoiber et al. (1986)
World, 1972-85	Estimating the annual volcanic flux	Stoiber et al. (1987)
Kilauea, 1985	Shallow magma processes, Pu'u O'o	Chartier et al. (1988)
Kilauea, 1979	SO_2 flux and earth tides	Connor et al. (1988)
Augustine, 1986	Scaling up degassing rates	Rose et al. (1988)
Kilauea, 1986	SO_2 related to magma supply rate	Andres et al. (1989)
Erebus, 1984-8	COSPEC paired with gas and particle samplers	Kyle et al. (1990)
Ruiz, 1985-8	Very large excess SO_2	Williams et al. (1990)
Etna, 1975-85	Long-term SO_2 average output	Allard et al. (1991)
Lascar, 1989	Excess SO_2 compared to surficial magma	Andres et al. (1991)
St. Helens, 1980-8	Exponential SO_2 decay after eruption	McGee (1992)
Stromboli, 1980-93	SO_2 flux and intrusive magma degassing budget	Allard et al. (1994)
Erebus, 1984-93	Shallow magma processes	Kyle et al. (1994)
Etna, 1987-94	Continuous COSPEC and high eruptive fluxes	Caltabiano et al. (1994)

advantage of ground-based platforms is that large data sets can be collected, which allows examination of the pattern of gas release in detail and enables more robust statistical averaging. In recent years the data collection and reduction processes have been automated (Kyle and McIntosh, 1989) and this has facilitated collection of large data sets which can be used for studies of surficial magmatic processes such as convection (Kyle et al., 1994).

SO_2 emissions and volcanic activity

Volcanoes release SO_2 at high rates during large explosive eruptions but these fluxes generally cannot be measured with COSPEC because large plume sizes, attenuation of ultraviolet radiation by ash and aerosols, and the geometric problems associated with traverses all cause difficulties. Instead the COSPEC is useful either during conditions of low-level explosive and effusive activity, continual open-vent degassing, or gas releases from shallow intrusions and domes. At any one time there are probably 50 to 100 fuming volcanoes in the world. The SO_2 emissions for these range from <10 to more than 5000 metric tonnes/day. The highest SO_2 emission rates measured at volcanoes by COSPECs were 32,000 t/d at Kilauea in 1984 (Greenland et al., 1985), 25,000 t/d at Etna in 1989 and 1991 (Caltabiano et al., 1994), and 24,000 t/d at Augustine in 1986 (Rose et al., 1988). Stoiber et al. (1983) broadly classified volcanic plumes based on their SO_2 flux as small (< about 200 t/d) moderate (200 to 1000 t/d) and large (>1000 t/d). Moderate and large SO_2 fluxes imply magma degassing because (1) SO_2 is an abundant magmatic gas, so magma degassing is its logical source, and (2) the main alternative source of these gaseous sulfur discharges, boiling of S-bearing hydrothermal fluids, seems unlikely, since boiling of hydrothermal fluids produces trivial amounts of SO_2 in comparison to other S-bearing gases and minerals, even when the fluids are heated to magmatic temperatures (Gerlach et al., 1995). A relationship between the rate of SO_2 release and earth tides has been shown at Kilauea (Fig. 27F; Conner et al., 1988).

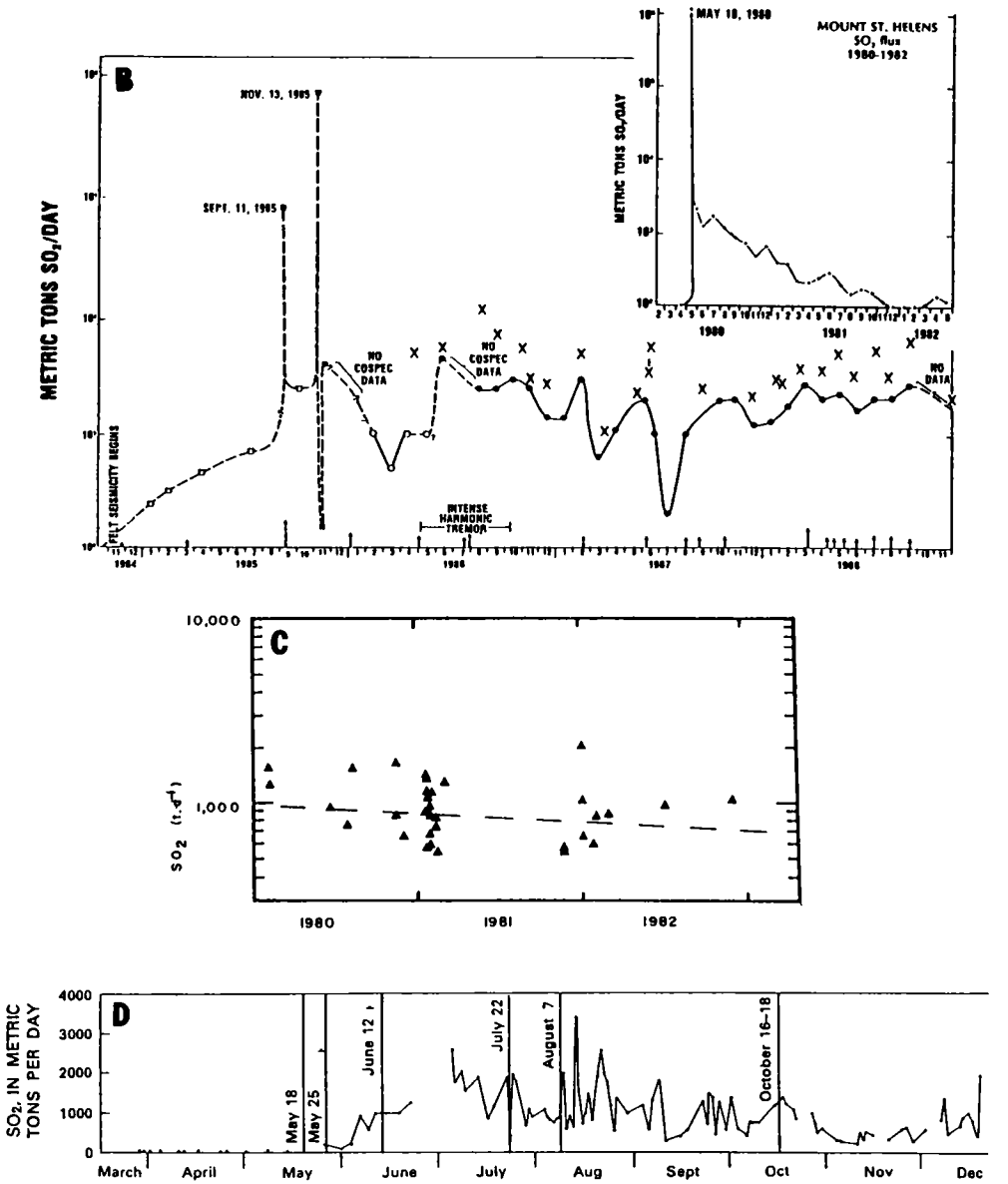

Figure 27 (continued).

(B) Nevado del Ruiz, 1984-88. Semilog plot of data collected at Ruiz, which shows a fairly steady emission rate of thousands of tons/day for years following the eruptions of 1985. Inset: data from Mount St. Helens for comparison. [Used by permission of the editor of Journal of Volcanology and Geothermal Research; Williams et al. (1990), Fig. 2, p. 56.]

(C) Masaya, 1980-82 (from Stoiber et al., 1986). Masaya is a basaltic shield characterized by lava lake and long term open vent degassing of about 1000 t/d.

(D) Mount St. Helens, 1980 (from Casadevall et al., 1981). The first several months of COSPEC data at Mount St. Helens, showing the relationship between explosive volcanic activity and the SO_2 flux.

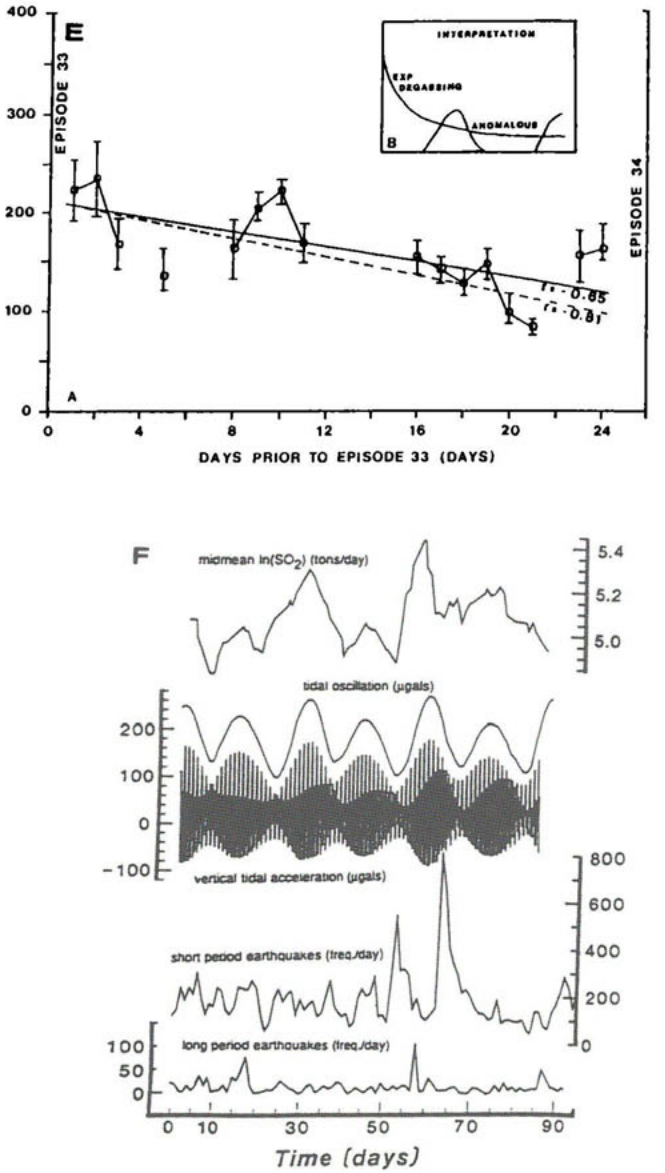

Figure 27 (continued):

E. Pu'u O'o, June 13-July 6, 1985. A daily record of degassing patterns of the ERZ vent during one repose period of 24 days. An exponential decrease with two anomalous periods was interpreted. [E and G by permission of the editor of Bulletin of Volcanology; Chartier et al. (1988), Figs. 9 and 11, respectively.]

F. Kilauea summit June 10-Sept 12, 1979 (from Connor et al., 1988). The daily fluxes are shown to correlate with vertical accelerations of earth tides.

SO_2 emission rates at volcanoes often correlate with eruptive activity. The COSPEC data sets from several volcanoes have shown a declining rate of SO_2 emission following a large eruption and coincidental with a decrease in volcanic activity. Such a pattern is best

shown by the data set from Mount St. Helens, 1980-86 (McGee, 1992; Fig. 27A). On another scale, measurements made at the Puu O'o vent at Kilauea between fountaining phases also show a generally declining trend of emissions (Chartier et al., 1988; Fig 27E). The tendency for SO_2 emission rates to decline at inactive open vents can be supported by other examples, but there is the expectation that frequent measurements might detect increases in SO_2 emissions which correlate with and precede renewed activity. This was first noted by Malinconico (1979) at Etna Volcano; volcanologists have noted this kind of correlation on several occasions since (e.g., Fig. 27D; cf. Fig. 33, below). Precursory increases in SO_2 flux are not observed consistently, however.

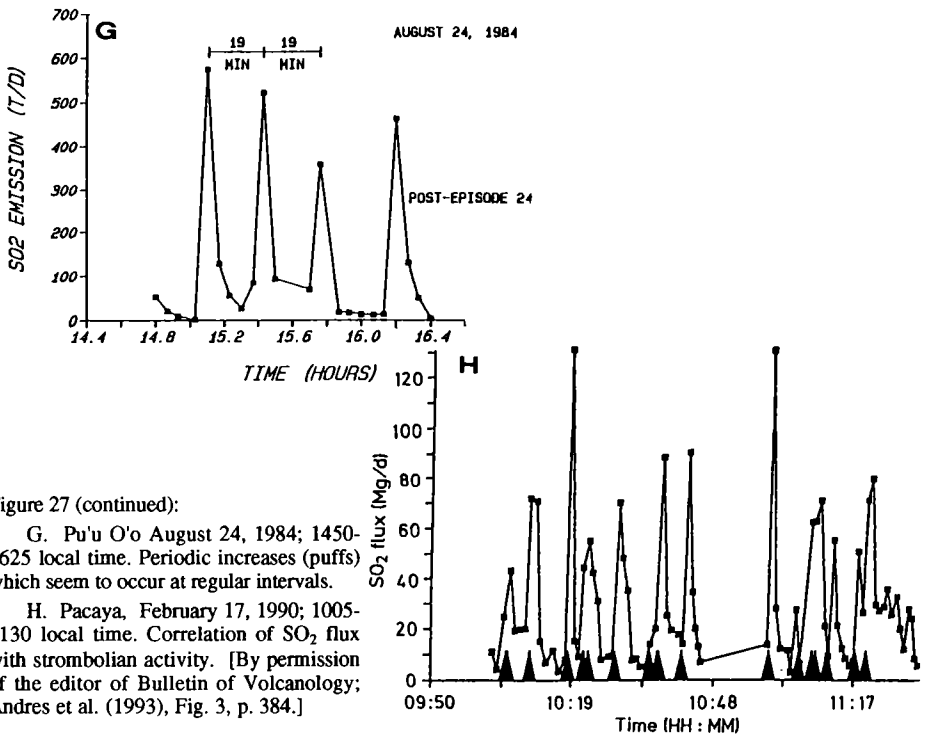

Figure 27 (continued):

G. Pu'u O'o August 24, 1984; 1450-1625 local time. Periodic increases (puffs) which seem to occur at regular intervals.

H. Pacaya, February 17, 1990; 1005-1130 local time. Correlation of SO_2 flux with strombolian activity. [By permission of the editor of Bulletin of Volcanology; Andres et al. (1993), Fig. 3, p. 384.]

The use of a COSPEC prior to a climactic eruption is of interest to volcanologists because the presence of SO_2 in a plume or eruption cloud is thought to be an indicator of near surface magma and an open vent, and thus gas emission measurements may provide a means of detecting changes associated with fracturing of the near surface rocks above a pressurized magma body. Before the Mount St. Helens eruption of 1980, the COSPEC measured generally very low SO_2 emission rates (Fig. 27D). By contrast, emission rates at Ruiz (Williams et al., 1986; 1990; Fig. 27B) were as high as several thousand tonnes/day before the main eruptive events. Similarly high SO_2 emissions were observed before the cataclysmic June 15, 1991 eruption at Mount Pinatubo (Daag et al., 1994). Such high (>1000 t/d) fluxes of SO_2 have come to mean that the volcano may be likely to erupt, although such observations are tempered by a lack of data on the background emissions of many volcanoes. Even with the uncertainties and the lack of many robust data sets, COSPEC gas emission measurements have been used on numerous occasions to try to help forecast eruptions, and following seismic monitoring, provide valuable information for volcanologists trying to understand evolving magmatic systems.

TOTAL OZONE MAPPING: SPECTROMETER DETERMINATIONS OF SO_2 EMISSIONS

Introduction

As noted earlier, sampling of volcanic gases is often impractical and hazardous; another major limitation stems from the sheer size of large, powerful eruptions. There are no ground-based techniques that have the capability to fully analyze large eruption plumes, which often exceed thousands of square kilometers in area. Observing phenomena of this size can only be accomplished by instruments aboard Earth-orbiting satellites. A powerful tool in the remote sensing of volcanic events was discovered quite by accident, after the launch of the Total Ozone Mapping Spectrometer (TOMS) in 1978 on NASA's Nimbus-7 satellite. Originally designed for globally mapping ozone by measuring the Earth's ultraviolet albedo, TOMS measured anomalous ozone values over Mexico after the eruption of El Chichón in 1982. It turned out that erupted sulfur dioxide was absorbing in some of the same UV wavelengths as used for ozone, and Krueger (1983) developed an algorithm to quantify SO_2.

One advantage of the TOMS instrument is its ability to provide full spatial coverage of large eruptions of sulfur dioxide. Perhaps equally valuable are the nearly continuous global data that the original and subsequent TOMS instruments have produced, recording explosive volcanic SO_2 emissions since late 1978, with the potential to continue this data collection through the turn of the century. Combined with other techniques TOMS data have been used to place constraints on annual emplacement of SO_2 into the atmosphere (Bluth et al., 1993), and to evaluate volcanic eruption sulfur budgets (Bluth et al., 1994a). In addition to estimating SO_2 emissions from individual eruptions, TOMS data have also aided studies of atmospheric circulation using volcanic injections of SO_2 as natural tracers (Schoeberl et al., 1993).

Due to the dynamic nature of eruption plumes, quantification of sulfur dioxide from TOMS measurements is rarely straightforward. A good deal of this section is devoted to discussion of some of the fundamentals of the TOMS instrument, along with the basics of determining SO_2 tonnages and limitations of the technique. A short summary of TOMS data follows, with specific applications to studies of magma degassing. More detailed descriptions of the TOMS instrument and theory behind TOMS-based SO_2 measurement can be found in Krueger (1983; 1985).

Method

Basic parameters. The Nimbus-7 satellite was launched into a sun-synchronous orbit, making a complete observation of the Earth every day in 13.7 orbits. Each orbit consists of a series of 2800 km-wide scans of 35 pixels each, with pixel resolution ranging from 50 km at the orbit center (nadir) to about 200 km at the orbit edges. Each scan takes approximately eight seconds to complete, thus the data comprising most volcanic SO_2 emissions can be collected within a few minutes, essentially giving a snapshot view of eruption clouds. The Nimbus TOMS measures the reflected sunlight of the Earth's surface in six ultraviolet wavelengths. From this information, both total column ozone and sulfur dioxide are calculated, based on the decrease in reflected light due to absorption and scattering by these gases (Krueger, 1983). Two bands which are unaffected by ozone or sulfur dioxide are used to calculate surface albedo (which can include both the Earth and some types of water clouds) or reflectivity.

TOMS instruments. The Nimbus TOMS provided data from November 1978 to its demise in May 1993. A second TOMS instrument was launched in August 1991 in a joint

U.S.–U.S.S.R. venture on board the Meteor-3 satellite. Although it uses essentially the same UV wavelengths, the Meteor TOMS is in a higher altitude, precessing orbit compared to Nimbus, resulting in a slightly larger footprint and less coverage at high latitudes. A third TOMS instrument is aboard NASA's Earth Probe satellite, launched in late 1994. The Earth Probe orbit is identical to that of the Nimbus satellite, and has modified wavelengths resulting in improved discrimination of SO_2. Future launches of TOMS instruments, by various agencies, are planned through the turn of the century.

Basic technique. Column amounts of SO_2 (ideally, the amount of gas between the TOMS instrument and the Earth's surface) are calculated in units of milli-atm cm (also known as Dobson units), the one-dimensional thickness of the gas layer at STP. Typical SO_2 clouds erupted from volcanoes and detected by TOMS range from 20 to several hundred milli-atm cm. The column mass of SO_2 is obtained by multiplying the average column amount of an integration region by its area and a conversion factor.

Background levels of SO_2 are determined by examining the areas adjacent to the volcanic cloud. SO_2 tonnages are calculated for the cloud(s) simply by adding the column masses from all the pixels within the cloud, and accounting for any non-zero background. The timing of the TOMS data collection is noted; this information may be used to calculate SO_2 dispersion during the time between eruption and subsequent TOMS orbits. If the SO_2 cloud is cohesive enough so that tonnages may be calculated on successive days, data are used to extrapolate to the time of eruption and better estimate an original emitted tonnage.

Limitations. The TOMS minimum detectable SO_2 mass depends on eruption, background, and meteorological conditions. Under normal operating conditions for the average scan position area (approximately 5000 km^2), the minimum SO_2 amount considered above noise in one pixel is about 2.5 kilotons (kt). However, single high-value pixels are generally assumed to be random noise, and 2-3 adjacent high-value pixels are usually required to represent a statistically valid SO_2 cloud. Based on the majority of pixel areas and actual SO_2 clouds found within the TOMS database, a practical lower range of detection is about 5-10 kt. However, towards the outer edges of the TOMS scan (where the footprint areas increase to 40,000 km^2) the minimum cloud detection might be no better than 50 kt SO_2.

The maximum amount of SO_2 detectable by TOMS has not been determined. Because the TOMS instrument measures UV reflectance rather than transmittance, even an optically opaque cloud will produce a signal. A cross-section through such a cloud would presumably reveal that absorption (i.e., SO_2 concentration) values reach a plateau; however the thickest cloud, or highest level of SO_2 concentration, known to date (Mount Pinatubo 1991) did not produce such a pattern in the TOMS data.

As the TOMS instrument uses reflected light, the data are valid only in sunlit portions of the orbit. Due to available sunlight, large algorithm errors caused by increasing light path length and screening by ozone place practical limits on the detection of eruptions to about 70° latitude in the hemispheric summer and 50° in winter. This restraint can be significant because of the numerous eruptions from volcanoes in Alaska, Kamchatka, and Iceland. However, there is one advantage at high latitudes because subsequent orbits overlap. At 60° during the hemispheric summer, two or three consecutive observations (at roughly 100 minute intervals) of an SO_2 cloud are often available, instead of the usual single daily observation.

There is little known regarding the minimum and maximum altitudes at which TOMS can detect and measure SO_2 clouds. The TOMS SO_2 algorithm was designed for stratospheric measurements, and the SO_2 cloud altitude clearly has an effect on retrievals.

For example, UV absorption of the sulfur dioxide molecule decreases as temperature rises (McGee and Burris, 1987). Since atmospheric temperature increases with lowering altitude below the tropopause, SO_2 clouds in the lower troposphere should be harder to detect. Other factors that hamper low-altitude detection include the increase in UV light scattering with atmospheric thickness and the increasing likelihood of interference from UV-reflecting water clouds between TOMS and a low altitude SO_2 cloud. Despite these hindrances, TOMS has observed lower tropospheric clouds (e.g., Galunggung 1982, Mauna Loa 1984).

Sources of error. It is important to recognize that the TOMS instruments were not optimally designed to directly measure sulfur dioxide; rather, SO_2 quantities are inferred from UV reflectance data based on an algorithm and the unique conditions surrounding each volcanic eruption. The method of using TOMS to quantify volcanic SO_2 emissions involves three types of uncertainties: (1) the measurement error of a scan pixel; (2) the cloud tonnage error, and (3) the error in extrapolating back to an original emission. Implicit in TOMS tonnage estimates are a number of assumptions and corrections, unique to each volcanic eruption, which will be briefly discussed here.

(1) The accuracy of a single TOMS measurement of SO_2 relies on instrument calibration and operating conditions, errors in assigning absorption coefficients, and the physical and chemical conditions within and surrounding the sulfur dioxide cloud (e.g., Krueger et al., 1990). A (correctable) scan bias occurs in the TOMS data retrieval due to changing sensitivity of the instrument to SO_2 as TOMS scans from nadir to the orbit edges. Changes in the Earth's UV reflectance, from high altitude water clouds as well as high albedos over ice-covered areas, have been correlated to linear, correctable effects on TOMS SO_2. Coemitted tephra and the transformation of erupted sulfur dioxide into sulfuric acid aerosols can also affect SO_2 retrievals, but their precise effects are not well known; these effects are under investigation using radiative transfer calculations.

Because of the limited amount of ground-based SO_2 data on large eruptions and the discrepancies among instrument sensitivities to SO_2, there have been very few opportunities to compare TOMS measurements to other data. One such opportunity arose after the September 1992 eruption of Mount Spurr, Alaska when the emitted SO_2 cloud drifted over an operating Brewer instrument (a ground-based UV spectrophotometer designed to measure ozone) in Toronto. TOMS data taken during two overpasses agreed within 20% to the ground-based measurements (A. Krueger, personal communication).

(2) Evaluations of cloud tonnages are largely affected by background levels, determination of cloud boundaries, and movement of the cloud between TOMS overpasses. Background levels vary with respect to latitude, meteorological conditions, and operating conditions of the TOMS instrument; the variable nature of TOMS background requires careful evaluation in order to discriminate and quantify the SO_2 cloud. Determination of cloud boundaries is vital because the TOMS method works best for compact clouds, or "spikes" of SO_2, rather than discriminating between background (zero level) and cloud boundaries. For diffuse clouds, either due to the nature of the eruption or from dispersion of an originally compact emission, the tonnage uncertainty increases. Due to the size or location of the SO_2 cloud, or orbit overlap at high latitudes, it is not uncommon for an SO_2 cloud to overlap adjacent scans. In these cases cloud movement between TOMS overpasses must be assessed in order to avoid counting the same SO_2 region twice.

(3) When estimating the original amount of SO_2 emitted by an eruption, it is necessary to account for changes in SO_2 amount between the time of eruption and the satellite

observation(s). This calculation assumes that measured tonnages are minimum values because of both chemical conversion of SO_2 to H_2SO_4 and subsequent rainout, and physical dissipation of SO_2 at the cloud margins to below the TOMS detection limits. The loss rate of most volcanic SO_2 clouds (to TOMS observation), while driven by chemical reaction rates, is also highly dependent on cloud altitude. If the erupted SO_2 remains below the tropopause there is more rapid conversion to sulfuric acid and rainout than in the drier, relatively less reactive conditions in the stratosphere. With large stratospheric clouds the amount lost at cloud boundaries is small compared to the mass of the SO_2 cloud (e.g., total cloud tonnage decreased by roughly 10% a day during the first week of observation following the 1991 Mount Pinatubo eruption; Bluth et al., 1992). In contrast, tonnages of small, tropospheric sulfur dioxide clouds with a high perimeter to mass ratio are more affected by physical and chemical processes, and commonly decrease by up to 50% per day (e.g., Bluth et al., 1994a).

The uncertainty involved in estimating the original emission of SO_2 generally decreases with the number of available measurements; thus the more days an SO_2 cloud is detectable by TOMS, the better the extrapolation. Krueger et al. (1990) considered both instrument and typical cloud/background parameters to estimate a total error of ±30% for the 1985 Nevado del Ruiz eruption, a figure which is typically used regarding TOMS tonnages. However, this error is not necessarily applicable to all eruptions. Work in progress to improve accuracy estimates of the TOMS data includes comparison of TOMS data to those of other instruments such as the Brewer spectrometer, and radiative transfer modeling of sulfur dioxide, tephra, and aerosols.

Data

During its 14-year lifetime, the Nimbus-7 TOMS instrument detected over 100 different volcanic eruption clouds. TOMS quantifying capabilities have ranged over three orders of magnitude, from 5 kt (essentially its lower limit of detection) to 20 Megatons (Mt) emitted from Mount Pinatubo in 1991 (Bluth et al., 1992). Figure 28 shows the larger eruptions from the TOMS database; some eruption clouds have been combined to represent a single event. The Volcanic Explosivity Index, or VEI, allows categorization of volcanic eruptions, based mainly on the height of the eruption column and amount of emitted tephra (Newhall and Self, 1982). TOMS detected every highly explosive eruption which occurred during its operation (i.e., the 11 eruptions of VEI ≥ 4), approximately 33% of VEI 3 eruptions, and about 10% of VEI 2 eruptions, using the database of the Smithsonian's Global Volcanism Network (Smithsonian Institution/SEAN, 1989) from 1979 to 1985 as the reported ground truth. Calibration and algorithm development are ongoing for the TOMS on Meteor-3 and no eruption tonnages have been quantified using this instrument.

Applications

General correlations of SO_2 outgassing with eruption characteristics. Differences in volcanic degassing between non-arc (divergent plate and hot spot) and arc (convergent plate) tectonic regimes are fairly evident in the TOMS data. Non-arc volcanoes typically erupt more often than arc volcanoes, but are less numerous worldwide; arc eruptions are by far the most violent (Smithsonian Institution/SEAN, 1989). As shown in Figure 29, there is a general increase in outgassed SO_2 with explosivity for arc eruptions but non-arc activity is less dependent on VEI. Non-arc volcanoes typically degas more sulfur-rich magmas and emit relatively greater amounts of sulfur dioxide for a given VEI. When considering the two regimes on a global basis we found a 2:1 ratio of arc to non-arc outgassing in the TOMS SO_2 database—a ratio dominated by two arc eruptions, El Chichón and Mount Pinatubo (Bluth et al., 1993).

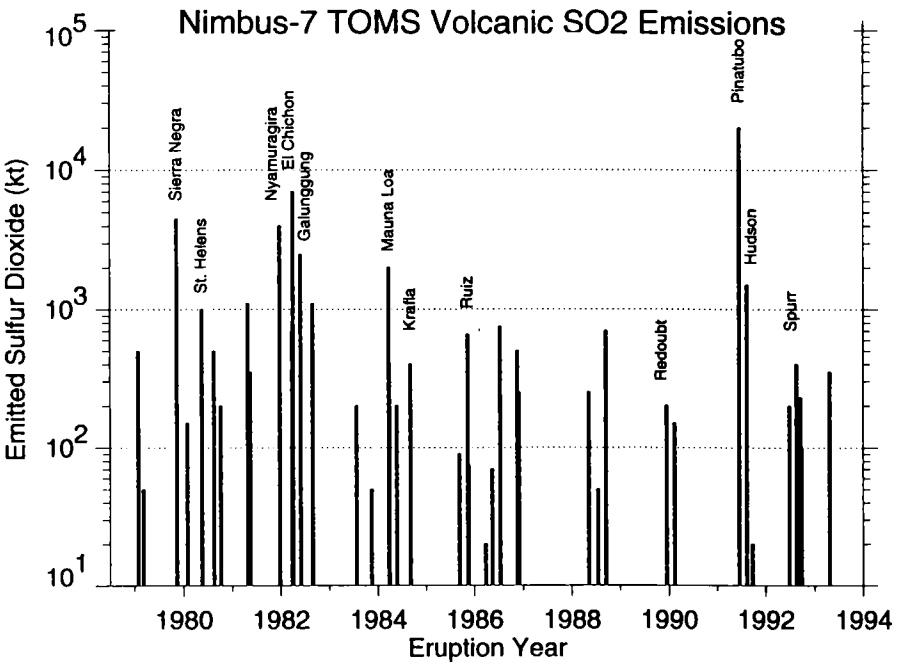

Figure 28. Inventory of TOMS SO_2 data from explosive eruptions, 1979-1992 (after Bluth et al., 1993). Most of the larger or well-known eruptions are labeled. Multiple eruptions from a single volcanic episode are combined, except for the three eruptions of Mount Spurr in 1992. The higher frequency of small eruptions observed prior to 1986 resulted from detailed searches through the TOMS database for all known eruptions using data from Smithsonian Institution/SEAN (1989).

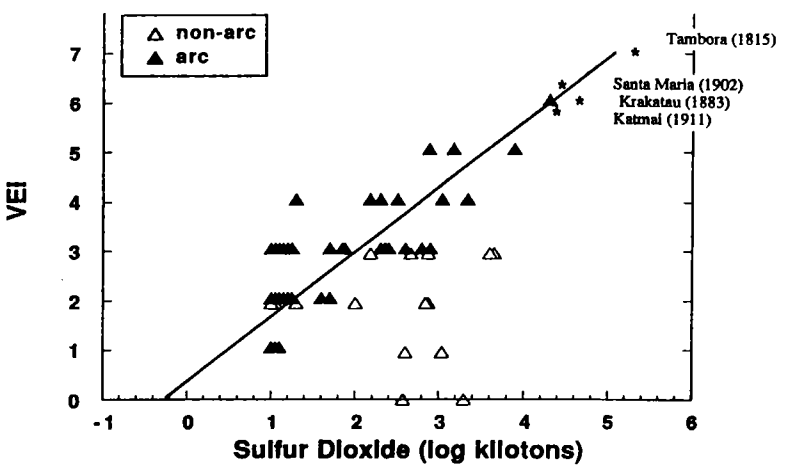

Figure 29. SO_2 outgassing by explosive eruptions compared to VEI (from Bluth et al., 1993). Data are separated by tectonic regimes to show relative contributions of volcanic activity as a function of explosivity. The TOMS SO_2-VEI regression line ($r^2 = 0.999$) is determined from average SO_2 for all VEI 4-6 eruptions between 1979 and 1992; VEI 2 and 3 averages are calculated using respective TOMS detection rates. Estimates of SO_2 emissions (*) from some historical, highly explosive eruptions are added for comparison.

Annual SO_2 emissions. In order to understand the impact of volcanism on the Earth's atmosphere, the eruption frequency and outgassing rates for the entire range of volcanic activity must be known. Non-explosive volcanoes (e.g., Etna, Kilauea) degas at relatively consistent rates, estimated at 9 Mt SO_2 annually (Stoiber et al., 1987). In contrast, forceful degassing characteristic of explosive eruptions (e.g., Mount Pinatubo) is notoriously sporadic and more difficult to quantify. Thus the total yearly volcanic flux of sulfur dioxide is not well constrained; previous ground-based estimates range from 1.5 to 50 Mt (see references within Bluth et al., 1993). The current man-made contribution is approximately 190 Mt/yr (Möller, 1984).

Using the TOMS data, Bluth et al. (1993) made the simplest estimate of annual SO_2 output by explosive volcanism from the total explosive SO_2, 52 Mt, over 14 years of observation — an average of 4 Mt/yr. But Figure 28 demonstrates the rather sporadic distribution of the "average" output. The dataset is sensitive to the SO_2 emissions of a few relatively large eruptions. For example, one could argue that the 14-year TOMS database is simply dominated by two eruptions, El Chichón and Mount Pinatubo; removing these would halve the calculated annual SO_2 flux for this period.

Seeking another way to address the temporal distribution of global volcanism, Bluth et al. (1993) linked the TOMS SO_2 data to a longer-term dataset of eruption explosivity (VEI) and frequency. Although virtually useless in connecting individual eruptions to SO_2 emissions (in Fig. 29, note the 2-3 order of magnitude ranges of SO_2 observed over VEI 3 or 4 eruptions), a general relationship between average sulfur dioxide emission and VEI has been observed previously by Stoiber et al. (1987). Likewise in Figure 29, a TOMS SO_2/VEI relationship can be determined from average SO_2 amounts for each VEI level (VEI 2 and 3 averages reflect the TOMS' detection rates of these eruptions). The relationship of eruption frequency to VEI over the past 200 years (Simkin, 1993) can then be used to determine the annual eruptive activity for each VEI category. Multiplying the two (average SO_2 and number of eruptions from VEI 0 - 7) produces a total SO_2 flux from explosive volcanism of approximately 4 Mt, in agreement with the simple average of the total TOMS SO_2 database. This suggests that the dominance of the total explosive SO_2 output by a few large eruptions is not unique to the past 14 years. Most volcanic emissions are apparently generated from non-explosive degassing, and combining the non-explosive (9 Mt) and explosive (4 Mt) outputs yields an annual flux of 13 Mt SO_2 from volcanoes. Therefore, it appears that the average annual volcanic emission of SO_2 to the Earth's atmosphere comprises less than 10% of the present-day anthropogenic flux. Even a Mount Pinatubo-sized eruption is small compared to the current annual anthropogenic SO_2 contribution to the atmosphere.

Although much smaller in SO_2 mass output, volcanic activity produces a disproportionately large climatic impact compared to anthropogenic sources because explosive volcanism has the ability to inject sulfur directly into the stratosphere. In the TOMS database 65% of the total 52 Mt SO_2 was emitted by eruptions of VEI 4 and above (Bluth et al., 1993), which implies that stratospheric injection of sulfur dioxide by volcanoes averages roughly 2.5 Mt/yr.

Tandem use with COSPEC. In short-lived, powerful eruptions, such as those of Mount Pinatubo in June 1991, the explosive emissions of SO_2 are usually much greater than the non-explosive contribution. These emissions are best quantified by TOMS. In contrast, eruptions such as exhibited by Mauna Loa and Etna outgas essentially all their sulfur non-explosively, and are better evaluated by COSPEC. To accurately assess the total sulfur budget for moderate strength volcanism such as that exhibited by Galunggung in 1982, a combination of remote sensing techniques is most appropriate.

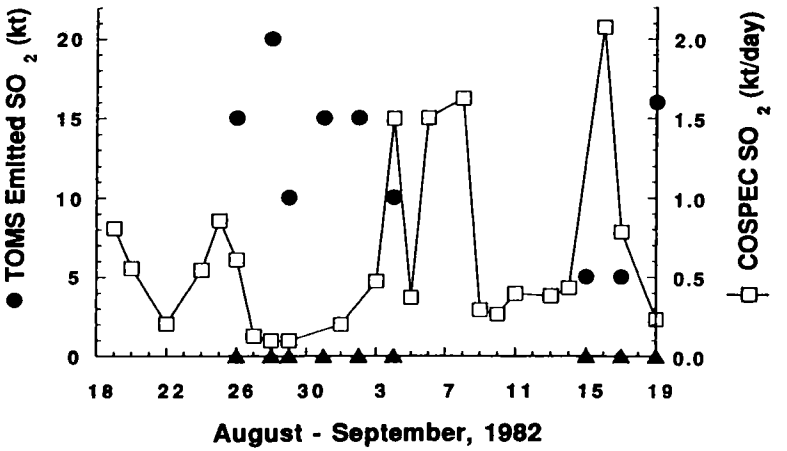

Figure 30. Comparison of TOMS and COSPEC SO_2 data for a coincident period of record of Galunggung eruptions in Indonesia, August 19 - September 19, 1982 (from Bluth et al., 1994a). Large Vulcanian eruptions reported by the Cikasasah Volcano Observatory are marked by filled triangles along the horizontal axis. Note that the TOMS and COSPEC data are plotted on different scales.

Galunggung awoke from 63 years of quiescence in April 1982. During its most violent period from April to October, the Cikasasah Observatory reported 88 eruptions (Katili and Sudradjat, 1984). Eruptions became less violent towards the end of September, but the volcano continued to erupt sporadically through January 1983. TOMS detected and measured 24 separate sulfur dioxide clouds from April 5 to September 19 (Bluth et al., 1994a). The rapid dispersion of the SO_2 clouds, altitude estimates of co-emitted ash clouds, and comparisons of cloud motion to tropospheric wind, suggest that most of the SO_2 remained below the tropopause. A total of just over 2000 kt SO_2 was produced primarily by the 24 explosive eruptions observed by TOMS, and to a smaller extent by the 64 explosive eruptions which were below the TOMS detection limit.

For the first time both TOMS and COSPEC were in operation during a coincident, 32-day period of explosive volcanism (Fig. 30). Bluth et al. (1994a) estimated that explosive outgassing of SO_2 (derived from TOMS) produced approximately six times the non-explosive emissions (estimated from COSPEC data; Badruddin, 1986). If this ratio remained relatively constant over the course of activity from April to September, approximately 350 kt would have outgassed non-explosively. COSPEC data indicate an additional 50 kt SO_2 were emitted by the less-violent activity from the end of September 1982 to the end of January 1983. Combining all the estimates of SO_2 emissions, Galunggung outgassed approximately 2500 kt of sulfur dioxide from both explosive and non-explosive activity between April 1982 to January 1983.

Excess SO_2 from convergent-plate volcanoes

Volatile exsolution models for Kilauea basalt containing 0.3 wt % H_2O, 0.07 wt % S, and 0.02-0.05 wt % CO_2 suggest that vigorous exsolution of dissolved sulfur (as SO_2) occurs only after the magma has ascended to shallow depths (estimated to be about 150 m) where pressures are <30 bar (Gerlach, 1986). The observed amounts of SO_2 emitted from Kilauea basalt are roughly in balance with the amounts that would be expected from the dissolved sulfur content of the magma and the volumes of magma extruded and degassed

Table 9. Comparisons of erupted magma masses and masses of sulfur released. Modified from Andres et al. (1991).

Volcano, date	*Erupted Magma Mass tonnes (10^6 g)*	*S mass tonnes (= 10^6 g)*	*Equiv % S wt %*
Stromboli, 1980-93	1.9×10^5/yr†	1.1×10^5/yr†	58†
Etna, 1975	4.0×10^4	7.5×10^3	15
Láscar, 1989	3.7×10^6	2.7×10^5	6.9
Lonquimay, 1989	1.1×10^5	3.5×10^3	3.1
Ruiz, 1985	3.5×10^7	3.3×10^5	0.93
Fuego, 1974	2.2×10^8	1.6×10^6	0.72
El Chichón, 1982	1.2×10^9	7.0×10^6‡	0.58
Pacaya, 1972	2.6×10^4	1.3×10^2	0.5
Agung, 1963	5.0×10^9	0.6×10^7	0.12
St. Helens, 1980	7.4×10^8	0.3×10^6	0.04
Mauna Loa, 1984	5.4×10^8	1.2×10^5	0.02

† From Allard et al. (1994); ‡slightly modified to reflect data of Bluth et al. (1993).

near the surface (Andres et al., 1989). These results are also likely to be true for eruptions of other tholeiitic basalts with similar low volatile contents, but they are at odds with SO_2 emissions depicted by TOMS and COSPEC data for eruptions of magma at convergent-plate volcanoes. For these systems, SO_2 emissions appear to be in excess of expected yields based on concentrations of dissolved sulfur, as represented by melt inclusions, and the quantity of erupted and near surface magma (Rose et al., 1982; Andres et al., 1991; Westrich and Gerlach, 1992; Allard et al., 1994; Gerlach et al., 1994, 1995; Gerlach and McGee, 1994). In many cases, the proportion of excess sulfur indicated by the SO_2 release is very large. Table 9 shows examples of the required sulfur contents of surficial coerupted magma that, if completely degassed, could account for the observed masses of released sulfur. The values are much higher than the sulfur content of the magma indicated by melt inclusions, except for Mauna Loa, which involves tholeiitic basalt likely to have a volatile content similar to that of Kilauea basalt. Most of the examples are for convergent plate volcanoes. The general lack of agreement in these cases shows that remote sensing of SO_2 is a poor way to estimate lava eruption rates and volumes for these systems, and that melt-inclusion methods are likely to underestimate sulfur yields during convergent plate volcanism (Devine et al., 1984; Palais and Sigurdsson, 1989) by large factors.

Comprehensive TOMS, COSPEC, and melt-inclusion data permit a comparison of SO_2 emissions based on remote sensing and melt inclusions for explosive volcanism at three convergent plate volcanoes. TOMS and COSPEC data from the climactic explosion of Mount St. Helens on May 18, 1980 to the last stages of quiescent dome degassing in September 1988 indicate a total SO_2 emission for the eruption of roughly 2 Mt (megaton) compared to a melt inclusion-based estimate for the eruption of 0.08 Mt (Gerlach and McGee, 1994). The total TOMS and COSPEC-based SO_2 emission estimate for the 1989-1990 eruption of Redoubt Volcano, Alaska, is approximately 1 Mt compared to a maximum emission estimate of 0.04 Mt from melt-inclusion data (Gerlach et al., 1994). The TOMS estimate for SO_2 emission during the 1991 eruption of Mount Pinatubo, Philippines, is about 20 Mt (Bluth et al., 1992), whereas the melt inclusions indicate no significant degassing of dissolved sulfur during magma ascent and eruption (Gerlach et al., 1995; see also Chapter 8). The sources of the excess sulfur are widely discussed and debated, but the remote sensing data for SO_2 and CO_2 and melt inclusion data for H_2O and CO_2 suggest that the Mount St. Helens dacite, the Redoubt andesites, and the Mount Pinatubo dacite were vapor-saturated at depth prior to eruption, and that sulfur in accumulated vapor provided the immediate source of excess sulfur for the SO_2 emissions (Westrich and

Gerlach, 1992; Gerlach et al., 1994; Gerlach and McGee, 1994; Wallace and Gerlach, 1994; Gerlach et al., 1995).

Detection of H_2S emissions. During the summer of 1992, Mount Spurr, Alaska ended a 39-year period of quiescence and emitted large SO_2 plumes during three separate eruptions June 27, August 18, and September 17 (Bluth et al., 1994b). After the August and September eruptions, an unusual pattern was observed: TOMS-measured SO_2 actually increased from the first to second day, before returning to a typical pattern of gradual cloud dispersion (Fig. 31). Both eruption plumes were observed after complete separation from the volcano, thus there was no possibility that the increase could have occurred from additional outgassing after the first TOMS overpass. An important implication for this retrieval pattern may be that significant H_2S emission occurred during the Spurr eruption.

Bluth et al. (1994b) first examined several other explanations. Measurement uncertainty was ruled out as the cause, based on the consistent SO_2 dispersion characteristics of the clouds after the initial days' low quantities. Neither interference from co-erupted ash, nor aerosol formation were consistent with the TOMS data. UV light scattering by the ash clouds, which Schneider et al. (1994) showed were coincident with the gas clouds, may have partially masked detection of sulfur dioxide, but TOMS reflectivity data showed no evidence of UV attenuation from ash particles. In addition, the slow fallout rate of micron-sized particles in the plume (Rose, 1993; Wen and Rose, 1994) indicated that any effect on TOMS measurements should have lasted for weeks, rather than only a single day. Radiative transfer modeling of ash and aerosol effects on TOMS retrievals suggest that the presence of either should cause measured SO_2 to increase, rather than be underestimated. Also, the aerosol effect should have increased with time, as more SO_2 converted to aerosol.

The eruption of H_2S, and oxidation to SO_2 subsequent to the first day, could explain the tonnage increases in the TOMS data. The amount of hydrogen sulfide required to produce the sulfur dioxide pattern observed in the TOMS data is roughly 75 kt H_2S for the August eruptions (a 3:1 SO_2:H_2S ratio), and 25 kt H_2S for the September eruption (a 6:1 ratio). Doukas and Gerlach (1994) report on evidence and a possible mechanism for hydrogen sulfide emissions from boiling of hydrothermal fluid within the volcano (see below). As discussed above under pressure effects, it is also possible that H_2S was a stable sulfur gas species in the magma at depth (Reaction 26, Fig. 14) and that rapid eruption and transport through the troposphere allowed a significant amount of it to reach the stratosphere and subsequently oxidize to SO_2. For example, Gerlach and Casadevall (1986b) suggested that sudden release of H_2S stabilized in magma at depth (Fig. 14) may have caused the high H_2S/SO_2 observed in Mount St. Helens plumes during explosive eruptions, including the May 18, 1980 climactic eruption plume (Casadevall et al., 1981; Hobbs et al., 1981), and that SO_2-related environmental effects of explosive volcanism may often require post-eruption oxidation of discharged H_2S.

The pattern of increasing SO_2 in this stratospheric cloud was also observed in the TOMS data immediately after the climactic May 18 eruption of Mount St. Helens in 1980. While the TOMS data cannot be used as definitive proof of H_2S gas emissions from either the Spurr or St. Helens eruptions, these results may open a new approach for investigating the degassing of magma-hydrothermal systems.

EMISSION RATES OF OTHER VOLCANIC GASES

Methods for measurement

Volcanologists have long recognized the value of remote sensing data on more species, but results of this sort are very sparse (Mori et al., 1993). An infrared gas spectrometer

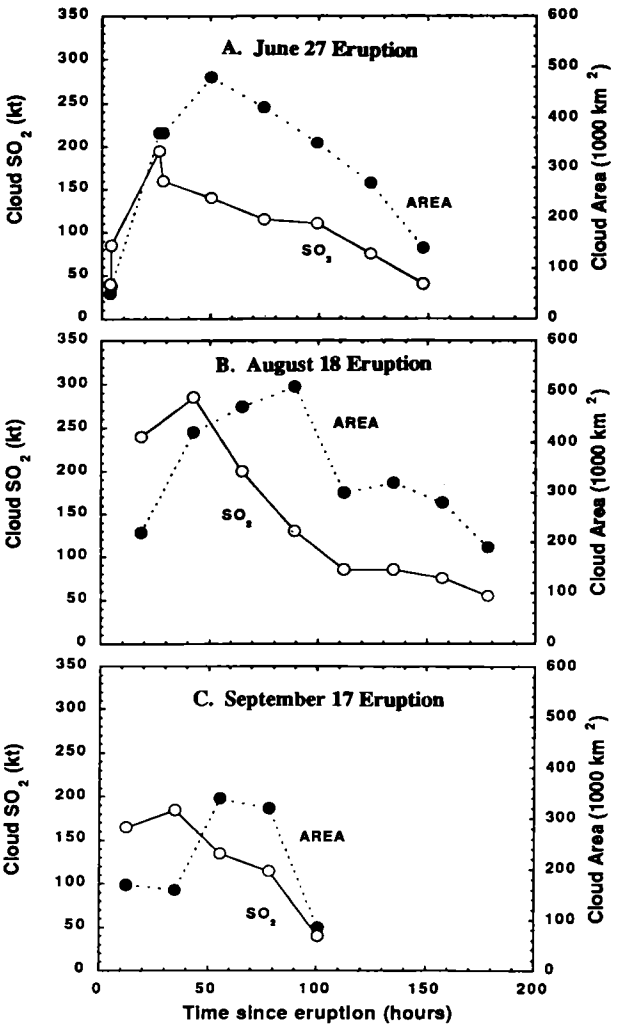

Figure 31. Comparison of cloud sulfur dioxide mass (open circles) and area (filled circles) as a function of time after eruptions of Mount Spurr, Alaska in 1992 (from Bluth et al., 1994b). (a) June 27 eruption. (b) August 18 eruption. (c) September 17 eruption.

(Miran) has been used to provide data on CO_2 fluxes of volcanic plumes at Mount St. Helens (Harris et al., 1981). This device is not a remote sensor, but requires direct sampling of the plume. This limitation means that the CO_2 concentrations of the plume must be mapped by aircraft traverses through the plume. As a result, the Miran has only been used in a few cases (Harris et al., 1981; Casadevall et al., 1987; Casadevall et al., 1994; Doukas and Gerlach, 1995). At Mount St. Helens Miran data on CO_2 were coupled with COSPEC determined SO_2 fluxes to allow comparison and ratioing of two species. Because most of the CO_2 may be lost from magmas before extensive degassing of SO_2—as discussed above for Kilauea volcano—there is a possibility that such data will be a more useful forecasting tool than SO_2 alone (Harris and Rose, 1994; Casadevall et al., 1994).

Methods of estimation

Combining flux measurements with compositional data on plumes and fumaroles gives estimated fluxes of additional species. For instance, by combining COSPEC SO_2 fluxes with direct gas samples that constrain the ratios of other species to SO_2, fluxes for all species in the samples can be estimated (e.g. Rose et al., 1986; McGee, 1992). When analytical data are not available for minor and trace species, thermochemical modeling can provide estimates of the appropriate ratios (Symonds et al., 1992). Combining the COSPEC with gas-filter sampling (Finnegan et al., 1989) also allows estimation of elemental fluxes (Phelan et al., 1982; Rose et al., 1988).

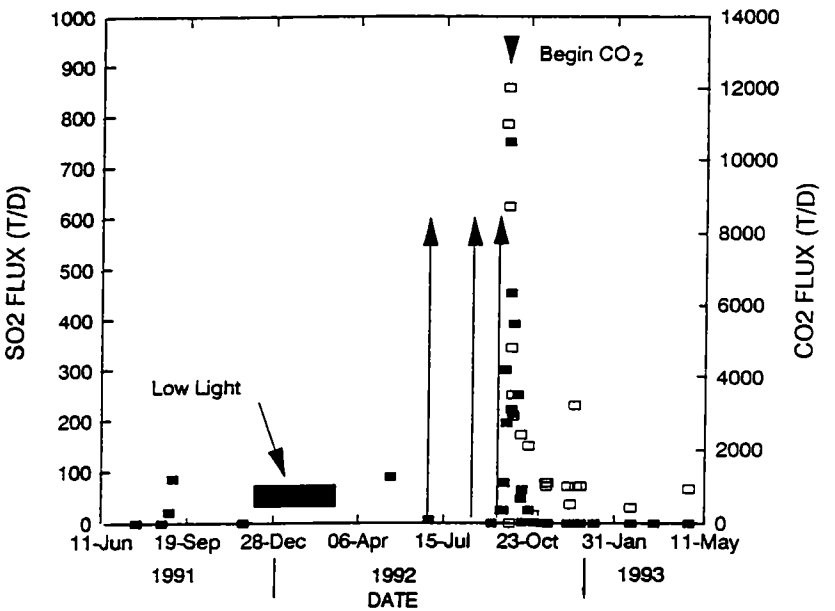

Figure 32. SO_2 and CO_2 emission-rate measurements for Crater Peak, Spurr Volcano, between 1991 and 1993. Solid squares and open squares give SO_2 (left vertical axis) and CO_2 (right vertical axis) fluxes, respectively. Arrows mark explosive eruptions. Solid bar indicates low light period when COSPEC measurements were not possible. From Doukas and Gerlach (1994).

Measuring both SO_2 and CO_2 emission rates–an example of the advantages

During the 1991-1993 activity of Crater Peak on Spurr Volcano, Doukas and Gerlach (1994) measured both SO_2 and CO_2 emission rates using COSPEC and Miran, respectively. Over this timeframe, there were three subplinian eruptions on June 27, August 18, and September 16-17, 1992. SO_2 measurements began on July 22, 1991 at the onset of precursory seismicity, whereas CO_2 fluxes were not initiated until September 25, 1992; flux measurements continued until April 24, 1993 (Fig. 32). Despite the elevated seismic activity and explosive eruptions, both indicating shallow intrusion of magma, SO_2 fluxes were generally <100 t/d during the 1991-1993 period, except during the eruptions themselves, as measured by TOMS (Bluth et al., 1994b), and between September 25 and October 10, shortly after the September eruption (Fig. 32). The <100 t/d fluxes are much lower than expected for a passively degassing volcano discharging moderately large

plumes. Other active volcanoes discharging plumes of moderate size generally emit 200 to 1000 t/d of SO_2 (e.g., Mount St. Helens, Fig. 27A, McGee, 1992; Redoubt, Casadevall et al., 1994), as did Crater Peak between September 25 and October 10, 1992 (Fig. 32). In contrast, the CO_2 emission rates from late 1992 to early 1993 were generally between 1000 and 12,000 t/d, similar to other volcanoes emitting moderately large plumes (e.g., Redoubt, Casadevall, 1994; Mount St. Helens, Harris et al., 1981). The generally lower than expected SO_2 emission rates, normal CO_2 fluxes, and CO_2/SO_2 ratios between 10-100, much higher than expected for gases from undegassed convergent-plate magmas (Fig. 10), led Doukas and Gerlach (1994) to suggest that the gases released from shallow magma encountered liquid water (possibly as hydrothermal fluid) inside the volcano. They speculate that scrubbing of sulfur dioxide by hydrolysis reactions with water masked the SO_2 degassing, but that boiling of hydrothermal fluid released CO_2 to the atmosphere. They also suggest that "drying out" of the channelways between September 25 and October 10, 1992 allowed a brief period of elevated SO_2 emissions. These results underscore the advantages to be gained from measuring emission rates of magmatic volatiles like CO_2, which are relatively insoluble in shallow magma and boiling water, for comparison with SO_2 emission rates.

GAS STUDIES TO ASSESS VOLCANIC HAZARDS

In addition to seismic and geodetic monitoring, gas studies play an important role in assessing volcanic activity. There are three basic gas-based approaches to assessing volcanic activity: (1) direct sampling of fumarolic or soil gases, (2) measuring gas emission rates, and (3) continuous monitoring of volcanic fumaroles and ambient air. The ideal gas program would integrate all three methods because each approach has advantages and disadvantages (Table 10). At some volcanoes, the gases vent into a crater lake and geochemical sampling of lake waters can detect changes in the degassing activity.

Direct gas sampling

Surveillance by direct gas sampling involves collecting gas samples from volcanic fumaroles at periodic intervals with the methods described above. It may also involve soil-gas sampling to detect diffuse degassing around the volcanic edifice. The time interval between sampling may vary depending on volcanic activity, logistical considerations, and available resources. Direct sampling of fumaroles is currently the only way to fully characterize the compositions of gases discharging from volcanoes. It is also the only way to collect isotopic data vital to constraining the origin(s) of individual gas species from potentially restless volcanoes (e.g., Sorey et al., 1993). Direct gas sampling can also capitalize on rare and urgent sampling opportunities because it requires a minimal amount of time and field equipment. Past studies have shown that direct gas sampling can determine the source(s) of the gases, including the presence or absence of subsurface magma (Allard et al., 1991b); if magma is present, these data can sometimes detect changes in its degassing state (Gerlach and Casadevall, 1986b; Tedesco et al., 1991). Chemical analyses of gases can also be used to estimate subsurface temperatures of volcanic-hydrothermal systems and to determine whether a system is heating up or cooling down (Tedesco and Sabroux, 1987). Moreover, direct gas sampling provides geochemical information on a volcano's hydrothermal system, which should be a part of an overall hazards assessment since a hydrothermal system may influence the eruptive style of a volcano.

Direct gas sampling is currently the most practical and cost effective way to geochemically characterize volcanoes with low gas fluxes. Surveillance of volcanoes with low gas fluxes requires methods that can detect magmatic gases in weak fumarolic

Table 10. Summary of advantages and disadvantages of gas geochemical methods to assess volcanic activity.

Advantages	*Disadvantages*
Direct Gas Sampling	
1. Characterizes complete gas composition.	1. Temporal resolution only as good as sampling frequency.
2. Only way to collect isotopic data on gases.	2. Labor intensive.
3. Requires minimal time and equipment.	3. Each sample requires human access to potentially dangerous volcanic vents.
4. Best way to study low-flux volcanoes.	4. Weather dependent.
5. Can detect subsurface temperature changes.	
6. Helps characterize volcano-hydrothermal systems.	
7. Enhances volcanic emission studies.	
8. Cheapest method.	
Measuring Gas Emission Rates	
1. Only way to measure fluxes of gas species.	1. Currently, only SO_2 and CO_2 are measured.
2. Best spatial coverage of volcanic degassing.	2. Temporal resolution only as good as measurement frequency.
3. Can be used during eruptions or during elevated volcanic activity when other methods are not feasible.	3. Labor intensive.
4. Only gas measurement method to estimate volumes of magma degassed.	4. Weather dependent.
5. Safest methods because it does not require human access to volcanic vents.	5. More expensive than gas sampling.
Continuous Monitoring	
1. Provides very frequent time-series data.	1. Ideal sensors for volcanoes not yet available
2. Can detect short-lived (hours to days) gas events.	2. Monitoring equipment exposed to geologic hazards.
3. Not weather dependent.	3. Servicing equipment requires human access to potentially dangerous volcanic vents.
4. Safer than direct gas sampling.	4. More expensive than gas sampling.
5. Easy direct comparison with telemetered geophysical data on same time scale.	

emissions, including species like CO_2 and He that may pass through hydrothermal or meteoric water that is often present at such volcanoes. Recent work (Baubron et al., 1990; Allard et al., 1991a) shows that significant degassing of CO_2 also occurs on the flanks of volcanoes as diffuse soil-gas emissions, which suggests that periodic soil-gas sampling may detect changes in activity at volcanoes with low gas fluxes. Emission-rate methods (below) are often not sensitive enough to detect low gas fluxes in the early stages of a magmatic intrusion. Direct gas sampling has the sensitivity required to potentially detect such disturbances, including any changes in CO_2 and He.

One main disadvantage of assessing volcanic activity with gas samples is that each time series of samples requires another trip to the collection site. This approach is satisfactory when one can collect and analyze samples faster than the rate at which gas compositions are changing. However, when available resources, weather conditions, or other problems restrict the sampling frequency, the samples may miss rapidly changing chemical events. Moreover, the duration of some gas events are so short (e.g., several hours long; McGee and Sutton, 1994) that it is impractical to detect them by gas sampling.

Measuring gas emission rates

Remote sensing and direct sampling of plumes are the only ways of obtaining gas flux information, which provide the best gauge of overall volcanic degassing. Because measurements are made on volcanic plumes rather than in close proximity to volcanic vents, these are also the safest geochemical assessment methods and can even be used during some volcanic eruptions. Current technology enables measurement of SO_2 and CO_2 emission rates by airborne or ground-based methods, and SO_2 emissions by satellite (see above). Measurement intervals depend on volcanic activity, weather, and available resources, and like direct gas sampling, one major problem with emission-rate studies is that the temporal resolution of the data is only as good as the sampling frequency. Another significant disadvantage is that SO_2 and CO_2 are the only species that can currently be measured by remote sensing or direct sampling of plumes. However, new methods capable of measuring other species are under development (e.g., K. McGee, personal communication, 1994) and these may make remote sensing a more attractive and cost-effective way to measure volcanic emissions.

Continuous monitoring of fumaroles and ambient air

Continuous monitoring is accomplished by collecting very frequent gas-concentration data (e.g., every 10 minutes) with sensors placed inside a fumarole or in the air or soil around a fumarole. The data are telemetered back to a remote site for analysis and interpretation. This method has the advantages of being much safer than direct gas sampling and has excellent temporal control that can detect hourly changes in the compositions of gas emissions (Sutton et al., 1992; McGee and Sutton, 1994). For example, both reduced-gas monitoring and SO_2 flux measurements detected a large gas release prior to the October 1986 lava extrusion at Mount St. Helens (Fig. 33; McGee and Sutton, 1994). The chief disadvantage of continuous monitoring is that suitable sensor technology for volcanic environments is still to be developed. For instance, species-selective sensors that can withstand the acid-gas attack in volcanic fumaroles are not yet available (Sutton et al., 1992). However, new advances in environmental sensors have made it possible to monitor specific species in the air around volcanic vents (Sutton, 1990). Future improvements in sensor technology will make continuous monitoring more attractive.

Sampling of volcanic crater lakes

About 88 of the world's 619 active volcanoes contain near-summit crater lakes (Rowe and Varekamp, 1993). In such cases, periodic sampling of crater lakes has many of the advantages (numbers 2-8, Table 10) and disadvantages (2-4, Table 10) of direct gas sampling and some of the advantages (1-2, 4, Table 10) of measuring gas emission rates (Giggenbach, 1974; Giggenbach and Glover, 1975; Menyailov, 1975; Takano, 1987; Takano and Watanuki, 1990; Rowe et al., 1992a,b; Brantley et al., 1993; Christenson and Wood, 1993; Ágústsdóttir and Brantley, 1994; Delmelle and Bernard, 1994).

An integrated approach to surveillance

Table 11 outlines surveillance methods for an idealized eruption. The application of the various techniques is closely related to the level of activity. During early and late stages, direct sampling, if possible, is the method of choice. The best time for direct gas sampling is typically late, after the big eruptions, but while the vent is still open. COSPEC and Miran measurements of SO_2 and CO_2 become feasible usually at some point before the climactic eruption and continue throughout the eruptive cycle, except during large explosive

Table 11. A model of gas studies throughout an idealized eruption sequence.

Sequence of events	*Timing*	*Vent characteristics*	*Sampling/Species*	*Expected Results*
repose period	years prior	background degassing	Direct: H_2O, CO_2, SO_2, H_2, H_2S, HCl, HF, CO, He, isotopes†	-establish baseline gas compositions -determination of sources of gases -background hydrothermal activity
onset of activity	>1 year prior	minor degassing: interactions with groundwater, rock, atmosphere	Direct: H_2O, CO_2, SO_2, H_2, H_2S, HCl, HF, CO, He, isotopes†	-increases in magmatic-gas components -CO_2 escape through diffuse cracks and soil -elevated hydrothermal activity
ramping up of activity	1-12 months prior	increase in vent degassing; vent opening	Direct: H_2O, CO_2, SO_2, H_2, H_2S, HCl, HF, CO, He, isotopes† COSPEC: SO_2 Miran: CO_2 Continuous Monitoring	-increases in magmatic-gas components -compositions of magmatic gases -fO_2 determination -low-level SO_2 and CO_2 degassing rates -periods of elevated degassing
paroxysmal eruption(s)	within months prior	open vent; minor, precursor eruptions	COSPEC: SO_2 Miran: CO_2 Continuous Monitoring TOMS: SO_2	-low-level SO_2 and CO_2 degassing rates -gas detection of intrusions -periods of elevated degassing -total SO_2 from explosive events
cataclysmic eruption	during	major explosive eruption	TOMS: SO_2	-total SO_2 degassed
recurring eruptions	days to months after	open vent; minor eruptions	TOMS: SO_2 COSPEC: SO_2 Miran: CO_2 Continuous Monitoring	-total SO_2 from explosive events -low-level SO_2 and CO_2 degassing rates -gas detection of intrusions -periods of elevated degassing
ramping down of activity	months to years after	open vent degassing; rare eruptive activity	Direct: H_2O, CO_2, SO_2, H_2, H_2S, HCl, HF, CO, He, isotopes† COSPEC: SO_2 Miran: CO_2	-evolution of magmatic-hydrothermal system -compositions of magmatic gases -fO_2 determination -gas-rock interactions -low-level SO_2 and CO_2 degassing rates

†Recommended isotopes for gas monitoring include δD and $\delta^{18}O$ for H_2O, $\delta^{13}C$ for CO_2, $\delta^{34}S$ for total S, and $^3He/^4He$.

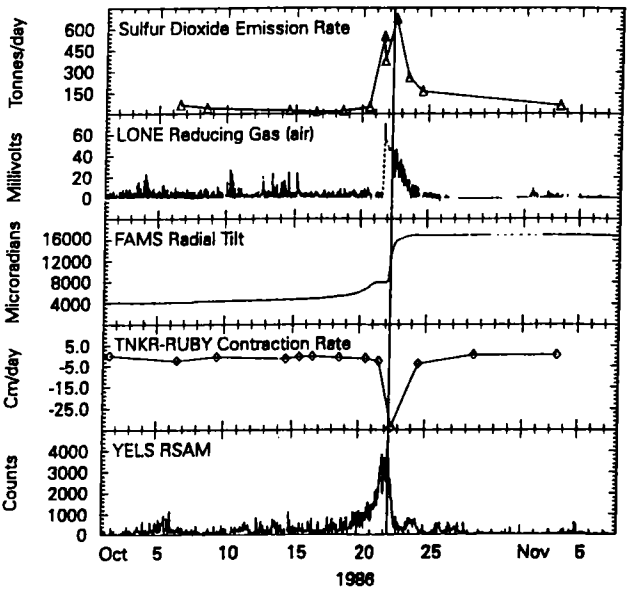

Figure 33. Plot of SO_2 emission rates, reducing-gas sensor data, tilt, electronic distance measurements (EDM), and seismic data at Mount St. Helens during October and November, 1986. Air reducing-gas data are from station LONE on the east side of the dome. The single datum on October 22 is shown enlarged and the dotted line represents the missing early portion of the reducing-gas peak. Tilt data are from FAMS (north side of dome); EDM data are from the line between TNKR (north crater floor) and RUBY (north side of dome); Seismicity is represented by hourly-averaged RSAM data from YELS (north crater floor). Vertical line represents the beginning of lava extrusion on 21 October 1986. Note that the increases in SO_2 fluxes and reducing-gas signals coincide with changes in tilt, EDM, and seismic data. From McGee and Sutton (1994).

eruptions. TOMS is useful (for SO_2) during the large explosive eruptions, but can't be used to measure lower-level emissions. The example shown in Figure 34 documents SO_2 emissions throughout 1980 at Mount St. Helens. Most of the data come from COSPEC observations, but the high spikes are TOMS data, taken during the major eruption of May 18. The ratio of explosive to non explosive degassing at Mount St. Helens in 1980 is roughly 5:1; ~1 Mt during the May 18 event and 220 Kt during non-eruptive days of 1980.

CONCLUSIONS

Volcanic gases contain H_2O, CO_2, SO_2, H_2, H_2S, HCl, HF, CO, S_2, COS, rare gases, and a number of trace-metal species. The main volcanic gases are H_2O, CO_2, and SO_2, although H_2S may be the dominant sulfur gas in equilibrium with some convergent-plate magmas at depth, and HCl may exceed total S in some convergent-plate volcanic gases. Gases discharging from convergent-plate volcanoes contain much more H_2O than gases from divergent-plate or hot-spot volcanoes, which have higher proportions of CO_2 and SO_2. Convergent-plate-volcano gases are also relatively enriched in HCl. These patterns reflect the tectonic origins of the respective magmas. Magmas from divergent-plate and hot-spot volcanoes derive volatiles primarily from the mantle, so they contain moderate amounts of C and S but are relatively depleted in H_2O and Cl compared to magmas from convergent-plate volcanoes, which contain volatiles from the subducted slab as well as the mantle, making them richer in H_2O and Cl.

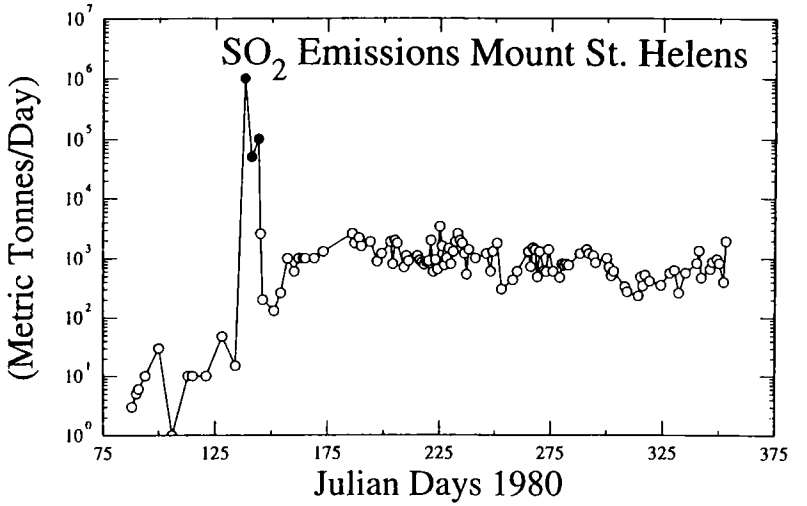

Figure 34. Combination of COSPEC (open circles) and TOMS (filled circles) data for Mount St. Helens in 1980. COSPEC data are from Casadevall et al. (1982); TOMS data are approximate. Highest spike of SO_2 emissions is on Julian day 138 (18 May), about 1 Mt, measured by TOMS.

The relative abundances of H_2, H_2S, and CO in volcanic gases depend on temperature, pressure, and bulk composition. For a given bulk atomic composition, the H_2/H_2O, SO_2/H_2S, and CO/CO_2 ratios increase with rising temperature and falling pressure. The abundances of H_2, H_2S, and CO also increase with the amounts of atomic H, H + S, and C, respectively, and with decreasing fO_2. The fO_2's of at least some high-temperature volcanic gases are apparently buffered by their respective lavas over a range of liquidus to solidus conditions. Thus, volcanic-gas data can provide independent constraints on fO_2 of magmas in addition to those provided by analyses of minerals and glasses in rocks.

Volcanic-gas studies contribute to the overall understanding of the storage and release of volatiles from magmas. One outstanding dilemma is that many andesitic-dacitic convergent-plate volcanoes emit more SO_2 during eruptions than can be explained by the amount of dissolved S released from erupted or near-surface magma. This also applies to CO_2 in the few cases where the appropriate CO_2 data exist. One emerging explanation is that many of these magmas may contain a separate gas phase at depth prior to eruption (see also Chapter 8). These andesitic-dacitic magmas also contain variable amounts of dissolved volatiles (mainly H_2O) that may exsolve from melt during ascent and eruption or at shallow depths by second boiling of magma (e.g., during crystallization of a dome). Most basaltic magmas also appear to contain dissolved volatiles and a separate gas phase. For instance, Kilauea magmas apparently saturate with CO_2-rich fluid at ~40 km depth, whereas most of the remaining volatiles exsolve at ≤150 m. This general feature of two-stage degassing may be common at hot-spot and divergent-plate volcanoes. Once a separate CO_2-rich fluid exists, it may scavenge other volatiles with especially low solubility (e.g., rare gases) from the melt.

Volcanic gases are one of several indicators used to understand and forecast volcanic activity. In particular, SO_2 fluxes correlate moderately well with volcanic activity, and have helped forecast some eruptions. However, SO_2-flux data have been much more successful at predicting the episodic eruptions or declining volcanic activity that follow an

initial cataclysmic eruption than in predicting the first explosive eruption itself. This suggests that prior to the vent-clearing eruption, a hydrothermal or impermeable-rock barrier may prevent some or all of the SO_2 from reaching the surface. Recent work indicates that magmatic CO_2 and He are less affected by hydrothermal barriers and may therefore provide an improved basis for forecasting initial eruptions.

The principal atmospheric and global impacts of volcanic eruptions occur through stratospheric injection of SO_2, which converts to sulfuric acid aerosols that block incoming solar radiation and contribute to ozone destruction. On average, volcanoes emit 13 Mt of SO_2 per year, of which 4 Mt comes from explosive eruptions and 9 Mt is emitted by passive degassing. This represents only 5-10% of the annual anthropogenic SO_2 flux, but its climatic and atmospheric impacts are greater because much of the volcanic SO_2 is injected explosively into the stratosphere where it is not readily rained out, unlike the SO_2 discharged into the troposphere. Over the past 14 years, the eruptions of El Chichón and Mount Pinatubo dominate the explosive SO_2 flux, suggesting that most of the stratospheric injections come from infrequent large eruptions.

Future studies should expand the data on high-temperature equilibrium com-positions of volcanic gases. These studies should include thermochemical evaluation of analytical data and retrieval of last equilibrium compositions and temperatures where possible by methods reviewed above. High sampling priorities include gases from hot-spot and divergent-plate volcanoes, especially those with alkaline and evolved magmas. More time-series samples from multiple vents on the same volcano are also needed. In addition, more work is needed to develop sensors that detect specific gas species and resist corrosion by acidic volcanic gases so that the true potential of time-series monitoring of fumaroles can be realized. A high priority for plume studies is to measure CO_2 emission rates, as well as the emission rates of other gas species, in addition to SO_2. Past studies show that, in addition to SO_2 fluxes, ratios of gas species change with volcanic activity. Multiple-species flux data would provide data on both emission rates and the ratios of gas species. Satellite-based systems that can detect multiple species well into the troposphere are also desirable and may offer the most cost-effective approach for measuring volcanic-gas emissions when combined with in-situ or continuous sensor data in the future. Such systems may provide the only practical means for observing volcanic emissions on a global scale. Finally, we need additional TOMS measurements of SO_2 emissions from large explosive eruptions to improve understanding of the atmospheric and climatic impacts of these volcanic events.

ACKNOWLEDGMENTS

Timely and detailed reviews by Patric Allard, Alain Bernard, Jake Lowenstern, and Ken McGee greatly improved an earlier draft of this paper. Mark Reed suggested the method of graphically displaying correspondence temperatures. Funding for this project was provided in part by the U.S. Geological Survey Volcano Hazards and Geothermal Studies Program and the U.S. Geological Survey Global Change and Climate History Program.

REFERENCES

Ágústsdóttir AM, Brantley SL (1994) Volatile fluxes integrated over four decades at Grímsvötn volcano, Iceland. J Geophys Res 99:9505-9522.

Allard P (1983) The origin of hydrogen, carbon, sulphur, nitrogen and rare gases in volcanic exhalations: evidence from isotope geochemistry. In: Tazieff H, Sabroux JC (eds) Forecasting Volcanic Events. Elsevier, Amsterdam, 337-386.

Allard P, Tazieff H, Dajlevic D (1979) Observations of sea floor spreading in Afar during the November 1978 fissure eruption. Nature 279:30-33.

Allard P, Carbonnelle J, Dajlevic D, Le Bronec J, Morel P, Robe MC, Maurenas JM, Faivre-Pierre R, Martin D, Sabroux JC, Zettwoog P (1991a) Eruptive and diffuse emissions of CO_2 from Mount Etna. Nature 351:387-391.

Allard P, Malorani A, Tedesco D, Cortecci G, Turi B (1991b) Isotopic study of the origin of sulfur and carbon in Solfatara fumaorles, Campi Flegrei caldera. J Volcanol Geotherm Res 48:139-159.

Allard P, Carbonnelle J, Métrich N, Loyer H, Zettwooog P (1994) Sulphur output and magma degassing budget of Stromboli volcano. Nature 368:326-330.

Alt JC (1994) A sulfur isotopic profile through the Troodos ophiolite, Cyprus: primary composition and the effects of seawater hydrothermal alteration. Geochim Cosmochim Acta 58:1825-1840.

Andres RJ, Rose WI (1994) Remote sensing spectroscopy of volcanic plumes and clouds. In: McGuire WJ, Kilburn CRJ, Murray JB (eds) Monitoring Active Volcanoes: Strategies, Procedures, and Techniques. University College of London Press, London, England (in press).

Andres RJ, Kyle PR, Stokes JB, Rose WI (1989) Sulfur dioxide emissions from episode 48A, East Rift Zone eruption of Kilauea volcano, Hawaii. Bull Volcanol 52:113-117.

Andres RJ, Rose WI, Kyle PR, deSilva S, Francis P, Gardeweg M, Moreno Roa H (1991) Excessive sulfur dioxide emissions from Chilean volcanoes. J Volcanol Geotherm Res 46:323-329.

Andres RJ, Rose WI, Stoiber RE, Williams SN, Matiás O, Morales R (1993) A history of sulfur dioxide emission rate measurements from Guatemalan volcanoes. Bull Volcanol 55:379-388.

Andres RJ, Kyle PR, Chuan RL (1994) Sulfur dioxide, particle and elemental emissions from Mount Etna, Italy during July 1987. Geologishe Rundschau (in press).

Baubron JC, Allard P, Toutain JP (1990) Diffuse volcanic emissions of carbon dioxide from Vulcano Island, Italy. Nature 344:51-53.

Badruddin M (1986) Pancaran gas SO_2 pada Letusan G. Galunggung, 1982. In: Katili JA, Sudradjat A, Kumumadinata K (eds) Letusan Galunggung 1982-1983. Direktorat Vulkanologi, Direktorat Jenderal Geologi Dan Sumberdaya Mineral, Departemen Pertambangan Dan Energi, Bandung, 285-301 (in Indonesian).

Bernard A (1985) Les mécanismes de condensation des gaz volcaniques. PhD dissertation, University of Brussels, Belgium (in French).

Bernard A, Symonds RB, Rose WI Jr (1990) Volatile transport and deposition of Mo, W and Re in high temperature magmatic fluids. Appl Geochem 5:317-326.

Berresheim H, Jaeschke W (1983) The contribution of volcanoes to the global atmospheric sulfur budget. J Geophys Res 88:3732-3740.

Bluth GJS, Doiron SD, Schnetzler CC, Krueger AJ, Walter LS (1992) Global tracking of the SO_2 clouds from the June, 1991 Mount Pinatubo eruptions. Geophys Res Lett 19:151-154.

Bluth GJS, Schnetzler CC, Krueger AJ, Walter LS (1993) The contribution of explosive volcanism to global atmospheric sulphur dioxide concentrations. Nature 366:327-329.

Bluth GJS, Casadevall TJ, Schnetzler CC, Doiron SD, Walter LS, Krueger AJ, Badruddin M (1994a) Evaluation of sulfur dioxide emissions from explosive volcanism: the 1982-1983 eruptions of Galunggung, Java, Indonesia. J Volcanol Geotherm Res (in press).

Bluth GJS, Scott CJ, Sprod IE, Schnetzler CC, Krueger AJ, Walter LS (1994b) Explosive SO_2 emissions from the 1992 eruptions of Mount Spurr, Alaska. In: Keith T (ed) Spurr 1992. U S Geol Surv Bull (in press).

Brantley SL, Ágústsdóttir AM, Rowe GL (1993) Crater lakes reveal volcanic heat and volatile fluxes. GSA Today 3:173-178.

Buat-Ménard P, Arnold M (1978) The heavy metal chemistry of atmospheric particulate matter emitted by Mount Etna volcano. Geophys Res Lett 5:245-248.

Caltabiano T, Gennaro D, Romano R (1994) SO_2 flux measurements at Mount Etna (Sicily). J Geophys Res (in press).

Carmichael ISE (1991) The redox states of basic and silicic magmas: a reflection of their source region? Contrib Mineral Petrol 106:129-141.

Casadevall TJ, Johnston DA, Harris DM, Rose WI, Malinconico LL, Stoiber RE, Bornhorst TJ, Williams SN (1981) SO_2 emission rates at Mount. St. Helens from March 29 through December, 1980. In: Lipman PW, Mullineaux DR (eds) The 1980 eruptions of Mount St. Helens, Washington. U S Geol Surv Prof Paper 1250:193-200.

Casadevall T, Rose W, Gerlach T, Greenland LP, Ewert J, Wunderman R, Symonds R (1983) Gas emissions and the eruptions of Mount St. Helens through 1982. Science 221:1383-1385.

Casadevall TJ, Rose WI Jr, Fuller WH, Hunt WH, Hart MA, Moyers JL, Woods DC, Chuan RL, Friend JP (1984) Sulfur dioxide and particles in quiescent volcanic plumes from Poás, Arenal, and Colima volcanos, Costa Rica and Mexico. J Geophys Res 89:9633-9641.

Casadevall TJ, Stokes JB, Greenland LP, Malinconico LL, Casadevall JR, Furukawa BT (1987) SO_2 and CO_2 emission rates at Kilauea volcano, 1979-1984. In: Decker RW, Wright TL, Stauffer PH (eds) Volcanism in Hawii. U S Geol Surv Prof Paper 1350:771-780.

Casadevall TJ, Doukas MP, Neal CA, McGimsey RG, Gardner CA (1994) Emission rates of sulfur dioxide and carbon dioxide from Redoubt volcano, Alaska during the 1989-1990 eruptions. J Volcanol Geotherm Res (in press).

Chaigneau M, Tazieff H, Febre R (1960) Composition des gaz volcaniques du lac de lave permanent due Nyiragongo (Congo belge). C R Acad Sci Paris, Ser D, 250:2482-2485.

Chartier TA, Rose WI, Stokes JB (1988) Detailed record of SO_2 emissions from Pu'u `O`o between episodes 33 and 34 of the 1983-86 ERZ eruption, Kilauea, Hawaii. Bull Volcanol 50:215-228.

Christenson BW, Wood CP (1993) Evolution of vent-hosted hydrothermal system beneath Ruapehu Crater Lake, New Zealand. Bull Volcanol 55:547-565.

Cole JW, Nairn IA (1975) Catologue of the active volcanoes of the world including solfatara fields—Part 22. New Zealand. Int'l Assoc Volcanol Chem Earth's Interior.

Connor CB, Stoiber RE, Malinconico, LL Jr (1988) Variation in sulfur dioxide emissions related to earth tides, Halemaumau crater, Kilauea volcano, Hawaii. J Geophys Res 93:14867-14871.

Daag A, Tubianosa B, Newhall C, Tungol N, Javier D, Dolan M, de los Reyes PJ, Arboleda R, Martinez M, Regalado MTM (1994) Monitoring sulfur dioxide emissions at Mount Pinatubo. In: Punongbayan RS, Newhall CG (eds) The 1991-1992 eruptions of Mount Pinatubo, Philippines. U S Geol Surv Prof Paper (in press).

Delmelle P, Bernard A (1994) Geochemistry, mineralogy, and chemical modelling of the acid crater lake of Kawah Ijen volcano, Indonesia. Geochim Cosmochim Acta 58:2445-2460.

Delorme H (1983) Composition chimique et isotopique de la phase gazeuse de volcans calcoalcalins: Amèrique Centrale et Soufrière de la Guadeloupe. Application à la surveillance volcanique. PhD disseration, University of Paris VII.

Devine JD, Sigurdsson H, Davis AN, Self S (1984) Estimates of sulfur and chlorine yields to the atmosphere from volcanic eruptions and potential climatic effects. J Geophys Res 89:6309-6325.

Doukas MP, Gerlach TM (1994) Results of volcanic gas monitoring during the 1992 eruption at Mt. Spurr. In: Keith T (ed) Spurr 1992. U S Geol Surv Bull (in press).

Ellis AJ (1957) Chemical equilibrium in magmatic gases. Am J Sci 255:416-431.

Finnegan DL, Kotra JP, Hermann DM, Zoller WH (1989) Use of ^{7}LiOH-impregnated filters for the collection of acidic gases and analysis by instrumental neutron activation analysis. Bull Volcanol 59:83-87.

Friend JP, Bandy AR, Moyers JL, Zoller WH, Stoiber RE, Torres AL, Rose WI, McCormick MP, Woods DC (1982) Research on atmospheric volcanic emissions: an overview. Geophys Res Lett 9:1101-1104.

Gantes M, Sabroux JC, Vitter G (1983) Chemical sensors for monitoring volcanic activity. In: Tazieff H, Sabroux JC (eds) Forecasting Volcanic Events. Elsevier, Amsterdam, 409-424.

Gerlach TM (1979) Evaluation and restoration of the 1970 volcanic gas analyses from Mount Etna, Sicily. J Volcanol Geotherm Res 6:165-178.

Gerlach TM (1980a) Evaluation of volcanic gas analyses from Kilauea Volcano. J Volcanol Geotherm Res 7:295-317.

Gerlach TM (1980b) Investigations of volcanic gas analyses and magma outgassing from Erta'Ale lava lake, Afar, Ethiopia. J Volcanol Geotherm Res 7:415-441.

Gerlach TM (1980c) Evaluation of volcanic gas analyses from Surtsey Volcano, Iceland, 1964-1967. J Volcanol Geotherm Res 8:191-198.

Gerlach TM (1980d) Chemical characteristics of the volcanic gases from Nyiragongo lava lake and the generation of CH_4-rich fluid inclusions in alkaline rocks. J Volcanol Geotherm Res 8:177-189.

Gerlach TM (1981) Restoration of new volcanic gas analyses from basalts of the Afar region: further evidence of CO_2-degassing trends. J Volcanol Geotherm Res 10:83-91.

Gerlach TM (1986) Exsolution of H_2O, CO_2, and S during eruptive episodes at Kilauea volcano, Hawaii. J Geophys Res 91:12177-12185.

Gerlach TM (1989a) Degassing of carbon dioxide from basaltic magma at spreading centers: I. Afar transitional basalts. J Volcanol Geotherm Res 39:211-219.

Gerlach TM (1989b) Degassing of carbon dioxide from basaltic magma at spreading centers: II. Mid-oceanic ridge basalts. J Volcanol Geotherm Res 39:221-232.

Gerlach TM (1993a) Oxygen buffering of Kilauea volcanic gases and the oxygen fugacity of Kilauea basalt. Geochim Cosmochim Acta 57:795-814.

Gerlach TM (1993b) Thermodynamic evaluation and restoration of volcanic gas analyses: An example based on modern collection and analytical methods. Geochem J 27:305-322.

Gerlach TM, Casadevall TJ (1986a) Evaluation of gas data from high-temperature fumaroles at Mount St. Helens, 1980-1982. J Volcanol Geotherm Res 28:107-140.

Gerlach TM, Casadevall TJ (1986b) Fumarole emissions at Mount St. Helens Volcano, June 1980 to October, 1981: degassing of a magma-hydrothermal system. J Volcanol Geotherm Res 28:141-160.

Gerlach TM, Graeber EJ (1985) Volatile budget of Kilauea volcano. Nature 313:273-277.

Gerlach TM, McGee KA (1994) Total sulfur dioxide emissions and pre-eruption vapor saturated magma at Mount St. Helens, 1980-1988. Geophys Res Lett (in review).

Gerlach TM, Nordlie BE (1975) The C-O-H-S gaseous systems, Part II: temperature, atomic composition, and molecular equilibria in volcanic gases. Am J Sci 275:377-394.

Gerlach TM, Taylor BE (1990) Carbon isotope constraints on degassing of carbon dioxide from Kilauea volcano. Geochim Cosmochim Acta 54:2051-2058.

Gerlach TM, Westrich HR, Casadevall TJ, Finnegan DL (1994) Vapor saturation and accumulation in magmas of the 1989-1990 eruption of Redoubt volcano, Alaska. J Volcanol Geotherm Res 62 (in press).

Gerlach TM, Westrich HR, Symonds RB (1995) Pre-eruption vapor saturation in magma of the climactic Mount Pinatubo eruption: Source of the giant statospheric sulfur dioxide cloud. In: Punongbayan RS, Newhall CG (eds) The 1991-1992 eruptions of Mount Pinatubo, Phillipines. U S Geol Surv Prof Paper (in press).

Getahun A, Reed MH, Symonds R (1994) Mount St. Augustine volcano fumarole wall rock alteration: mineralogy, zoning, and numerical models of its formation process. J Volcanol Geotherm Res (in review).

Giggenbach WF (1974) The chemistry of Crater Lake, Mt. Ruapehu (New Zealand) during and after the 1971 active period. New Zealand J Sci 17:33-45.

Giggenbach WF (1975) A simple method for the collection and analysis of volcanic gas samples. Bull Volcanol 39:15-27.

Giggenbach WF (1980) Geothermal gas equilibria. Geochim Cosmochim Acta 44:2021-2032.

Giggenbach WF (1987) Redox processes governing the chemistry of fumarolic gas discharges from White Island, New Zealand. Appl Geochem 2:143-161.

Giggenbach WF (1992) Isotopic shifts in waters from geothermal and volcanic systems along convergent plate boundaries and their origins. Earth Planet Sci Lett 113:495-510.

Giggenbach WF, Glover RB (1975) The use of chemical indicators in the surveillance of volcanic activity affecting the crater lake on Mt. Ruapehu, New Zealand. Bull Volcanol 39:70-81.

Giggenbach WF, Goguel RL (1989) Collection and analysis of geothermal and volcanic water and gas discharges. DSIR Chemistry Rept CD 2401.

Giggenbach WF, Le Guern F (1976) The chemistry of magmatic gases from Erta'Ale, Ethiopia. Geochim Cosmochim Acta 40:25-30.

Giggenbach WF, Matsuo S (1991) Evaluation of results from second and third IAVCEI field workshops on volcanic gases, Mt Usu, Japan, and While Island, New Zealand. Appl Geochem 6:125-141.

Giggenbach WF, Sheppard DS (1989) Variations in the temperature and chemistry of White Island fumarole discharges 1972-85. New Zealand Geol Surv Bull 103:119-126.

Gill JB (1981) Orogenic andesites and plate tectonics. Springer-Verlag, Berlin.

Graedel TE (1978) Chemical compounds in the atmosphere. Academic Press, New York.

Greenland LP (1987a) Hawiian eruptive gases. In: Decker RW, Wright TL, Stauffer PH (eds) Volcanism in Hawii. U S Geol Surv Prof Paper 1350:781-790.

Greenland LP (1987b) Composition of gases from the 1984 eruption of Mauna Loa volcano. In: Decker RW, Wright TL, Stauffer PH (eds) Volcanism in Hawii. U S Geol Surv Prof Paper 1350:781-790.

Greenland LP, Rose WI, Stokes JB (1985) An estimate of gas emissions and magmatic gas content from Kilauea volcano. Geochim Cosmochim Acta 49:125-129.

Harris DM, Rose WI (1994) Dynamics of carbon dioxide emissions, magma crystallization and magma ascent: hypothesis, theory and application to Mount St. Helens. Bull Volcanol (in review).

Harris DM, Sato M, Casadevall TJ, Rose WI Jr, Bornhorst TJ (1981) Emission rates of CO_2 from plume measurements. In: Lipman PW, Mullineaux DR (eds) The 1980 eruptions of Mount St. Helens, Washington. U S Geol Surv Prof Paper 1250:201-207.

Heald EF, Naughton JJ, Barnes IL Jr (1963) Use of equilibrium calculations in the interpretation of volcanic gas samples. J Geophys Res 68:545-557.

Hobbs PV, Radke LF, Eltgroth MW, Hegg DA (1981) Airborne studies of the emissions from the volcanic eruptions of Mount St. Helens. Science 211:816-818.

Holloway JR (1977) Fugacity and activity of molecular species in supercritical fluids. In: Fraser DG (ed) Thermodynamics in Geology. Reidel Publishing Co, Dordrecht, Holland, 161-181.

Huntingdon AT (1973) The collection and analysis of volcanic gases from Mount Etna. Philos Trans R Soc London, Ser A, 274:119-128.

Ito E, Harris DM, Anderson AT Jr (1983) Alteration of oceanic crust and geologic cycling of chlorine and water. Geochim Cosmochim Acta 47:1613-1624.

Jaggar TA (1940) Magmatic gases. Am J Sci 238:313-353.

Katili JA, Sudradjat A (1984) Galunggung: The 1982-1983 eruption. Report of the Volcanological Survey of Indonesia, Republic of Indonesia.

Kodosky LG, Motyka RJ, Symonds RB (1991) Fumarolic emissions from Mount St. Augustine, Alaska,

1979-1984: degassing trends, volatile sources, and their possible role in eruptive style. Bull Volcanol 53:381-394.

Krauskopf KB (1957) The heavy metal content of magmatic vapor at 600°C. Econ Geol 52:786-807.

Krauskopf KB (1964) The possible role of volatile metal compounds in ore genesis. Econ Geol 59:22-45.

Krueger AJ (1983) Sighting of El Chichón sulfur dioxide clouds with the Nimbus 7 Total Ozone Mapping Spectrometer. Science 220:1377-1379.

Krueger AJ (1985) Detection of volcanic eruptions from space by their sulfur dioxide clouds. American Institute of Aeronautics and Astronautics, AAIA 23rd Aerospace Sciences Meeting, AIAA-85-0100, January 14-17, Reno, Nevada, 1-5.

Krueger AJ, Walter LS, Schnetzler CC, Doiron SD (1990) TOMS measurement of the sulfur dioxide emitted during the 1985 Nevado del Ruiz eruptions. J Volcan Geotherm Res 41:7-15.

Kyle PR, McIntosh WC (1989) Automation of a correlation spectrometer for measuring volcanic SO_2 emissions. New Mexico Bur Mines Mineral Res Bull 131:158.

Kyle PR, Meeker K, Finnegan D (1990) Emission rates of sulfur dioxide, trace gases and metals from Mount Erebus, Antarctica. Geophys Res Lett 17:2125-2128.

Kyle PR, Sybeldon LM, McIntosh WC, Meeker K, Symonds R (1994) Sulfur dioxide emission rates from Mount Erebus, Antarctica. In: Kyle P (ed) Volcanological Studies of Mount Erebus, Antarctica. Antarctic Res Series, Washington, DC (in press).

Lazrus AL, Cadle RD, Gandrud BW, Greenberg JP, Huebert BJ, Rose WI (1979) Trace chemistry of the stratosphere and of volcanic eruption plumes. J Geophys Res 84:7869-7875.

Le Guern F, Gerlach TM, Nohl A (1982) Field gas chromatograph analyses of gases from a glowing dome at Merapi volcano, Java, Indonesia, 1977, 1978, 1979. J Volcanol Geotherm Res 14:223-245.

Magro G, Pennisi M (1991) Noble gases and nitrogen: mixing and temporal evolution in the fumarolic fluids of Vulcano, Italy. J Volcanol Geotherm Res 47:237-247.

Malinconico LL (1979) Fluctuations in SO_2 emissions during recent eruptions of Etna. Nature 278:43-45.

Matsuo S (1961) On the chemical nature of fumaorlic gases of volcano, Showashinzan, Hokkaido, Japan. J Earth Sci Nagoya Univ 9:80-100.

Matsuo S, Suzuoki T, Kusakabe M, Wada H, Suzuki M (1974) Isotopic and chemical compositions of volcanic gases from Satsuma-Iwojima, Japan. Geochem J 8:165-173.

Matsuo S, Ossaka J, Hirabayashi J, Ozawa T, Kimishima K (1982) Chemical nature of volcanic gases of Usu volcano in Japan. Bull Volcanol 45:261-264.

McGee K (1992) The structure, dynamics and chemical composition of non-eruptive plumes from Mount St. Helens. J Volcanol Geotherm Res 51:269-282.

McGee K, Sutton AJ (1994) Eruptive activity at Mount St. Helens, Washington, USA, 1984-1988: a gas geochemistry perspective. Bull Volcanol (in press).

McGee TJ, Burris J Jr (1987) SO_2 absorption cross sections in the near U.V. J Quant Radiative Transfer 37:165-182.

Menyailov IA (1975) Prediction of eruptions using changes in compositions using changes in compositions of volcanic gases. Bull Volcanol 39:112-125.

Menyailov IA, Nikitina LP (1980) Chemistry and metal contents of magmatic gases: the new Tolbachik volcanoes case (Kamchatka). Bull Volcanol 43:197-205.

Menyailov IA, Nikitina LP, Shapar VN, Pilipenko VP (1986) Temperature increase and chemical change of fumarolic gases at Momotombo volcano, Nicaraqua, in 1982-1985: are these indicators of a possible eruption? J Geophys Res 91:12199-12214.

Millán MM, Hoff RM (1978) Remote sensing of air pollutant by correlation spectroscopy—instrumental response characteristics. Atmos Environ 12:853-864.

Mizutani Y (1962a) Chemical analysis of volcanic gases. J Earth Sci Nagoya Univ 10:125-134.

Mizutani Y (1962b) Origin of lower temperature fumarolic gases at Showashinzan. J Earth Sci Nagoya Univ 10:135-148.

Mizutani Y (1978) Isotopic compositions of volcanic steam from Showashinzan volcano, Hokkaido, Japan. Geochem J 12:57-63.

Mizutani Y, Sugiura T (1982) Variations in chemical and isotopic compositions of fumarolic gases from Showashinzan volcano, Hokkaido, Japan. Geochem J 16:63-71.

Möller D (1984) Estimation of the global man-made sulphur emission. Atmos Environ 18:19-27.

Mori T, Notsu K, Tohjima Y, Wakita H (1993) Remote detection of HCl and SO_2 in volcanic gas from Unzen volcano, Japan. Geophys Res Lett 20:1355-1358.

Nemoto T, Hayakawa M, Takahashi K, Oana S (1957) Report on the geological, geophysical, and geochemical studies of Usu volcano (Showashinzan). Geol Surv Japan Rep 170:1-149.

Newhall CG, Self S (1982) The volcanic explosivity index (VEI): An estimate of explosive magnitude for historical volcanism. J Geophys Res 87:1231-1238.

Nordlie BE (1971) The composition of the magmatic gas of Kilauea and its behavior in the near surface environment. Am J Sci 271:417-463.

Palais JM, Sigurdsson H (1989) Petrologic evidence of volatile emissions from major historic and prehistoric volcanic eruptions. In: Berger A, Dickinson RE, Kidson JW (eds) Understanding Climate Change. Am Geophys Union Monograph 52:31-53.

Peacock SM (1990) Fluid processes in subduction zones. Science 248:329-337.

Phelan JM, Finnegan DL, Ballantine DS, Zoller WH, Hart MA, Moyers JL (1982) Airborne aerosol measurements in the quiescent plume of Mount St. Helens: September, 1980. Geophys Res Lett 9:1093-1093.

Quisefit JP, Toutain JP, Bergametti G, Javoy M, Cheynet B, Person A (1989) Evolution versus cooling of gaseous volcanic emissions from Momotombo Volcano, Nicaragua: Thermochemical model and observations. Geochim Cosmochim Acta 53:2591-2608.

Rose WI (1993) Comment on "another look at the calculation of fallout tephra volumes" by Judy Fierstein and Manuel Nathenson. Bull Volcanol 55:372-374.

Rose WI, Chuan RL, Cadle RD, Woods DC (1980) Small particles in volcanic eruption clouds. Am J Sci 280:671-696.

-Rose WI Jr, Stoiber RE, Malinconico LL (1982) Eruptive gas compositions and fluxes of explosive volcanoes: Budget of S and Cl emitted from Fuego volcano, Guatemala. In: Thorpe RS (ed) Orogenic Andesites and Related Rocks. Wiley and Sons, New York, NY, 669-676.

Rose WI, Symonds RB, Chartier T, Stokes JB, Brantley S (1985) Simultaneous experiments with two correlation spectrometers at Kilauea and Mount St. Helens. EOS Trans Am Geophys Union 66:1142.

Rose WI, Chuan RL, Giggenbach WF, Kyle PR, Symonds RB (1986) Rates of sulfur dioxide and particle emissions from White Island volcano, New Zealand, and an estimate of the total flux of major gaseous species. Bull Volcanol 48:181-188.

Rose WI, Heiken G, Wohletz K, Eppler D, Barr S, Miller T, Chuan RL, Symonds, RB (1988) Direct rate measurements of eruption plumes at Augustine volcano: a problem of scaling and uncontrolled variables. J Geophys Res 93:4485-4899.

Rowe GL (1991) The acid crater lake system of Poás volcano, Costa Rica: geochemistry, hydrology, and physical characteristics. PhD Dissertation, Pennsylvania State University, University Park, PA

Rowe GL, Varekamp JC (1993) A call for contributions to the IWGCL crater and caldera lake database. International Working Group on Crater Lakes (IWGCL) Newsletter 6:54-61.

Rowe GL Jr, Brantley SL, Fernandez M, Fernandez JF, Borgia A, Barquero J (1992a) Fluid-volcano interaction in an active stratovolcano: the crater lake system of Poás volcano, Costa Rica. J Volcanol Geotherm Res 49:23-51.

Rowe GL Jr, Ohsawa S, Takano B, Brantley SL, Fernandez JF, Barquero J (1992b) Using crater lake chemistry to predict volcanic activity at Poás volcano, Costa Rica. Bull Volcanol 54:494-503.

Schidlowski M (1986) The atmosphere. In: Hutzinger O (ed) The Natural Environment and the Biogeochemical Cycles. Springer Verlag, New York.

Schneider DJ, Rose WI, Kelley L (1994) Tracking of the 1992 Crater Peak/Spurr volcano eruption clouds using AVHRR. In: Keith T (ed) Spurr 1992. U S Geol Surv Bull (in press).

Schoeberl MR, Doiron SD, Lait LR, Newman PA, Krueger AJ (1993) A simulation of the Cerro Hudson SO_2 cloud. J Geophys Res 98:2949-2955.

Shepherd ES (1921) Kilauea gases, 1919. Hawaiian Volcano Obs Bull 9:83-88.

Shinohara H, Giggenbach WF, Kazahaya K, Hedenquist JW (1993) Geochemistry of volcanic gases and hot springs of Satsuma-Iwojima, Japan: following Matsuo. Geochem J 27:271-285.

Sigvaldason GE, Elisson G (1968) Collection and analysis of volcanic gases at Surtsey, Iceland. Geochim Cosmochim Acta 32:797-805.

Simkin T (1993) Terrestrial volcanism in space and time. Ann Rev Earth Planet Sci 21:427-452.

Smithsonian Institution/SEAN, 1989, Global Volcanism 1975-1985. Prentice-Hall, Englewood Cliffs, New Jersey, and American Geophysical Union, Washington, DC.

Sorey ML, Kennedy BM, Evans WC, Farrar CD, Suemnicht GA (1993) Helium isotope and gas discharge variations associated with crustal unrest in Long Valley Caldera, California, 1989-1992. J Geophys Res 98:15871-15889.

Spycher NF, Reed MH (1988) Fugacity coefficients of H_2, CO_2, CH_4, H_2O and of H_2O-CO_2-CH_4 mixtures: A virial equation treatment for moderate pressures and temperatures applicable to calculations of hydrothermal boiling. Geochim Cosmochim Acta 52:739-749.

Stevenson DS (1993) Physical models of fumarolic flow. J Volcanol Geotherm Res 57:139-156.

Stoiber RE, Jepsen A (1973) Sulfur dioxide contributions to the atmosphere by volcanoes. Science 182:577-578.

Stoiber RE, Rose WI Jr (1974) Fumarolic incrustations at active Central American volcanoes. Geochim Cosmochim Acta 38:495-516.

Stoiber RE, Malinconico LL Jr, Williams SN (1983) Use of the Correlation Spectrometer at Volcanoes. In: Tazieff H, Sabroux JC (eds) Forecasting Volcanic Events. Elsevier Science Publishers, Amsterdam, 425-444.

Stoiber RE, Williams SN, Huebert BJ (1986) Sulfur and halogen gases at Masaya Caldera complex, Nicaragua: total flux and variations with time. J Geophys Res 91:12215-12231.

Stoiber RE, Williams SN, Huebert BJ (1987) Annual contribution of sulfur dioxide to the atmosphere by volcanoes. J Volcanol Geotherm Res 33:1-8.

Stolper E, Newman S (1994) The role of water in the petrogenesis of Mariana trough magmas. Earth Planet Sci Lett 121:293-325.

Sutton AJ (1990) Chemical sensors for volcanic gases with a compilation of commercial availability. U S Geol Surv Open-File Rept 90-44.

Sutton AJ, McGee KA, Casadevall TJ, Stokes JB (1992) Fundamental volcanic-gas-study techniques: an integrated approach to monitoring. In: Ewert JW, Swanson DA (eds) Monitoring volcanoes: techniques and strategies used by the staff of the Cascades Volcano Observatory, 1980-90. U S Geol Surv Bull 1966:181-188.

Symonds R (1993) Scanning electron microscope observations of sublimates from Merapi volcano, Indonesia. Geochem J 26:337-350.

Symonds RB, Reed MH (1993) Calculation of multicomponent chemical equilibria in gas-solid-liquid systems: Calculation methods, thermochemical data and applications to studies of high-temperature volcanic gases with examples from Mount St. Helens. Am J Sci 293:758-864.

Symonds RB, Rose WI, Reed MH, Lichte FE, Finnegan DL (1987) Volatilization, transport and sublimation of metallic and non-metallic elements in high temperature gases at Merapi Volcano, Indonesia. Geochim Cosmochim Acta 51:2083-2101.

Symonds RB, Rose WI, Gerlach TM, Briggs PH, Harmon RS (1990) Evaluation of gases, condensates, and SO_2 emissions from Augustine Volcano, Alaska: the degassing of a Cl-rich volcanic system. Bull Volcanol 52:355-374.

Symonds RB, Reed MH, Rose WI (1992) Origin, speciation, and fluxes of trace-element gases at Augustine volcano, Alaska: insights into magma degassing and fumarolic processes. Geochim Cosmochim Acta 56:633-657.

Takano B (1987) Correlation of volcanic activity with sulfur oxyanion speciation in a crater lake. Science 235:1633-1635.

Takano B, Watanuki K (1990) Monitoring of volcanic eruptions at Yugama crater lake by aqueous sulfur oxyanions. J Volcanol Geotherm Res 40:71-87.

Taran YA, Rozhkov AM, Serafimova EK, Esikov AD (1991) Chemical and isotopic compositions of magmatic gases from the 1988 eruption of Klyuchevskoy volcano, Kamchatka. J Volcanol Geotherm Res 46:255-263.

Taylor BE (1986) Magmatic volatiles: isotopic variations of C, H, and S. In: Valley JW, Taylor HP, O'Neil JR (eds) Stable isotopes in high temperature geological processes. Rev Mineral 16:185-225.

Tazieff H, Le Guern F, Carbonnelle J, Zettwoog P (1972) Etude chimique des fluctuations des gaz éruptifs de volcan Erta'Ale (Afar, Ethiopia). C R Acad Sci Paris, Ser D, 274:1003-1006.

Tedesco D, Sabroux JC (1987) The determination of deep temperatures by means of the CO-CO_2-H_2-H_2O geothermometer: an example using fumaroles in the Campi Flegrei, Italy. Bull Volcanol 49:381-387.

Tedesco D, Toutain JP, Allard P, Losno R (1991) Chemical variations in fumarolic gases at Vulcano Island (Southern Italy): seasonal and volcanic effects. J Volcanol Geotherm Res 45:325-334.

Wallace PJ, Gerlach TM (1994) Magmatic vapor source for SO_2 released during volcanic eruptions: evidence from Mount Pinatubo. Science 265:497-499.

Wen S, Rose WI (1994) Retrieval of sizes and total masses of particles in volcanic clouds using AVHRR bands 4 and 5. J Geophys Res 99:5421-5431.

Westrich HR, Gerlach TM (1992) Magmatic gas source for the stratospheric SO_2 cloud from the June 15, 1991, eruption of Mount Pinatubo. Geology 20:867-870.

Williams SN (1993) Galeras volcano, Colombia: perspectives from a researcher and survivor. Geotimes 38-6:12-14.

Williams SN, Stoiber RE, Garcia NP, Londoño AC, Gemmell JB, Lowe DR, Connor CB (1986) Eruption of the Nevado del Ruiz volcano, Colombia, on 13 November 1985: gas flux and fluid geochemistry. Science 233:964-967.

Williams SN, Sturchio NC, Calvache MLV, Mendez RF, Londoño AC, García NP (1990) Sulfur dioxide from Nevado del Ruiz volcano, Colombia: total flux and isotopic constraints on its origin. J Volcanol Geotherm Res 42:53-68.

Woods A (1993) Moist convection and the injection of volcanic ash into the atmosphere. J Geophys Res 98:17627-17636.